Monitoring and Characterization of Crystal Nucleation and Growth during Batch Crystallization

Somnath Shivaji KADAM

Monitoring and Characterization of Crystal Nucleation and Growth during Batch Crystallization

Proefschrift

ter verkrijging van de graad van doctor aan de Technische Universiteit Delft, op gezag van de Rector Magnificus prof. ir. K.C.A.M. Luyben, voorzitter van het College voor Promoties, in het openbaar te verdedigen op vrijdag 8 juni 2012 om 10:00 uur

door

Somnath Shivaji KADAM

Master of Science in Industrial Chemistry, Technical University of Munich and National University of Singapore geboren te Mumbai, India. Dit proefschrift is goedgekeurd door de promotor:

Prof. dr. ir. A. I. Stankiewicz

Copromotor:

Dr.ir. H. J. M. Kramer

Samenstelling promotiecommissie:

Rector Magnificus, voorzitter

Prof. dr. ir. A. I. Stankiewicz, Technische Universiteit Delft, promotor Dr. ir. H. J. M. Kramer, Technische Universiteit Delft, copromotor

Prof. Z. K. Nagy, Loughborough University
Prof. G. Coquerel, University of Rouen

Prof. dr. ir. L. A. M. van der Wielen, Technische Universiteit Delft Prof. dr. ir. P. M. J. Van den Hof, Technische Universiteit Eindhoven

Dr. P. J. Daudey, Albermarle Catalysts B.V.

Prof.ir. J. Grievink, Technische Universiteit Delft, reservelid

Dr. Ir. Joop H. ter Horst heeft als begeleider in belangrijke mate aan de totstandkoming van het proefschrift bijgedragen.

Dit werk is financieel ondersteund door Institute for Sustainable Process Technology.

ISBN 978-94-6191-301-2

Copyright © 2012 by Somnath Shivaji Kadam.

All rights reserved. No part of the material protected by this copyright notice may be reproduced or utilized in any form or by any means, electronic or mechanical, including photocopying, recording or by any information storage and retrieval system, without written permission from the copyright owner.

Printed in the Netherlands by Ipskamp Drukkers.



Contents

1	Introduction			
	1.1	Crysta	allization fundamentals	3
		1.1.1	Principles of crystallization	3
		1.1.2	Crystal nucleation	4
		1.1.3	Crystal growth	7
		1.1.4		10
	1.2	State-	of-the-art	11
		1.2.1	Crystallization domain understanding	12
		1.2.2	Methods of characterizing crystallization	14
		1.2.3	Monitoring crystallization process	16
	1.3		enges in understanding, characterizing and monitoring batch	18
		crysta	llization processes	
		1.3.1	Crystallization domain understanding	18
		1.3.2	Crystallization process characterization	19
		1.3.3	Crystallization process monitoring	20
	1.4	Proble	em statement	21
	1.5	Thesis	s outline	22
	1.6	Projec	et organization	24
2	A New View on Crystal Nucleation		iew on Crystal Nucleation	29
	2.1	Introd	luction	31
	2.2	Exper	imental	32

		2.2.1	Solubility measurements	32
		2.2.2	MSZW measurements	33
		2.2.3	Cooling crystallization on a 3 mL scale	34
		2.2.4	Unstirred cooling experiments on a 1 mL scale	34
	2.3	Resul	ts	34
		2.3.1	MSZW of paracetamol in water	35
		2.3.2	Scale up rule for MSZW	37
		2.3.3	Single nucleus mechanism	39
	2.4	Discu	ssions	42
	2.5	Concl	usions	43
3	Αľ	New V	iew on the Metastable Zone Width	47
	3.1	Introd	luction	49
	3.2	Mode	l structures	50
		3.2.1	Stochastic model	51
		3.2.2	Conventional population balance model	54
	3.3	Exper	imental	55
		3.3.1	Attrition size and threshold crystal volume fraction determination	55
		3.3.2	MSZW measurements	56
	3.4	Resul	ts and discussions	57
		3.4.1	Attrition size and threshold crystal volume fraction determination	57
		3.4.2	Parameter estimation	58
		3.4.3	Effect of volume on MSZW	61

		3.4.4 Transition volume determination as a function of nucleation rate	62
		3.4.5 MSZW measurements	63
		3.4.6 Nucleation mechanism above the transition volume	67
	3.5	Conclusions	69
	3.6	Nomenclature	69
4	A (Comparative Study of ATR-FTIR and FT-NIR	73
	Sp	ectroscopy	
	4.1	Introduction	75
		4.1.1 Available concentration measurement techniques	75
		4.1.2 Incentive for the work and the approach	78
	4.2	Experimental	78
	4.3	Results and discussions	83
		4.3.1 Spectral features	83
		4.3.2 Partial least square modeling	86
		4.3.3 Solubility curve determination	90
		4.3.4 Batch experiments	93
		4.3.5 Associated problems	96
	4.4	Conclusions	96
5	Ra	pid Online Calibration for ATR-FTIR spectroscopy	103
	5.1	Introduction	105
	5.2	Experimental details	107
	5.3	Process model development and parameter estimation	110

	5.4	Result	ts and discussions	112
		5.4.1	Spectral features	112
		5.4.2	Validation of the PLS model	113
		5.4.3	Batch cooling crystallization	113
		5.4.4	Semi-industrial scale experiments	114
		5.4.5	Online calibration	116
		5.4.6	Parameter estimation and model validation	119
	5.5	Concl	usions	124
	5.6	Apper	ndix	125
6	Raj	pid Cr	ystallization Process Development Strategy	131
	6.1	Introd	luction	133
	6.2	Incent	tive for the work	137
	6.3	Skid d	design and its advantages	138
		6.3.1	Instrument skid	139
		6.3.2	Pump skid	140
		6.3.3	Advantages of the skid design	140
	6.4	Exper	imental	141
	6.5	Result	ts	146
		6.5.1	Solubility measurements	146
		6.5.2	Slurry test	147
		6.5.3	Infrared spectrum	148
		6.5.4	Combined characterization and PAT tool selection at lab scale	149

		6.5.5	Combined calibration and characterization at industrial scale	150
		6.5.6	Gaining process insights	152
	6.6	Concl	usions	154
7	Conclusions and recommendations			159
Suı	nma	ry		169
Sar	nenv	atting		173
Lis	List of Publications			179
Cu	rricul	lum V	itae	181
Acl	know	ledge	ments	183

	Chapter 1
Introduction	

Crystallization is a separation and purification technique which involves a phase change into a crystalline product from a solution or a melt.¹ Solution is a homogeneous mixture of two or more species and may be in solid, liquid or gaseous state. Discrepancy exists over the definition of a melt in literature but melt usually refers to materials which are solids at room temperature and are heated to get the liquid state.^{1, 2} Crystallization can lead to high purities in a single step under relatively mild conditions. The resultant crystals, under ideal conditions, flow freely when conveyed, are easy to handle and pack. It is due to these advantages of crystallization that 60% of the end products in the chemical industry are manufactured in particulate form.³ Products separated and purified by crystallization are commonly used in day-to-day life and include table salt, sugar, active pharmaceutical ingredients like paracetamol and ibuprofen, fertilizers like ammonium sulfate etc.

Batch mode of operation for crystallization process is often preferred for production of these products. Batch crystallization is used when the production rates are smaller, very expensive materials are handled, losses are to be kept at minimum, same equipment has to be used for multiple products etc.¹ The advantages of batch crystallization lies in its ease of operation and requirement of relatively simple equipments. On the other hand a major disadvantage associated with it is inconsistent and usually poor product quality. Quality of the crystalline product, which is defined in terms of the Crystal Size Distribution (CSD), purity, kind of solid state etc., is related to its performance when used as an ingredient during subsequent processes. Also quality of the product from batch crystallization process has a strong influence on the efficiency of downstream operations like filtration and drying.

This chapter aims at identifying the challenges which must be addressed in order to achieve consistent product quality during batch crystallization. The chapter starts with the fundamentals of the crystallization process and then identifies three basic requirements based on which strategies for process and equipment design, process development, and process control can be developed. Successful application of these strategies would lead to consistent product quality during batch crystallization. The three fundamental requirements are related to the crystallization domain understanding, methods of process characterization and process monitoring. The state-of-the-art in these requirements is discussed and the challenges associated with them are highlighted. Based on the challenges, a problem statement is formulated followed by the outline of the thesis which explains how each chapter in the thesis contributes to the solution of the problem.

1.1 Crystallization fundamentals

1.1.1 Principles of crystallization

For crystallization to occur from a clear liquid solution, there must be a driving force. The driving force for crystallization is known as supersaturation $\Delta\mu$ and for one component crystals in solution it is defined as⁴

$$\Delta \mu = \mu_s - \mu_c \tag{1.1}$$

where μ_s and μ_c are the chemical potentials of a molecule in the solution and in the bulk of crystal phase respectively. When the solution is dilute enough, the supersaturation is approximated in terms of the concentration ratio and is expressed as

$$S = \frac{c}{c^*(T)} \tag{1.2}$$

or as relative supersaturation σ expressed as

$$\sigma = S - 1 \tag{1.3}$$

where c is the actual concentration and $c^*(T)$ is the saturation concentration at the temperature T. When S>1, the solution is supersaturated and in the supersaturated solution nucleation, growth and other crystallization phenomena like agglomeration can occur. When S=1, the solution is saturated and at that condition, solid and liquid are in equilibrium. When S<1, the solution is undersaturated and no crystallization can occur.

The undersaturated and supersaturated regions are separated by the solubility curve as shown in Figure 1.1.

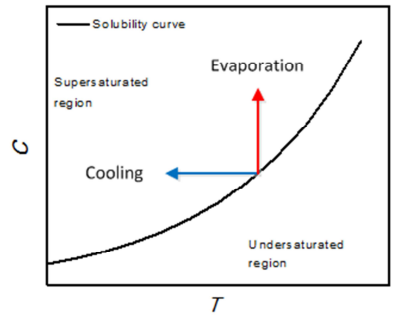


Figure 1.1: The concentration (*C*) - temperature (*T*) diagram representing the solubility curve, the undersaturated and the supersaturated regions.

A solution can be transferred into a supersaturated state by cooling the solution, evaporation of the solvent, addition of an anti-solvent to reduce the solubility of the solute in solvent, chemical reaction leading to the formation of a less soluble product from soluble reactants, or by combination of two or more of the above techniques. The choice of a technique for supersaturation generation depends on several factors like the steepness of the solubility curve with respect to the temperature, the volatility of the solvent, the heat sensitivity of the components etc.

Interestingly, crystal nucleation or formation of a new solid phase from the clear liquid phase seldom occurs immediately on entering the supersaturated region. On the contrary a metastable zone (MSZ) exists where a clear solution is meta stable, which means that, despite the existence of a supersaturation no crystal formation occurs at least not within a certain amount of time. The reason for existence of the MSZ could be understood when the nucleation process is considered in details.

1.1.2 Crystal nucleation

Nucleation is the formation of new, small, crystalline entities in a liquid phase. In unseeded batch crystallization processes it marks the start of a phase transformation and is responsible for the initial crystal population, which develops into the final crystalline product by other crystallization phenomena like crystal growth and agglomeration. Nucleation can be classified based on the presence or the absence of the crystalline material in solution.² If nucleation occurs in the absence of crystalline material of its own kind, it is called as primary nucleation. Primary nucleation can occur in a clear supersaturated solution or on the surface of foreign particles or on the surfaces of the equipment. The former case is called as primary homogeneous nucleation while the latter is known as primary heterogeneous nucleation. On the other hand, if nucleation occurs in the vicinity of the crystalline material itself it is classified as secondary nucleation. Secondary nucleation can occur in several ways.5 Tiny crystallites formed on the surface of a seed crystal during processing can, when added to a supersaturated solution, be removed from the surface and act as nuclei, a phenomenon that is known as initial breeding.6 At high supersaturations in melts, dendrite like outgrowths may form from the crystalline material. At even higher supersaturations, irregular polycrystalline aggregates may form. Fragmentation of the dendrites and the polycrystalline aggregates can serve as the source of secondary nuclei.7 Fragmentation of the crystalline material may take place under the influence of a fluid shear leading to the formation of secondary nuclei. Fragile crystals and the crystals with outgrowths like dendrites are especially susceptible to fluid shear.8

Contact nucleation is probably the most common secondary nucleation mechanism in industrial crystallizers. Contacts nucleation is a result of micro abrasion which occurs when crystal-crystal, crystal-impeller, crystal-crystallizer wall come in contact.⁹ The overview of the important types of nucleation is given in Figure 1.2.

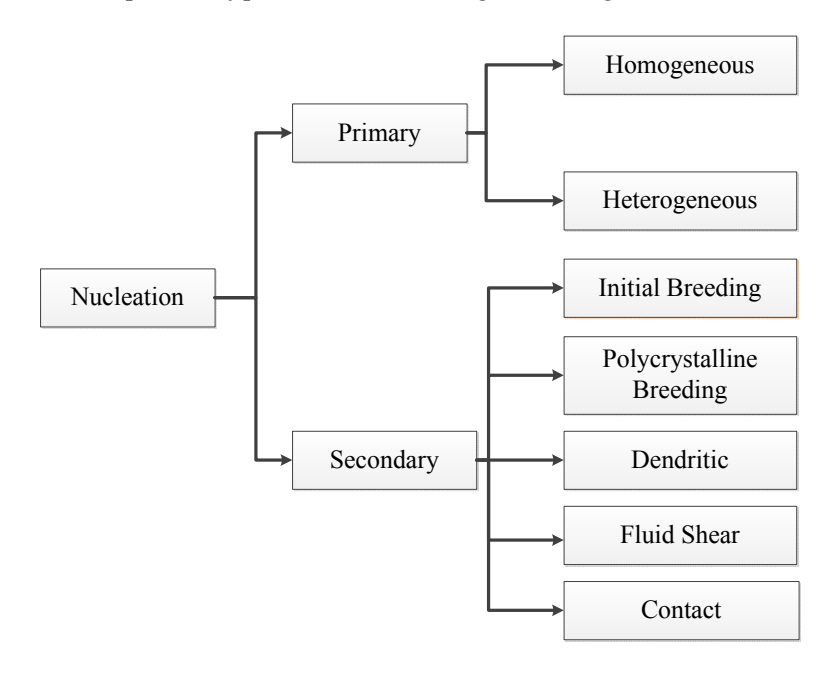


Figure 1.2: Important types of nucleation

Nucleation from a clear solution does not start immediately upon entering the supersaturated region. For nucleation to occur molecules have to come together to form clusters. Formation of the molecular clusters is a stochastic process.¹⁰ According to the Classical Nucleation Theory (CNT) nucleus is most likely a result of a sequence of molecular addition according to the scheme below²

$$M + M \rightleftharpoons M_2$$

$$M_2 + M \rightleftharpoons M_3$$
.....
$$M_{n-1} + M \rightleftharpoons M_n$$

In a supersaturated solution where $\Delta \mu = \mu_s - \mu_c > 0$ the solute molecules are not uniformly distributed but group together in arrays, known as clusters. According to the CNT, these clusters are spherical in shape and they exhibit periodicity similar to a

crystal. The clusters continuously alter their sizes by either the attachment or the detachment of a single molecule. The addition of molecules to a cluster leads to the decrease in free energy per unit volume of the cluster of ΔG_{ν} . On the other hand, the formation of a cluster leads to a free energy increase ΔG_{A} due to the formation of a surface with surface area A' and free energy per unit area of cluster γ between the cluster and the solution. For a spherical cluster of radius r, the overall free energy between the solute in cluster and the solute in solution can be written as r

$$\Delta G = \frac{4}{3}\pi r^3 \Delta G_V + 4\pi r^2 \gamma \tag{1.4}$$

The two terms on the right hand side of equation 1.4 depend differently on the cluster radius r and are also of opposite signs. Hence as r increases, ΔG goes through a maximum when critical size of the cluster r_c is reached as shown in Figure 1.3.

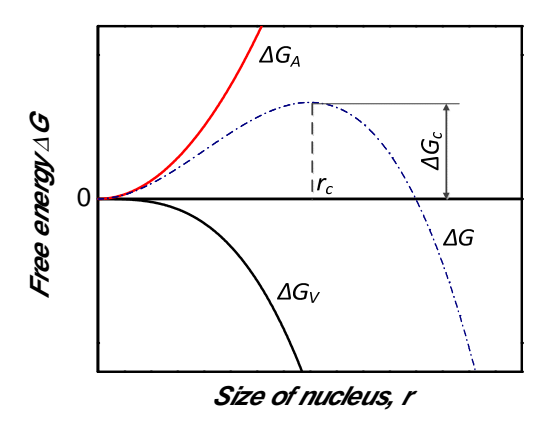


Figure 1.3: Free energy change during nucleation (Mullin 2001).²

From Figure 1.3, it is evident that the clusters with the size above the critical cluster size r_c would be stable. The critical cluster size is an inverse function of supersaturation: as the supersaturation increases, the critical cluster size decreases.

For nucleation to occur, energy equal to ΔG_c must be produced in the system.² The production of this energy can be understood by considering the energy of a fluid at constant temperature and pressure. The energy of a fluid is actually a mean of energies which fluctuate at different locations within the fluid. The fluctuations of energy manifests itself into fluctuations in molecular velocities and supersaturations.

Nucleation is favored at those locations within the fluid where the energy rises temporarily above ΔG_c .² The statistical distribution of energies within the fluid makes the nucleation process stochastic.

The requirement of the critical cluster size r_c and the energy equal to or greater than ΔG_c is usually not met immediately upon entering the supersaturated region. This leads to the existence of the metastable region next to the solubility curve.

The energy barrier for nucleation ΔG_c can be obtained by calculating the maximum of the function in equation 1.4. The rate at which the clusters cross the energy barrier ΔG_c per unit volume can be expressed in form of Arrhenius equation and gives the primary nucleation rate J^{12}

$$J = A \exp\left(\frac{-\Delta G_c}{kT}\right) \tag{1.5}$$

where A is the kinetic pre-exponential factor, k is the Boltzmann constant and T is the temperature.

1.1.3 Crystal growth

Nuclei are not detected as soon as they are formed but they have to grow into crystals of a detectable size. The theories which describe crystal growth can be broadly classified under three main categories viz. surface energy theory, diffusion theory and adsorption layer theory.

In 1878 Gibbs initiated the surface energy theory by postulating that the total surface energy of a crystal in equilibrium with its surrounding at constant temperature and pressure would be minimum for a given crystal volume.² Hence in a supersaturated solution the crystal growth would be such that the crystal develops into an "equilibrium shape" and the total surface energy of the crystal is minimized. The equilibrium shape of a crystal is related to the free energy of the faces and the crystal faces grow at rates proportional to their respective surface energies. Surface energy is inversely proportional to the lattice density of the plane indicating that the faces with high millers indices grow faster than those with lower millers indices.²

The diffusion theory of crystal growth considers the deposition of the solids on the crystal face as a diffusion process. According to the diffusion theory, the rate of crystal growth is proportional to the concentration difference between the solid surface and the bulk of the solution. It is assumed that a stagnant film exists of a liquid adjacent to

the growing crystal face through which the molecules of the solute have to diffuse.¹³ The diffusion theory was extended to diffusion-reaction theory by Berthoud¹⁴ and Valeton¹⁵ when it was found out that the solution in contact with the crystal surface is supersaturated and not saturated. Berthoud and Valeton suggested that the deposition of the mass on the crystal surface takes place in two steps. The first step is the diffusion of the solute molecules from the bulk solution to the crystal surface and it is followed by the second step where the solute molecules arrange themselves into a crystal lattice by a first order reaction. The two steps are schematically represented in Figure 1.4. It is assumed that there is no accumulation of solute at the interface.

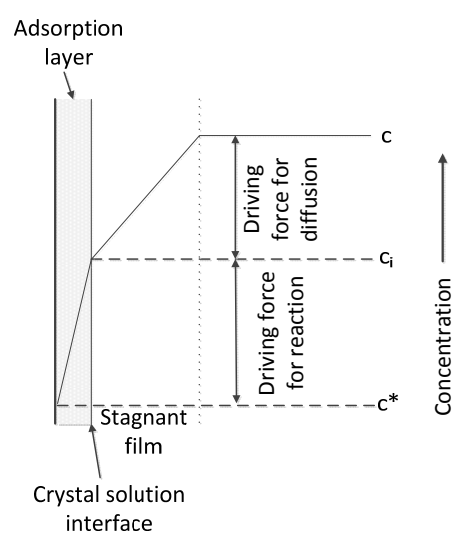


Figure 1.4: Schematics of the diffusion theory (Mullin 2001).² The schematics is for illustration purposes only. The concentration profile may not be linear within the adsorption layer and the driving forces for diffusion and reaction may not be of equal magnitudes.

The diffusion and reaction steps can be mathematically represented as

$$\frac{dm}{dt} = k_d A(c - c_i) \quad \text{(diffusion)} \tag{1.6}$$

$$\frac{dm}{dt} = k_r A (c_i - c^*)^r \text{ (reaction)}$$
 (1.7)

where m is the mass of solute deposited in time t, k_d is the co-efficient of mass transfer by diffusion, A is the surface area of the crystal, k_r is the rate constant for surface

reaction (integration step) and r is the order of reaction, c is the solute concentration in bulk (supersaturated), c^* is the equilibrium concentration, c_i is the solute concentration in solution at the crystal-solution interface. For sake of convenience the growth rate is obtained by eliminating the interfacial concentration and using the overall concentration difference as

$$\frac{dm}{dt} = k_G A (c - c^*)^g \tag{1.8}$$

where *k*^{*G*} and *g* are overall crystal growth co-efficient and the crystal growth exponent.

The adsorption layer theory is based on the assumption that the growth units of the crystallizing substance loose one degree of freedom when they arrive at the crystal face.² The units are not integrated immediately into the crystal lattice but are free to migrate over the crystal face or the terrace as shown in Figure 1.5 a. until they are integrated in the crystal lattice at positions which are most favored energetically i.e. where the attractive forces are the largest. These positions are called the kinks where the growth unit experiences attractive forces from three sides. A slightly less favorable position is called the step with attractive forces from two sides. Ideally the step-wise build-up will continue until the whole plane is completed as seen in Figure 1.5 b. There after a 2D nucleus or a center of crystallization must be formed on the surface (Figure 1.5 c) before the growth continues.

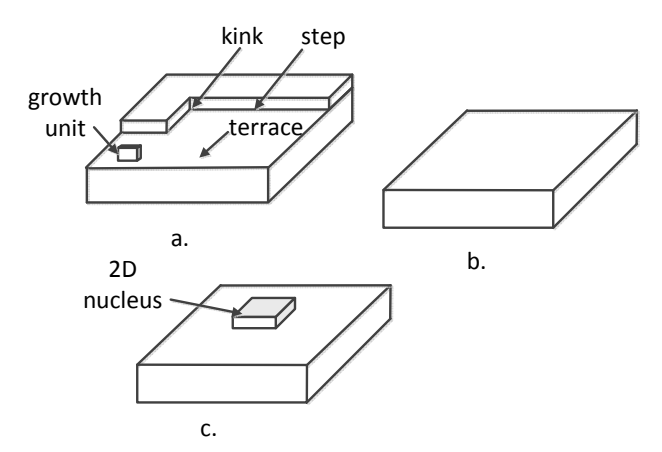


Figure 1.5: Schematic of adsorption layer theory without dislocation in crystal lattice (Mullin 2001). a.) different integration sites on the crystal face b.) completed face c.) 2D nucleus on a crystal surface.

1.1.4 Metastable zone width

As has been explained in section 1.1.2, nucleation does not start immediately upon entering the supersaturated region. In the supersaturated region, molecules have to come together to form clusters which must grow to a critical cluster size r_c to be stable nuclei. Such a zone within the supersaturated region where the molecular clusters try to transform into stable nuclei is called the metastable zone (MSZ). Once the stable nuclei are formed they grow into crystals of detectable size. To measure the metastable zone width (MSZW), solution is cooled usually at a constant speed. One side of the metastable zone is determined by the saturated temperature of the measured solution, the solubility curve, while the other is other is determined by the temperature at which crystals are first detected, the MSZ limit. The width of the metastable zone gives an indication of tendency of the crystallization system to nucleate. If the metastable zone width is large the crystallization system has less tendency to nucleate and vice-versa. Conventionally MSZW is treated as a reproducible quantity and hence it is represented as a curve next to the solubility curve as shown in Figure 1.6.

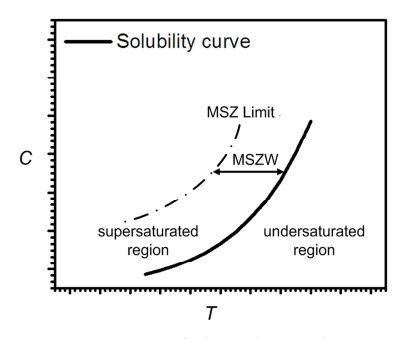


Figure 1.6: Conventional representation of the phase diagram

Apart from nucleation rates, MSZW is a complex and not fully understood function of growth rate, rate of supersaturation generation, mixing conditions, detection technique etc. For batch cooling crystallization, it is usually measured by cooling the undersaturated solution at a constant cooling rate until the crystals are detected.

Even if nucleation from clear solution is not possible within the MSZ during constant supersaturation increase, crystal growth is possible. Hence, the metastable zone is commonly used as the operating window during batch crystallization process. The seeding operation is performed within the MSZ wherein small amount of crystals with

pre-determined properties are inserted in an attempt to start the crystallization process reproducibly.^{1, 2} Seeding circumvents the possibility of nucleation from the clear solution and is expected to help in avoiding the associated irreproducibility in start of the batch. Care must be taken to avoid seeding too close to the MSZ limit or the solubility curve. Seeding close to the MSZ limit can promote undesirable crystallization phenomena like uncontrolled secondary nucleation and agglomeration while seeding close to the solubility curve can lead to low crystal growth rates and hence longer batch times.¹

1.2 State-of- the-art

The quality of the crystalline product, which is defined in terms of the Crystal Size Distribution (CSD), purity, kind of solid state etc., is related to its performance when used as an ingredient during subsequent processes. Also the quality of the product from batch crystallization process has a strong influence on the efficiency of downstream operations like filtration and drying. Hence achieving desirable crystalline product quality consistently is essential. Apart from the product efficacy and the process efficiency, there are regulatory considerations for pharmaceutical crystallization laid down by the Food and Drug Administration (FDA) which require predictive outcome of the crystallization process. To achieve it FDA has issued regulatory frameworks like the Process Analytical Technology (PAT) and the Quality by Design (QbD).¹⁶ PAT does not require following a fixed batch recipe but allows manipulation of the batch recipe based on the analytical tools to achieve a desired outcome. QbD is based on exploring the variable space to identify a set of variables which will allow achievement of desirable product quality consistently. There are three basic requirements that enable consistent product quality while adhering to the regulatory frameworks viz.

- 1. A proper understanding of the crystallization domain
- 2. Proper methods of characterizing the crystallization phenomena
- 3. Ability to monitor the process variables and hence the crystallization phenomena in situ.

A brief state-of-the-art in above three basic requirements is presented in sections 1.2.1 to 1.2.3.

1.2.1 Crystallization domain understanding

a. Nucleation

Nucleation results from aggregation of molecules in a supersaturated solution and is usually the first step in crystallization. Nucleation plays a very important role in determining final crystalline properties like the crystal structure and the size distribution. In spite of the strong impact of nucleation on subsequent processes and the final product quality, accurate description of the process is still missing. There are primarily two theories which are used to describe the nucleation process.

Classical Nucleation Theory(CNT):

CNT is used commonly to describe the nucleation process. The thermodynamic part of the CNT developed by Gibbs¹⁷ towards the end of 19th century is presented in section 1.1.2. Equation 1.5 represents the steady state nucleation rate based on the CNT. The pre-exponential factor of the CNT from equation 1.5 is postulated to be in between 10¹⁵ to 10²⁵ m⁻³s⁻¹ but is usually difficult to measure.⁴ Due to the high values of the pre-exponential factor, CNT usually over predicts the nucleation rates by several orders of magnitudes, sometimes by even 130 orders of magnitude compared to the experiments.¹⁸

One of the important features of the CNT is that the local density is the differentiating criteria between the two phases.¹⁹ This criteria is probably enough to differentiate phases when condensation of vapor to liquid droplet is considered but is insufficient when crystallization from solution is considered.²⁰ For crystals in solution, periodicity in structure could be another distinguishing criteria between two phases. Application of CNT to crystallization from solution would then mean that the density fluctuations and structural fluctuations occur simultaneously when crystals are formed.²¹ In other words, as soon as the molecules form clusters, they cluster gains the periodicity of the crystals.

Two-step nucleation:

According to the two-step nucleation model, the density fluctuations occur initially and are followed and superimposed by structural fluctuations.^{21, 22} For crystallization this means that a droplet of dense liquid is formed initially in the supersaturated solution which is followed by nucleation of a crystal showing periodicity within the droplet. Hence according to the two-step nucleation model, two energy barriers must

be crossed before nucleation occurs.²² Experimental data supporting the two-step nucleation model were obtained mainly for proteins, especially for lysozyme, by dynamic and static light scattering studies. These studies performed during lysozyme crystallization showed that monomers aggregate rapidly in diffusion limited aggregation regime to form clusters which progressively restructure into compact structures at the later stages of aggregation.²³ Although promising experimental results supporting the two-step nucleation model have been published for proteins, the applicability of the model to smaller organic molecules is still not established.

It is especially interesting to identify if the smaller organic molecules show small structured aggregates in the solution like dimers or chains before forming part of a nucleus. If small structured aggregates are present, then the nucleation for small molecules will not follow the two step nucleation model. This is because, unlike the two step nucleation model, structuring would already begin in the solution before the formation of a dense liquid phase.

b. Metastable Zone Width (MSZW)

The MSZW which is conventionally represented as in Figure 1.6, represents the operating window for the crystallization process.

The concept of the metastable zone was first put forward by Ostwald.²⁴ According to Ostwald, there exists a region in the concentration-temperature diagram where crystallization can only occur in presence of the crystalline material.²⁵ The metastable zone is bounded by the stable zone where the crystallization cannot occur even in presence of crystals and a labile zone where spontaneous nucleation can occur. Miers and Isaac²⁵ made the first attempt to measure the metastable zone width in 1907 with the help of refractive index measurements. They measured the MSZ limit for the binary mixture of selol and betol and coined a new term "supersolubility" for the MSZ limit. In their attempt they changed the definition of MSZ limit from the point at which spontaneous nucleation occurs to the point at which the crystallization is detected. In this thesis the term metastable zone limit will be used and it refers to the temperature at which the crystals are detected. One of the prominent studies in the second half of the twentieth century on MSZW measurements was done by Nyvlt.26 Nyvlt measured the MSZW of more than 25 substances at 250 mL when they were crystallized by cooling from their aqueous solutions. He also investigated the effect of cooling rate on the MSZW. During the analysis, Nyvlt considered MSZW to be a reproducible property for a give cooling rate, experimental set-up and the model system. MSZW increases with

increase in cooling rate. MSZW measurements have continued to intrigue researchers after Nyvlt and several attempts have been made to investigate the effect of various process parameters like solids contact, thermal history, detection technique etc. on the MSZW measurements.²⁷⁻²⁹ Interestingly, volume is not considered to be a parameter which would influence the MSZW. But when the energy barrier of Figure 1.3 is revisited a contradictory insight emerges. If MSZW measurement would be performed at increasingly higher volumes, the absolute number of the molecular clusters that would reach critical size would increase. This might also translate in some molecular cluster reaching the critical size at an earlier stage compared to molecular clusters in smaller volumes which would lead to a smaller MSZW at higher volumes. Surprisingly the effect of volume on MSZW is not investigated and the MSZW measured at lab scale is used to design crystallizers at industrial scale, to develop crystallization processes and to implement control strategies at industrial scale.

1.2.2 Methods for characterizing crystallization

a. Nucleation

Characterization of nucleation has always been a challenge for researchers primarily due to the fact that the nuclei cannot be detected in situ as soon as they reach the critical size. The nuclei have to grow into crystals of detectable sizes after which the characterization becomes possible.4 One of the first steps for characterization of nucleation were taken by Christiansen and Nielsen in 1951.30 They measured the induction times for barium sulfate precipitation in a glass "cross-mixer" which consisted of a mixing chamber, two inflow channels for two components and one outflow channel for the mixture. After mixing of the two components the induction time was noted. The induction time is the time required for detecting crystallization/precipitation after attainment of a desired supersaturation. They observed that the time required for precipitation to occur is inversely proportional to the initial concentration of barium sulfate at a constant temperature. Induction time measurements were later performed by other researchers by rapidly cooling undersaturated solutions at different temperatures to a desired supersaturation under stirred conditions and noting the time it takes for crystals to appear after attainment of the desired supersaturation.31,32

An interesting double pulse method to decouple nucleation from growth was put forward by Tammann³³ and later demonstrated by Galkin.³⁴ They reduced the

supersaturations even before the crystals were detected to a level where the nucleation rate was almost zero but the crystal growth was possible.

MSZW measurements can also be employed to determine the nucleation rates. Nyvlt²⁶ measured MSZW for 25 model systems and determined their nucleation rates. He assumed that for a certain period of time, the nucleation rate is equal to the rate of supersaturation generation (which is related to the MSZW) and the effect of growth on supersaturation depletion can be neglected. Due to the ease of measurements, MSZW have been commonly used to determine the nucleation kinetics.

b. Growth

Characterization of the crystal growth is done by measuring the growth rate of different faces of a single crystal, by following the weight increase by the crystals or the shift in the Crystal Size Distribution (CSD) or by measuring the supersaturation depletion.^{1, 35} Growth rate measurements of the different faces of a single crystal in a stagnant solution do not always provide quantitative data that could be used in the designing of the process but they do provide qualitative insights.³⁶ In certain cases, the growth kinetics obtained based on single crystal studies in stagnant solutions may even match the growth kinetics obtained in fluidized bed crystallizer under controlled conditions of solution velocity and supersaturation.^{37, 38} In fluidized bed crystallizer, the crystals with similar size are suspended in a flowing solution. The flow rate of the solution is adjusted such that the crystals are neither carried by the solution nor do they sink to the bottom of the crystallizer. By measuring the difference between the initial size and the final size of the crystals, the average crystal growth rate can be calculated. A Mixed Suspension Mixed Product Removal (MSMPR) configuration is also commonly used to obtain crystal growth kinetics by following the CSD with time and in combination with the population balance equations.³⁹ The methods described above to measure growth rate are time consuming and require significant number of data points to obtain growth kinetics. As an alternative the growth rate can be determined from the decrease in the solution concentration as a function of time in a seeded batch crystallizer.40,41

c. Metastable Zone Width (MSZW)

Polythermal method²⁶ is commonly used to characterize the MSZW in which a clear undersaturated solution is cooled under controlled conditions until crystals are detected at the MSZ limit. The slurry is then heated slowly until the crystals dissolve at the saturation temperature. The difference between the saturation temperature and the

MSZ limit is the metastable zone width.² The MSZW is a function of the detection technique used for detecting the crystals.⁴ A certain minimum volume fraction of the crystals must be present in order to be detected by most detection techniques.⁴ The commonly used techniques for MSZW measurement are visual observation, turbidity, light beam obscuration, calorimetry, ATR-FTIR spectroscopy, UV-vis spectroscopy, in situ imaging, Focused Beam Reflectance Measurements (FBRM) etc.^{29, 35, 42, 43} A detailed overview of different techniques used for measuring MSZW is available in the literature.⁴⁴

1.2.3 Monitoring crystallization process

The variables which are commonly monitored during a batch crystallization process are concentration of the solute in the solution and the CSD. Monitoring of the kind of solid state might also be important for model systems exhibiting polymorphic forms. The state-of-the-art in monitoring concentration and CSD is presented in following sections.

a. Concentration monitoring

Several techniques have been reported in the past to monitor the concentration and hence the supersaturation. They are based on measurement of a wide range of properties such as the refractive index,⁴⁵ the conductivity of the solution,⁴⁶ the density of the liquid phase,⁴⁷ the heat flux accompanying crystallization,⁴⁸ the absorbance of the electromagnetic light by the solution,⁴⁹⁻⁵¹ etc. A correlation is established between these properties and the concentration which could be in form of a simple univariate calibration or a more complex multivariate calibration.

Helt and Larson used the differential refractometer to monitor the supersaturation online during the crystallization of potassium nitrate.⁴⁵ The differential refractometer consisted of two cells one of which consisted a reference liquid and the other consisted of the circulated sample. The differences in the refractive indices of the sample and the reference liquid led to the deflection of light which was measured. Hlozn et. al. used the electrical conductivity of the ammonium aluminium sulphate aqueous solution to determine the concentration during the crystallization process.⁴⁶ To measure the conductivity they had to pump the sample through the conductometer and use a predetermined calibration curve to convert the conductivity reading to the concentration value. Gutwald and Mersmann used density meter combined with hydrocyclone to determine the supersaturation during the crystallization process.⁴⁷ The ability to monitor concentration during the process allowed them to compare the crystalline product quality obtained by the constant supersaturation method with the

constant cooling rate method. Fevotte and Klein used the heat released during crystallization to determine the concentration of the dissolved solute in a calorimeter.⁴⁸ They observed that the calorimetry gives better results when used offline.

The attenuated total reflectance (ATR) Fourier transform infrared (FTIR), the Fourier transform (FT) near infrared (NIR) and ultraviolet visible (UV-vis) are the most common techniques which are based on the absorbance of the electromagnetic light. Dunuwila and Berglund⁴⁹ demonstrated the use of the ATR-FTIR spectroscopy for online concentration measurements during the crystallization of maleic acid from water. Thereafter, this technique has been used by many researchers for concentration monitoring during crystallization.⁵²⁻⁵⁴ The use of NIR for in-line concentration measurement of a drug during crystallization has been reported by Zhou et al.⁵⁰ Howard et al.⁵¹ have reported the use of ATR UV-vis for concentration measurements during the polymorphic transformation of sodium benzoate from IPA/water mixture, while the details of the calibration process for ATR UV-vis were reported by Abu Bakar et al.⁵⁵

b. CSD monitoring

CSD can be monitored either offline, online or in-situ. Offline monitoring of the size distribution relies heavily on good sampling which is difficult to achieve. Also, the sample might change while being transferred to the offline instrument making it difficult to capture the dynamics of the process accurately.⁵⁶ Several methods are available now days which make it possible to monitor the CSD online or in situ. One of the most common online techniques used is the laser diffraction which is based on forward light scattering. In this technique, the particles are illuminated by a beam of visible light which results into a diffraction pattern. This diffraction pattern is inverted to reconstruct the size distribution by using certain mathematical techniques.⁵⁷ In-situ CSD can be obtained by using techniques based on ultrasound extinction and laser back diffraction. The technique based on ultrasound extinction is based on the measurement of the attenuation of the ultrasound while passing through the slurry. One of the main advantages of this technique is that it can work with slurry concentrations of almost 40 vol. %.58 The focused beam reflectance measurements (FBRM) measures the back diffraction properties of the suspension taking solvent and solute properties like the refractive index and the morphology into account. The technique measures chord length distribution from which the particle size distribution is generated with the help of first principle models.⁵⁹ Coulter counter which was primarily developed for sizing blood cells and cell culture can also be used for measuring particle size distributions. In

order to do so particles are suspended in a weak electrolyte and are passed through an orifice which separates two electrodes.⁶⁰ When a particle passes through the orifice, it displaces volume of electrolyte equal to its own volume which causes an increase in the electrical impedance. The change in the electrical impedance generates voltage pulses proportional to the volume of the particle which can be used for determining volume diameter of particle. In situ imaging can also be used for measuring CSD. Imaging is free from the assumptions about the shape of the crystals which is made in many techniques. Imaging allows determination of size and shape in a single measurement. As the measurement of size is based on direct observation and as no calibration is involved, interpretation of the data becomes easy.⁶¹

1.3 Challenges in understanding, characterizing and monitoring of batch crystallization processes

In spite of the progress in understanding, characterizing and monitoring of the batch crystallization processes over the last century, several challenges still remain which hinder the rapid design, process development, process scale-up, and the development of effective control strategies. Interestingly, the number of challenges encountered from the designing of a crystallizer to the development of control strategies are the same. These challenges are highlighted in the sections 1.3.1 to 1.3.3.

1.3.1 Crystallization domain understanding

- CNT predicts nucleation rates which could be several orders of magnitude larger than the experimentally measured nucleation rates. This indicates that the description of the nucleation process provided by the CNT is inadequate. The two step nucleation theory seems to describe crystallization of few model systems, especially proteins, sufficiently but its applicability to crystallization of small organics is debatable as the dense liquid phase has not been observed yet and the structuring of the small organic molecules in solution before formation of nucleus has not been ruled out.
- Primary nucleation is a stochastic process. This means that the time required for each molecular cluster in a supersaturated solution to reach critical size would be different. As a result of this stochastic nature of nucleation, the MSZW would also be a stochastic property and not deterministic as it is conventionally treated. Hence it is necessary to address the gap in understanding of the MSZW and sequence of events which leads to detection of crystals at the MSZ limit.

• It is a common practice to determine the crystallization process operating window at a small volume in the lab scale and use it for designing a process at industrial scale.³⁵ This method of designing the crystallization process is based on the assumption that the volume has no effect on the operating window or the MSZW. The lack of MSZW data at different volumes in literature means that this assumption is unverified. Hence designing, operating and controlling crystallization based on this unverified assumption may lead to batch-to-batch variations resulting from unexpected nucleation events within the MSZW.

1.3.2 Crystallization process characterization

- The use of MSZW in the current manner in which nucleation and growth are coupled leads to the overestimation of number of primary nuclei and also the primary nucleation rates. Characterization of nucleation rates by induction time measurements which requires attaining desired supersaturation very rapidly is feasible only at small volumes. The use of double pulse method for characterizing nucleation works well for slow growing systems like protein crystals but it is difficult to apply for systems which display a fast growth rate. Hence it is essential to find a way of characterizing crystal nucleation which would decouple crystal nucleation and growth, can be used at different volumes and also be applicable to a wide variety of model systems displaying both slow and fast growth rates.
- Polythermal method is commonly used to measure MSZW during batch crystallization processes.²⁶ MSZW is a complex and not fully understood function of cooling, nucleation and growth rates, of process conditions, such as the stirring speed and the used detection technique.⁴ In spite of the difficulties associated in the interpretations of the MSZW measurements, they are often used in characterizing the operating window and for determining the seeding point. The MSZW is also considered constant at different volume which has led to characterization models which are independent of volume.²⁶
- Crystal growth is characterized by using either direct methods of looking at CSD or indirect methods which look at change in certain property of the solution as the crystals grow. The direct methods usually require assumption about particle shape which may not be the actual shape of the crystals, or may require physical properties which are not easily available. In situ imaging does not require any assumption of the particle shape but is limited in the concentration of the solid particles which can be observed. The indirect

methods of following certain properties of the liquid phase may display a lag as the properties may not change until substantial growth has occurred.

1.3.3 Crystallization process monitoring

- Measurement of concentration with differential refractometer requires strict regulation of the conditions in the experimental setup. This might become very tedious when done in the presence of crystals.⁴⁵ The measurement of the conductivity as a means to determine the concentration is restricted to conducting solvents.46 The measurement of the density offers a reasonably good means on the lab scale when pure solutions are employed and the conditions are controlled. Its application on industrial scale is still not widely accepted as it is sensitive to unknown impurities and the temperature changes. Also it needs crystal free liquid for measurements, making the setup complicated with a solid-liquid separation unit.⁴⁷ The heat generation accompanying crystallization could be used to determine the crystallization rate and hence indirectly to determine concentration, but the results are reliable and accurate only when done offline. This could be because of the low enthalpy of crystallization for most crystallizing systems.⁴⁸ The measurement of the absorbance of the electromagnetic radiations could be used in-situ for concentration monitoring during crystallization. But it is not known if the performance of the spectroscopy based techniques is dependent on the crystallizing systems. Also the monitoring of concentration during crystallization with the spectroscopy based techniques is limited to the lab scale and technical issues that will arise while using these techniques at industrial scale are not know.
- With the exception of microscopy, the particle size cannot be measured directly. The CSD obtained from an instrument depends on the physical response of the analytical instrument with respect to the physical characteristic of the particles like their sizes and shapes. Most of the analytical instruments assume that the particles are spherical in shape. But even for spherical particles there are discrepancies in the size data obtained which result from the different equivalent diameters measured, and these discrepancies are typically within 10% in terms of median diameter by volume.⁵⁷ The use of microscopy for measuring particles sizes in-situ is a promising alternative but the quality of images obtained in practical situations is limited.⁶¹ The other challenges that in-

situ imaging faces are that the imaging sensors can handle low solid concentrations and the image analysis algorithms are not robust.

1.4 Problem statement

This thesis aims at addressing the challenges mentioned in section 1.3 in a manner which would be beneficial for designing crystallizers, developing crystallization processes, scaling them up and developing control strategies at industrial scale. The primary research objective of this thesis is as follows

To develop domain knowledge and tools for rapid monitoring and characterization of crystal nucleation and growth in order to facilitate rapid strategies for process and equipment design, process development, and process control during industrial batch crystallization processes.

To achieve the primary research objective, the following sub-goals must be realized

1.4.1 Developing crystallization domain knowledge

- a. Investigating whether there is a discrepancy between the measured nucleation rates and those predicted by the classical nucleation theory.
- b. Identifying the sequence of events between the birth of the primary nuclei and the detection of crystals at the MSZ limit. Investigating whether the stochastic nature of nucleation actually leads to stochastic MSZWs or the conventional understanding of deterministic MSZW holds.
- c. Identifying if MSZW is dependent on volume.

1.4.2 Crystallization process characterization

- a. Developing methods which would enable rapid characterization of nucleation and growth.
- b. Developing methods which would allow for quick estimation of the operating region during batch crystallization and its dependency on the scale of operation.

1.4.3 Crystallization process monitoring

a. Investigating which spectroscopic techniques are most suitable for the in situ monitoring of the solute concentration during batch crystallization processes.

b. Investigating the feasibility of laboratory calibration methods for concentration sensors at industrial scale.

1.4.4 Crystallization process development

a. Demonstrating a rapid crystallization process development strategy from lab scale to industrial scale by combining process monitoring and characterization.

1.5 Thesis outline

The thesis consists of five technical chapters which contribute towards either crystallization domain knowledge, process characterization, process monitoring or combination of them as shown in the Figure 1.7.

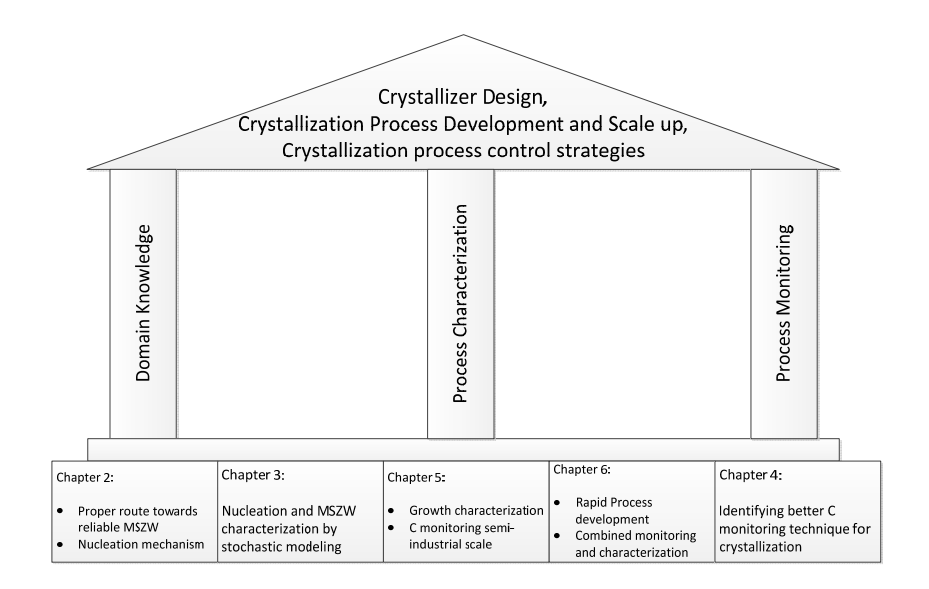


Figure 1.7 : Schematics of the thesis setup.

The detail contents of the technical chapters are as follows,

In chapter 2 a proper route towards reliable MSZW data is presented. A common assumption that the MSZW is constant at different volumes was tested by performing MSZW measurements at 1 mL and 1 L scales for paracetamol-water model system. Based on the MSZW measurements a scale up rule for MSZWs is formulated from 1 mL to 1 L scale. In addition a new nucleation mechanism which can explain the MSZW at

different volumes was postulated. Validation of the new nucleation mechanism is described with in situ imaging. The scientific and industrial implications of the new nucleation mechanism are also discussed.

In chapter 3 a stochastic model based on the Poisson's law is presented which can be used to obtain nucleation kinetics based on the MSZW measurements. The capabilities of the stochastic model to describe the effect of volume on MSZW are presented and compared with deterministic population balance model and the experimental measurements at different volumes. The stochastic model predicts a transition volume above which the MSZW changes from stochastic to practically deterministic. Experiments are used to verify if such a transition volume exists and the implications of the volume effect on MSZW for determining process operating window are discussed.

In chapter 4 a comparison between ATR-FTIR and FT-NIR spectroscopy is presented which was done with the motivation of identifying a concentration monitoring technique which works best for the crystallization process. The comparison between ATR-FTIR and FT-NIR spectroscopy is described for four different model systems in the presence and the absence of crystals. The comparison is also intended to answer if different techniques for concentration monitoring have same accuracy for a given model system and if the accuracy of both techniques stays same for all model systems.

In chapter 5 the pitfalls associated with the use of calibration model developed for ATR-FTIR spectroscopy at lab scale on industrial scale are described. A rapid method of calibration at semi-industrial scale is proposed and is demonstrated during ammonium sulfate batch crystallization. Parameter estimates for the population balance obtained with use of both concentration measurements and CSD measurements are compared with the parameter estimates obtained based on just the CSD measurements in order to investigate which method of parameter estimation is better.

In chapter 6 a rapid strategy for crystallization process development based on the unique skid based configuration of the PAT tools is presented. Combined calibration of the PAT tools and process characterization is demonstrated which can be done rapidly and is free from assumption that the solubility curve and the MSZW stays same at industrial scale. Use of in situ imaging is shown to give new process insights especially in the nucleation mechanism.

1.6 Project Organization

The work reported in this thesis is performed as a part of the project "Intelligent Observer and Controller for Pharmaceutical Batch Crystallization" and is financially supported by the Institute for Sustainable Process Technology (ISPT). ISPT is a cooperation between industry, universities and knowledge institutes which aims at speeding up innovation processes and make them more efficient than they are at present. The ISPT strives to improve the competitive position of the Dutch Process Industry.

The overall objective of the project is the development and the demonstration of the technical feasibility of a protocol and the necessary tools for the rapid and systematic identification of the optimal control strategy for batch cooling crystallization in a pharmaceutical plant. The major activities that will enable meeting of the objectives are

- 1. Introduction of measurement tools for crystallization in a pharmaceutical plant
- 2. Automated evaluation of the crystallization process
- 3. Controlling the process

Several industrial and academic partners have collaborated to achieve the overall objective. The partners include Albemarle Catalysts Company BV, DSM, FrieslandCampina, Merck Sharp and Dohme, Technical University of Delft-Process and Energy department, Technical University of Delft - Delft Centre for Systems and Control, and Technical University of Eindhoven - Control Systems group.

The work reported in this thesis is the contribution of the Technical University of Delft – Process and Energy department.

1.7 References

- (1) Myerson, A. S., *Handbook of Industrial Crystallization*. 2nd ed.; Butterworth-Heinemann: Woburn, MA, 2002.
- (2) Mullin, J. W., Crystallization. Fourth ed.; Butterworth-Heinemann: Oxford, 2001.
- (3) Christofides, P. D.; El-Farra, N.; Li, M.; Mhaskar, P., Model-based control of particulate processes. *Chemical Engineering Science* **2008**, 63, (5), 1156-1172.
- (4) Kashchiev, D.; van Rosmalen, G. M., Review: Nucleation in solutions revisited. *Crystal Research and Technology* **2003**, 38, (7-8), 555-574.

(5) Nyvlt, J., Nucleation and Growth Rate in Mass Crystallization. *Prog. Crystal Growth and Charact.* **1984**, 9, 335-370.

- (6) Ting, H. H.; McCabe, W. L., Supersaturation and Crystal Formation in Seeded Solutions. *Industrial & Engineering Chemistry* **1934**, 26, (11), 1201-1207.
- (7) van der Heijden, A. E. D. M.; van der Eerden, J. P.; van Rosmalen, G. M., The secondary nucleation rate: a physical model. *Chemical Engineering Science* **1994**, 49, (18), 3103-3113.
- (8) Sung, C. Y.; Estrin, J.; Youngquist, G. R., Secondary nucleation of magnesium sulfate by fluid shear. *AIChE Journal* **1973**, 19, (5), 957-962.
- (9) Wissing, R.; Elwenspoek, M.; Degens, B., In situ observation of secondary nucleation. *Journal of Crystal Growth* **1986**, 79, (1-3, Part 2), 614-619.
- (10) Kashchiev, D., *Nucleation: Basic Theory with Application*. ed.; Butterworth-Heinemann: Oxford, 2000.
- (11) Vekilov, P. G., Nucleation. *Crystal Growth & Design* **2010**, 10, (12), 5007-5019.
- (12) Volmer, M., Kinetic der Phasenbildung. ed.; Steinkpoff: Leipzig, 1939.
- (13) Nernst, W., Die Therorie Der Reaktionsgescwindigkeit in heterogenen Systemen. Z. Physik. Chem. **1904**, 47, 52-55.
- (14) Berthoud, A., The theorie de la formation des faces d'un cristal. *J. Chem. Phys.* **1912**, 10, 624-635.
- (15) Valeton, J. J. P., Wachstum und Aufloesung der Kristalle. Zeitschrift feur Kristallographie **1924**, 59, 483.
- (16) Gad, S. C., *Pharmaceutical manufacturing handbook: Regulations and quality*. John Wiley and Sons: New Jersey, 2008.
- (17) Gibbs, J. W., On the equilibrium of heterogeneous substances. *Trans. Connect. Acad. Sci.* **1876**, 3, 108-248.
- (18) Fokin, V. M.; Zanotto, E. D., Crystal nucleation in silicate glasses: the temperature and size dependence of crystal/liquid surface energy. *Journal of Non-Crystalline Solids* **2000**, 265, (1–2), 105-112.
- (19) Oxtoby, D. W., Crystal nucleation in simple and complex fluids. *Philosophical Transactions of the Royal Society of London. Series A:*
 - Mathematical, Physical and Engineering Sciences 2003, 361, (1804), 419-428.
- (20) Vekilov, P. G., Dense Liquid Precursor for the Nucleation of Ordered Solid Phases from Solution. *Crystal Growth & Design* **2004**, 4, (4), 671-685.
- (21) Talanquer, V.; Oxtoby, D. W., Crystal nucleation in the presence of a metastable critical point. *The Journal of Chemical Physics* **1998**, 109, (1), 223-227.
- (22) Wolde, P. R. t.; Frenkel, D., Enhancement of Protein Crystal Nucleation by Critical Density Fluctuations. *Science* **1997**, 277, (5334), 1975-1978.

(23) Georgalis, Y. U., P.; Raptis, J.; Saenger, W., Lysozyme Aggregation Studied by Light Scattering. I. Influence of Concentration and Nature of Electrolytes *Acta. Crystallogr.*, Sect D: Biol. Crystallogr. **1997**, 53, 691-702.

- (24) Ostwald, W., Z. Physik. Chem. 1897, 22, 302.
- (25) Miers, H. A.; Isaac, F., The Spontaneous Crystallisation of Binary Mixtures. Experiments on Salol and Betol. *Proceedings of the Royal Society of London. Series A* **1907**, 79, (531), 322-351.
- (26) Nývlt, J., Kinetics of nucleation in solutions. *Journal of Crystal Growth* **1968**, 3-4, (0), 377-383.
- (27) Mullin, J. W.; Gaska, C., The growth and dissolution of potassium sulphate crystals in a fluidized bed crystallizer. *The Canadian Journal of Chemical Engineering* **1969**, 47, (5), 483-489.
- (28) Söhnel, O.; Nýavlt, J., Induction time in batch crystallisation. *Kristall und Technik* **1976**, 11, (3), 239-244.
- (29) Nagy, Z. K.; Fujiwara, M.; Woo, X. Y.; Braatz, R. D., Determination of the Kinetic Parameters for the Crystallization of Paracetamol from Water Using Metastable Zone Width Experiments. *Industrial & Engineering Chemistry Research* **2008**, 47, (4), 1245-1252.
- (30) Christiansen, J. A., Nielsen, A. E., On the Kinetics of Formation of Precipitates of Sparingly Soluble Salts. *Acta. Chem. Scand.* **1951**, 05, 673-674.
- (31) Schöll, J.; Vicum, L.; Müller, M.; Mazzotti, M., Precipitation of L-Glutamic Acid: Determination of Nucleation Kinetics. *Chemical Engineering & Technology* **2006**, 29, (2), 257-264.
- (32) Qu, H.; Louhi-Kultanen, M.; Kallas, J., In-line image analysis on the effects of additives in batch cooling crystallization. *Journal of Crystal Growth* **2006**, 289, (1), 286-294.
- (33) Tammann, G., Die Aggregatzustaende. 2nd ed.; Voss: Leipsig, 1922.
- (34) Galkin, O.; Vekilov, P. G., Direct Determination of the Nucleation Rates of Protein Crystals. *The Journal of Physical Chemistry B* **1999**, 103, (49), 10965-10971.
- (35) Tavare, N. S., Batch Crystallizers: A Review. *Chem. Engg. Comm.* **1987**, 61, (1:6), 259-318.
- (36) Omar, W.; Al-Sayed, S.; Sultan, A.; Ulrich, J., Growth rate of single acetaminophen crystals in supersaturated aqueous solution under different operating conditions. *Crystal Research and Technology* **2008**, 43, (1), 22-27.
- (37) Mullin, J. W., Garside, J., Trans. I. Chem. E. 1967, 45, 285-291.
- (38) Mullin, J. W., Garside, J., Trans. I. Chem. E. 1968, 46.

(39) Randolph, A. D., Larson, M. A., *Theory of Particulate Processes*. 2nd ed.; Academic Press: San Diego, 1988.

- (40) Tavare, N. S., Garside, J., Chem. Eng. Res. Des. 1986, 64, 109-118.
- (41) Glade, H.; Ilyaskarov, A. M.; Ulrich, J., Determination of Crystal Growth Kinetics Using Ultrasonic Technique. *Chemical Engineering & Technology* **2004**, 27, (7), 736-740.
- (42) Liang, K.; White, G.; Wilkinson, D.; Ford, L. J.; Roberts, K. J.; Wood, W. M. L., Examination of the Process Scale Dependence of l-Glutamic Acid Batch Crystallized from Supersaturated Aqueous Solutions in Relation to Reactor Hydrodynamics. *Industrial & Engineering Chemistry Research* **2004**, 43, (5), 1227-1234.
- (43) Titiz-Sargut, S.; Ulrich, J., Application of a protected ultrasound sensor for the determination of the width of the metastable zone. *Chemical Engineering and Processing: Process Intensification* **2003**, 42, (11), 841-846.
- (44) Noriaki, K., A new interpretation of metastable zone widths measured for unseeded solutions. *Journal of Crystal Growth* **2008**, 310, (3), 629-634.
- (45) Helt, J. E.; Larson, M. A., Effects of temperature on the crystallization of potassium nitrate by direct measurement of supersaturation. *AIChE Journal* **1977**, 23, (6), 822-830.
- (46) Hlozn; yacute; Ladislav; Sato, A.; Kubota, N., On-Line Measurement of Supersaturation during Batch Cooling Crystallization of Ammonium Alum. *JOURNAL OF CHEMICAL ENGINEERING OF JAPAN* **1992**, 25, (5), 604-606.
- (47) Gutwald, T.; Mersmann, A., Batch cooling crystallization at constant supersaturation: Technique and experimental results. *Chemical Engineering & Technology* **1990**, 13, (1), 229-237.
- (48) Fevotte, G.; Klein, J. P., A new policy for the estimation of the course of supersaturation in batch crystallization. *The Canadian Journal of Chemical Engineering* **1996**, 74, (3), 372-384.
- (49) Dunuwila, D. D.; Berglund, K. A., ATR FTIR spectroscopy for in situ measurement of supersaturation. *Journal of Crystal Growth* **1997**, 179, (1-2), 185-193.
- (50) Zhou, G. X.; Crocker, L.; Xu, J.; Tabora, J.; Ge, Z., In-line measurement of a drug substance via near infrared spectroscopy to ensure a robust crystallization process. *Journal of Pharmaceutical Sciences* **2006**, 95, (11), 2337-2347.
- (51) Howard, K. S.; Nagy, Z. K.; Saha, B.; Robertson, A. L.; Steele, G.; Martin, D., A Process Analytical Technology Based Investigation of the Polymorphic Transformations during the Antisolvent Crystallization of Sodium Benzoate from IPA/Water Mixture. *Crystal Growth & Design* **2009**, *9*, (9), 3964-3975.

(52) Togkalidou, T.; Fujiwara, M.; Patel, S.; Braatz, R. D., Solute concentration prediction using chemometrics and ATR-FTIR spectroscopy. *Journal of Crystal Growth* **2001**, 231, (4), 534-543.

- (53) Borissova, A.; Khan, S.; Mahmud, T.; Roberts, K. J.; Andrews, J.; Dallin, P.; Chen, Z.-P.; Morris, J., In Situ Measurement of Solution Concentration during the Batch Cooling Crystallization of l-Glutamic Acid using ATR-FTIR Spectroscopy Coupled with Chemometrics. *Crystal Growth & Design* **2008**, *9*, (2), 692-706.
- (54) O'Sullivan, B.; Glennon, B., Application of in Situ FBRM and ATR-FTIR to the Monitoring of the Polymorphic Transformation of d-Mannitol. *Organic Process Research & Development* **2005**, 9, (6), 884-889.
- (55) Bakar, M. R. A.; Nagy, Z. K.; Rielly, C. D., Seeded Batch Cooling Crystallization with Temperature Cycling for the Control of Size Uniformity and Polymorphic Purity of Sulfathiazole Crystals. *Organic Process Research & Development* **2009**, 13, (6), 1343-1356.
- (56) Yu, Z. Q.; Chew, J. W.; Chow, P. S.; Tan, R. B. H., Recent Advances in Crystallization control: An Industrial Perspective. *Chemical Engineering Research and Design* **2007**, 85, (7), 893-905.
- (57) Kaye, B. H.; Alliet, D.; Switzer, L.; TurbittDaoust, C., The effect of shape on intermethod correlation of techniques for characterizing the size distribution of powder
- .1. Correlating the size distribution measured by sieving, image analysis, and diffractometer methods. *Particle & Particle Systems Characterization* **1997**, 14, (5), 219-224.
- (58) Neumann, A. M.; Kramer, H. J. M., A Comparative Study of Various Size Distribution. *Particle & Particle Systems Characterization* **2002**, 19, (1), 17-27.
- (59) Barthe, S.; Rousseau, R. W., Utilization of Focused Beam Reflectance Measurement in the Control of Crystal Size Distribution in a Batch Cooled Crystallizer. *Chemical Engineering & Technology* **2006**, 29, (2), 206-211.
- (60) Kersting, K., Specific problems using electronic particle counters. *Aquatic Ecology* **1985**, 19, (1), 5-12.
- (61) Larsen, P. A.; Rawlings, J. B.; Ferrier, N. J., Model-based object recognition to measure crystal size and shape distributions from in situ video images. *Chemical Engineering Science* **2007**, 62, (5), 1430-1441.
- (62) Shekunov, B.; Chattopadhyay, P.; Tong, H.; Chow, A., Particle Size Analysis in Pharmaceutics: Principles, Methods and Applications. *Pharmaceutical Research* **2007**, 24, (2), 203-227.

Chapter 2

A New View on Crystal Nucleation

This chapter is published as:

Kadam S. S., Kramer H. J. M., ter Horst, J. H. "Combination of a Single Primary Nucleation event and Secondary Nucleation in Crystallization Processes." Cryst. Growth. Des., **2011**, 11(4), 1271-1277.

The quality of a crystalline product is defined by its crystal size distribution, purity, morphology and kind of solid state. It is highly influenced by the nucleation behavior during the crystallization process. A convenient and often used experimental method for determining nucleation behavior is by measuring MetaStable Zone Widths (MSZW) in relatively small volumes. However, to what extent these can be related to nucleation behavior on larger (industrial) scales is not known. Two major reasons for this are the lack of experimental data for MSZW measurements on different scales and the incomplete understanding of the complexity of processes determining the MSZW. In order to investigate the relationship between nucleation behaviour for paracetamol in water at 1 mL and 1 L scale, MSZW measurements were performed. Well controlled MSZW measurements at 1 mL displayed large variations. This implies that at this scale a large number of experiments have to be performed to achieve a statistically sound experimental description of the MSZW. In contrast to the 1 mL experiments, the MSZW measurements performed at 1 L scale showed hardly any variations. The measured MSZW values at the 1 L scale corresponded to the onset of the MSZW distribution at the 1 mL scale, implying a simple scale up rule for laboratory MSZW data to larger scales. Careful in situ observation during several cooling crystallization experiments of paracetamol in water on a 3 mL scale showed the presence of a single crystal preceding the outburst of nuclei. This would imply that initially a single nucleus forms which, after growth to a considerable size, undergoes secondary nucleation. An abundance of fragments originate from this single crystal after secondary nucleation. This observation implies that the crystals produced in an industrial crystallizer originate all from one single crystal and are formed by secondary nucleation. Visualization experiments with other model systems showed that the mechanism is not limited to paracetamol but seems to occur more generally.

2.1 Introduction

The crystal product quality (crystal size distribution, kind of solid state, purity, morphology) in pharmaceuticals, agrochemicals, specialty and fine chemicals is highly influenced by the conditions prevailing during the crystallization process. These industrial crystallization processes generally are performed on a scale exceeding multiple cubic meters. Of the several phenomena occurring during crystallization, nucleation defines the initial population of crystals, determines the initial state of successive processes like crystal growth and hence, largely determines the product quality. For instance, nucleation of a large number of crystals at the start of a batch cooling crystallization would lead to a relatively small final crystal mean size. One strategy towards an improved control over the product quality is to control the nucleation behavior in industrial crystallization processes.

An often used and relatively fast experimental method for determining the nucleation behavior is by measuring Metastable Zone Widths (MSZW).²⁻⁵ During a MSZW measurement a solution is cooled, usually with a constant rate. One side of the metastable zone is determined by the saturation temperature of the measured solution, the solubility curve; while the other side is determined by the temperature at which the crystals are first detected, the MSZ limit. The MSZW then is determined by the difference between saturation temperature and MSZ limit.⁶ In principle, nucleation takes place before detection as the nuclei are small and have to grow to be detected. The detection largely depends on the resolution of the detection technique.⁷⁻¹⁰ A large MSZW is associated with a large supersaturation needed to nucleate the crystal product. With knowledge about the MSZW the occurrence of primary nucleation during industrial crystallization can be circumvented by e.g., adding seed crystals when the solution is positioned within the metastable zone.⁶ Seeding of crystals of one of the enantiomers within the MSZ of both is commonly employed during preferential crystallization of that enantiomer from its racemic solution.¹¹

The MSZW is not a fixed thermodynamic property. In fact it is a complex and not fully understood function of the cooling, nucleation and growth rates, of the process conditions such as the stirring speed and of the used detection technique.⁷ The lack of MSZW data on different scales indicates that there is no validated and robust rule for scaling up MSZW data obtained in the laboratory to industrial scale. Hence, from an industrial point of view it is important to find scale up rules for the MSZW while from

a scientific point of view an experimental study in the MSZW might reveal relevant nucleation mechanisms. This study investigates 1. a proper route towards reliable MSZW data 2. the relationship between the MSZW at different scales and 3. the underlying nucleation mechanism.

2.2 Experimental

Paracetamol (99.9% pure, Sigma Aldrich) in demineralized water was used as a crystallizing system for MSZW measurements at 1 mL and 1 L scale. Paracetamol in demineralized water, isonicotinamide (99.9% pure, Sigma) in 1 butanol (reagent grade, Sigma Aldrich), isonicotinamide in absolute ethanol (99.8%, Sigma Aldrich) and succinic acid (>99%, Merck) in demineralized water were used as the model crystallizing systems to perform the cooling experiments at 3 mL.

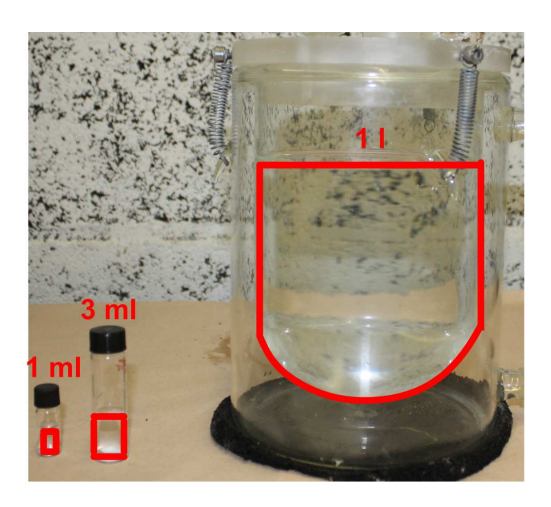


Figure 2.1: The three different volumes at which the experiments were performed. 1 mL vial, 3 mL vial and a 1 L crystallizer.

2.2.1 Solubility measurements

The paracetamol solubility measurements in water were performed using a multiple reactor setup (Crystal16, Avantium Technologies). The setup consists of 16 magnetically stirred 1 mL vials in which transmission of light through the solution was recorded. Slurries with the concentrations of 0.015 g/mL, 0.022 g/mL, 0.032 g/mL and 0.047 g/mL were prepared in the vials and were stirred at 700 rpm. The heating and

cooling rates employed were 0.3 °C/minute and 0.5 °C/minute respectively. Upon heating a vial in the setup, the transmission of the light through the solution became 100% at a certain temperature. That temperature was taken as the saturation temperature of that sample. The heating and cooling cycles were repeated at least 8 times per concentration to have a better estimate of the solubility.

2.2.2 MSZW measurements

MSZW measurements of paracetamol in water were performed on a 1 L scale using a jacketed glass crystallizer connected to a RK8KP Lauda thermostatic bath. The solution was stirred at 700 rpm using an IKA RET basic C stirring hotplate. The presence of crystals was detected by an in-situ camera (1μ m/pixel, Perdix analytical systems). The MSZW measurements of paracetamol in water on a 1 mL scale were performed using a multiple reactor setup (Crystal16, Avantium Technologies). The solution was stirred at 700 rpm with a magnetic stirrer. The presence of crystals was detected by the decrease in transmission of light through the vial.

About 50 mL of undersaturated solutions with paracetamol concentrations of 0.015 g/mL, 0.022 g/mL, 0.032 g/mL and 0.047 g/mL were prepared at 35, 45, 55 and 65 °C respectively in order to fill 16 vials of 1 mL with the same solution at a time. This was done to avoid concentration fluctuations between the vials. These solutions were cooled at a rate of 0.5 °C/minute. The temperature at which crystals were detected was taken as the metastable zone limit. The solutions were then heated at 5 °C/minute and held at a temperature approximately 5 °C above their saturation temperatures for an hour to allow complete crystal dissolution. The heating and cooling cycles were repeated approximately 10 times per sample at 1 mL scale. Because of a small constant temperature difference between actual temperature in the vial and the set temperature of the vial, a recalibration of Crystal16 set temperature was performed. In this way, the difference between actual and set temperature was kept within 0.1 °C. At a 1 L scale four identical experiments were carried out for each concentration with the same heating and cooling rates employed at 1 mL scale. Experiments on a 1 L scale were reproducible within half a degree and hence only four experiments per concentration were carried out. After the experiments, XRPD patterns were collected to make sure that the same polymorph was crystallized.

2.2.3 Cooling crystallizations on a 3 mL scale

Experiments at 3 mL were carried out in another multiple reactor setup (Crystalline, Avantium Technologies). The setup consists of 8 glass reactors which can be stirred by both magnetic and overhead stirrers. Experiments in four of the reactors could be followed with the help of the particle visualization module (Avantium Technologies) consisting of in-situ cameras with resolution of 5-11 µm/pixel and depth of field of 2.5 mm. 16 batch cooling crystallization experiments were performed for paracetamol in water (0.022 g/mL) to visualize crystallization at an early stage and validate the proposed nucleation mechanism. The cooling rate employed was 0.5 °C/minute. The experiments were performed by using either a magnetic or an overhead stirrer. Similar experiments were performed with the use of overhead stirrers for the crystallizing system of isonicotinamide in ethanol (0.120 g/mL), isonicotinamide in 1-butanol (0.071 g/mL) and succinic acid (0.082 g/mL) in water.

2.2.4 Unstirred cooling experiments on a 1 mL scale

Unstirred cooling experiments were performed at 1 mL scale with paracetamol concentration of 0.015 g/mL to verify if a single crystal is obtained in unstirred conditions. Initially an undersaturated solution was prepared in deionized water at 30 °C . The solution was filtered and introduced into a clean vial consisting of a magnetic stirrer. The solution in the vial was maintained at 30 °C while stirring for an hour to make sure that paracetamol was completely dissolved. The stirring was then turned off and the solution was allowed to come to room temperature without stirring. The stirrer bar was allowed to stay in the vial to investigate if the stirrer surface acts as a nucleation site and also to make sure that no impurities are introduced while removing the stirrer.

2.3 Results

First, MSZW measurements for paracetamol crystallization in water at different scales are compared (section 2.3.1) from which a scale up rule is formulated (section 2.3.2). Then the nucleation mechanism occurring during these experiments is investigated and discussed (section 2.3.3).

2.3.1 MSZW of paracetamol in water

Paracetamol Solubility

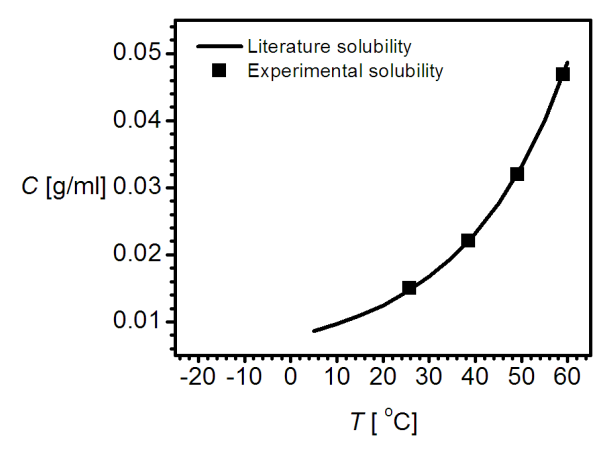


Figure 2.2: Temperature dependent solubility of paracetamol in water. The solid line is the solubility curve from literature¹² while the solid squares represent experimentally determined solubility.

The average values of the experimentally determined solubilities are shown in Figure 2.2 along with the solubility line reported in the literature. Eight measurements were performed per concentration to determine the solubility curve. Samples of the same concentration showed a saturation temperature within 0.7 °C of the average temperature. As can be seen from Figure 2.2, there is a very good agreement between our data and the solubility reported in the literature.

MSZW at 1 mL

The metastable zone width (MSZW) of a sample at a certain cooling rate is the difference between its saturation temperature and its MSZ limit. The MSZ limit is that temperature at which crystals are first detected upon cooling down a clear solution. Figure 2.3 shows the MSZW measurements of 0.015 g/mL paracetamol in water. 198 experiments were carried out at 1 mL scale using a cooling rate of 0.5 °C/minute. At the concentration used these solutions have a saturation temperature of 25.8 °C.

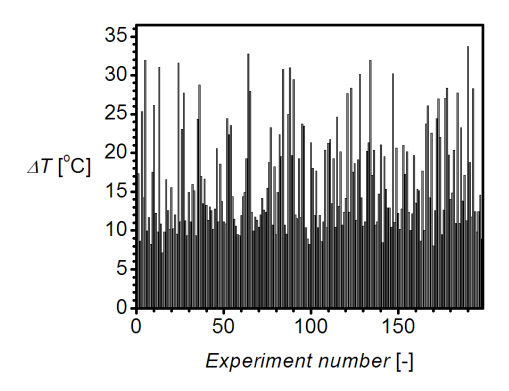


Figure 2.3: Distribution of the MSZW ΔT for a paracetamol concentration of 0.015 g/mL at 1 mL for 198 experiments.

We noted a substantial variation in the 1 mL MSZW measurements and therefore performed 198 experiments on this scale. The MSZW measured were between 7.2 °C and 33.8 °C. The variation was therefore in the order of 26 °C. These measurements show that in this case, a single MSZW limit measurement at 1 mL scale gives statistically insignificant results. They furthermore show that the MSZ limit is not a fixed quantity.

In order to determine the number of data points required to capture the MSZW variation at 1 mL scale, the cumulative average and cumulative standard deviation were determined (Figure 2.4). After approximately 150 experiments, the cumulative standard deviation becomes constant. It indicates that at a 1 mL scale at least 150 experiments are necessary to accurately capture the variations in MSZW measurements.

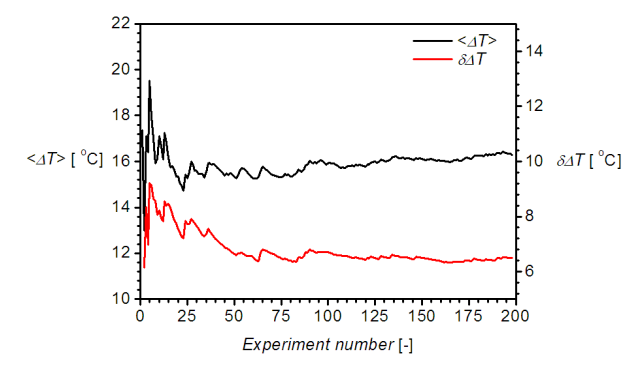


Figure 2.4: The cumulative average $\langle \Delta T \rangle$ and the cumulative standard deviation $\delta \Delta T$ become constant after approximately 150 experiments.

MSZW at 1 L

Interestingly, the variations in the MSZW are very low when the measurements are performed at 1 L scale, as seen in Figure 2.5. For the same paracetamol concentration of 0.015 g/mL as in the 1 mL experiments the spread of MSZW at 1 L scale was within 0.5 $^{\circ}$ C: all MSZW were between 7.0 and 7.5 $^{\circ}$ C.

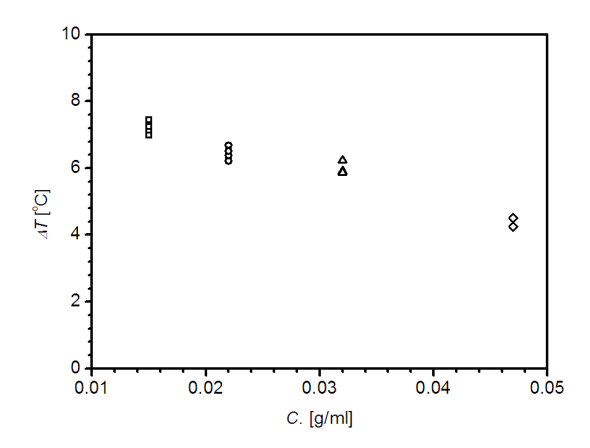


Figure 2.5: Distribution of the MSZW ΔT for paracetamol concentrations of 0.015 g/mL, 0.022 g/mL, 0.032 g/mL and 0.047 g/mL at 1 L (4 experiments per concentration).

2.3.2 Scale up rule for MSZW

The relation between the MSZW measurements at the different scales can be analyzed in term of the probability given by eq. 2.1. For N isolated experiments under equal conditions, the probability that the MSZW is ΔT or smaller is given as

$$P(\Delta T) = \frac{N^{+}(\Delta T)}{N} \tag{2.1}$$

where $N^+(\Delta T)$ is the number of experiments in which crystals are detected within a MSZW of ΔT . The plots are represented in Figure 2.6.

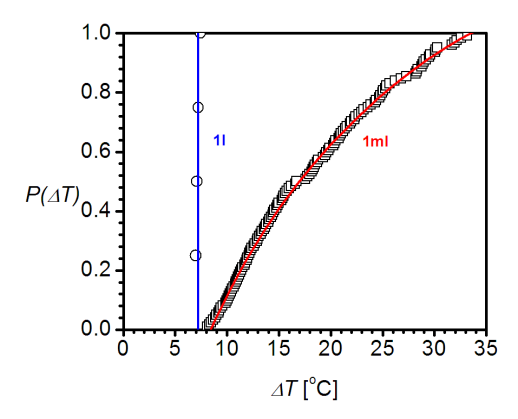


Figure 2.6: The probability distribution of the MSZW ΔT for a paracetamol concentration of 0.015 g/mL in water at a cooling rate of 0.5 °C/minute. Squares: 1 mL experiments; Circles: 1 L experiments. The lines are guides to the eye.

As can be seen in Figure 2.6, the probability of crystal detection shows a large variation for the 1 mL experiments while this variation is absent for 1 L experiments. More strikingly, it is observed that this narrow distribution of MSZW at 1 L is at the onset of the MSZW distribution at the 1 mL scale.

This relationship between MSZW at the 1 mL and 1 L scales is also observed with other concentrations as shown in Figure 2.7. It shows the solubility as a function of temperature as well as all measured MSZ limits on 1 mL and 1 L scale.

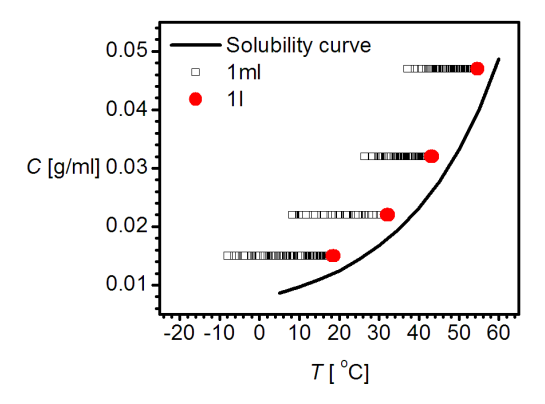


Figure 2.7: The relation between the MSZW at 1 mL and 1 L scales. The smallest MSZW measured on a 1 mL scale coincide with those measured on a 1 L scale.

For all 4 concentrations tested a large variation in the MSZ limit was measured for the 1 mL scale, while the MSZ limit for the 1 L scale experiments was found to be within 0.5°C. At the lowest value of the MSZ limit measured on a 1 mL scale, all MSZ limits on the 1 L scale were obtained. This gives a clear relationship between MSZW for paracetamol in water on a 1 mL and 1 L scale: the smallest MSZW measured at 1 mL coincides with the MSZW at 1 L.

The variations in the MSZ limit at 1 mL can be attributed to the stochastic nature of nucleation.¹³⁻¹⁵ In a supersaturated solution, solute molecules come together to form a cluster. The cluster grows by the attachment of molecules and decays in size by the detachment of molecules. Nucleation is therefore a process where clusters randomly change size until they decay or reach a size which enables it to grow without the chance of dissolution.^{6, 16} Due to this inherent random nature of the nucleation process, the temperature at which nucleation would be detected during continuous cooling is not a fixed quantity.

For the 1 L scale experiments the variations in the MSZ limit are very small. This could be explained by considering the volume of 1 L to consist of thousand 1 mL compartments. A nucleation event in any one of these small volumes would lead to nucleation in the entire crystallizer: the probability for nucleation in the larger volume is much larger. Thus, the outburst of nuclei on a 1 L scale coincides with the onset in the distribution of nucleation on a 1 mL scale as is seen in Figures 2.6 and 2.7.

2.3.3 Single nucleus mechanism

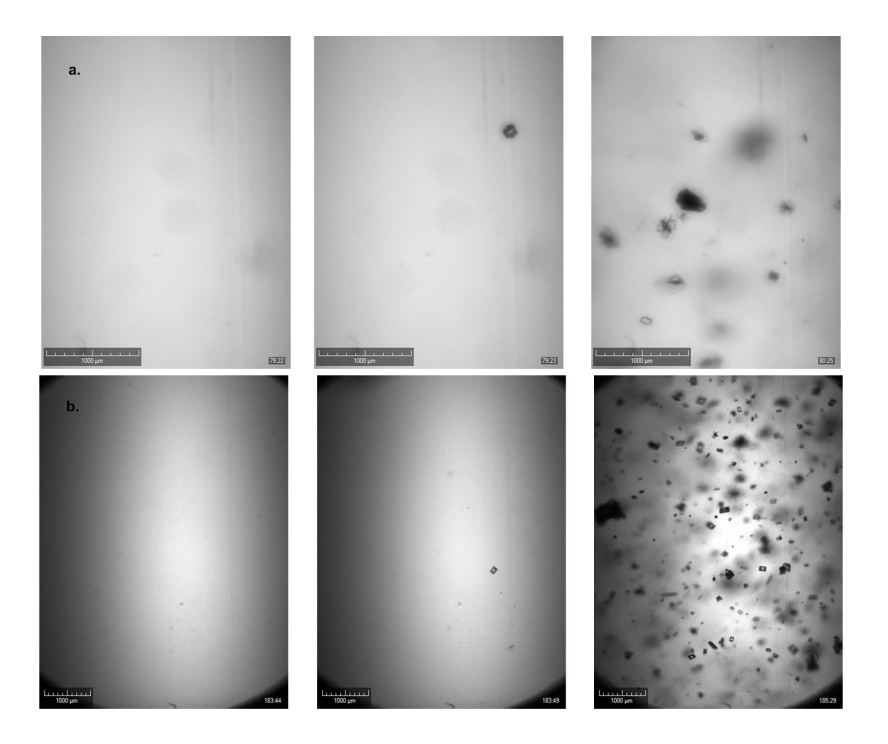
This relationship for MSZW between two volumes could be explained by assuming that in both scales a single primary nucleus is formed. This nucleus grows out to a particular size and undergoes secondary nucleation. In the clean and closed system under consideration, the possible secondary nucleation mechanisms are fluid shear induced crystal breakage and attrition by crystal-impeller or crystal-wall collision. Although the possibility cannot be entirely excluded, the fluid shear induced secondary nucleation is less probable under supersaturations encountered in this work. This mechanism generally occurs when the crystal develops dendrite-like outgrowths on its surfaces which only occur at high supersaturations or in melt crystallization. Attrition by crystal impeller collision has been previously recognized as the most common

secondary nucleation mechanism by many researchers.¹⁷⁻¹⁹ Attrition occurs when the crystal grows to a minimum attrition size.

This mechanism of a single primary nucleation event followed by secondary nucleation also was proposed for chiral symmetry breaking in sodium chlorate crystallization.²⁰ Sodium chlorate is an achiral compound of which the crystals are optically active. Crystallization from an unstirred solution results in a 50:50 mixture of levo and dextro crystals. However, evaporative crystallization in stirred solutions resulted in a product of crystals with a single handedness.

Experimental validation of the single nucleus mechanism

The single parent crystal was actually detected in the 3 mL scale cooling crystallization experiments. In order to increase the size at which crystal undergoes attrition an overhead stirrer was used instead of a magnetic stirrer. When a magnetic stirrer was used, the single crystal underwent attrition within 5-10 seconds of its first appearance on the camera while with overhead stirrer the attrition occurred after approximately 30 seconds. Figure 2.8a shows images during the MSZW measurement in which clearly a single crystal could be seen passing the camera several times before the actual outburst of secondary nuclei.



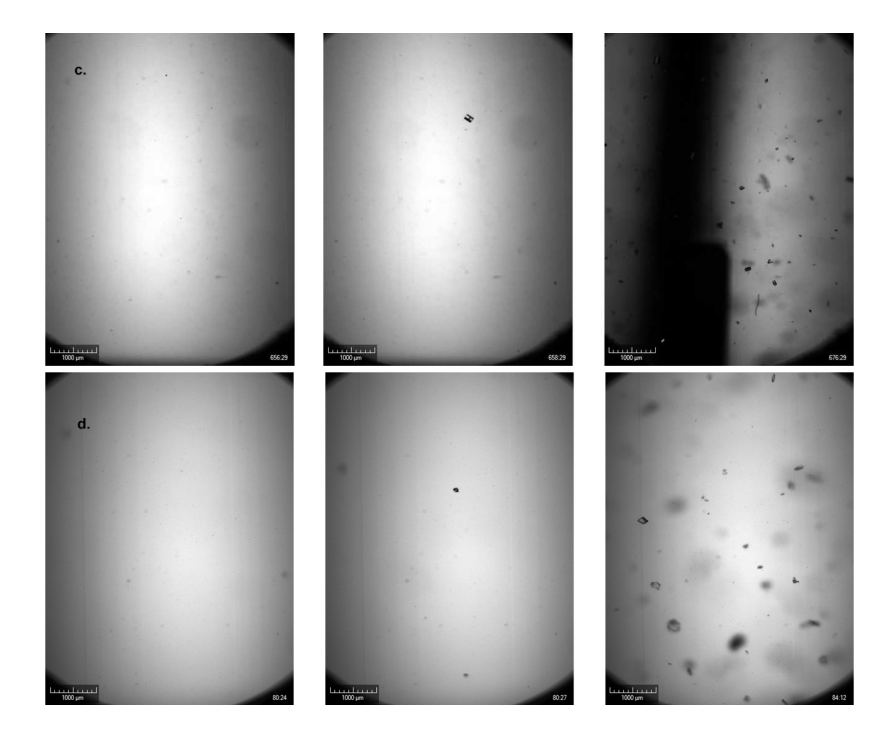


Figure 2.8: Images from a MSZW measurement at a 3 mL scale showing the clear supersaturated solution, the single parent crystal and the suspension after attrition of the single parent crystal for a. paracetamol (0.047 g/mL) in water; b. isonicotinamide (0.071 g/mL) in 1-butanol; c. isonicotinamide (0.120 g/mL) in ethanol; d. succinic acid (0.082 g/mL) in water. The dark part in Figure 2.8c (right side image) is the stirrer.

The single crystal was also observed for other crystallizing systems as shown in Figure 2.8b-d, indicating that the single nucleus mechanism might be a generally occurring mechanism.

This work shows that many processes perceived to be governed by the formation of crystals from primary nucleation may well instead be dominated by secondary nucleation of a single parent crystal.

2.4 Discussions

Contrary to the classical view that during cooling crystallization many nuclei appear by primary nucleation, it is shown during our experiments that only a single stable nucleus is born which eventually induces secondary nucleation. This single nucleus mechanism is consistent with the indications received in earlier studies.²⁰

Care was taken while experimenting to minimize the chances of the single nucleus originating from outside the solution. This nucleus is thus very likely formed by some kind of heterogeneous primary nucleation.⁶

At the moment, the birthplace of the single heterogeneous nucleus is not known. It could have been born in the bulk of the liquid, at the interface between wall and liquid, at the interface between stirrer and liquid, at the line between wall, liquid and air or at the interface between air and liquid. In the two day long unstirred cooling experiments in a 1 mL vial, a single crystal was observed at the interface between air and liquid (Figure 2.9). Although this provides an indication for the birthplace of the nucleus, further research would be necessary to ascertain its location.



Figure 2.9: Single crystal of paracetamol probably formed at the air-liquid interface.

The single nucleus grows into a parent crystal in the supersaturated solution. Apparently, no other crystal is present in the solution during this phase of the process.

After reaching an appropriate size at which the parent crystal can undergo attrition, crystal fragments start appearing.

This mechanism has industrial as well as scientific implications. Local variations in supersaturations in large industrial crystallizers might well be responsible for occurrence of the single nucleus mechanism at industrial scales. Industrially, it would be interesting to exploit the mechanism for crystallization control purposes. In a large volume, after the attrition of the single crystal, the fragments may not provide sufficient surface to consume the supersaturation upon their growth. More attrition events then are needed to increase the number of crystals and their total surface area which will complicate the control over the Crystal Size Distribution.²¹ It will be scientifically challenging to establish the origin of the single crystal and to exploit this by either enhancing or avoiding this single nucleus mechanism using templates. ²²

2.5 Conclusion

MSZW measurements were performed on 1 mL and 1 L scales. At small volumes, a large variation was measured. Hence at small volumes multiple (around 150) MSZW measurements should be performed to get an accurate MSZW distribution. Strikingly, the variations in the MSZW when measured at a larger volume (1 L) were almost absent. A relationship between MSZW at 1 mL and 1 L scale for paracetamol in water was found: the onset of the 1 mL MSZW distribution coincides with the MSZW at 1 L.

Another important result was obtained by in situ observation of crystals during cooling crystallization. These experiments revealed that a single crystal was present before an outburst of crystals was observed. The results indicate that only a single nucleus is formed which then grows out to a single crystal, sufficiently large to undergo attrition giving rise to an outburst and the detection of crystals. Other crystallization systems show similar behavior, indicating the generality of the single nucleus mechanism.

2.6 References

- 1. Myerson, A. S., *Handbook of Industrial Crystallization*. 2nd ed.; Butterworth-Heinemann: Woburn, US, 2002.
- 2. Nývlt, J.; Rychlý, R.; Gottfried, J.; Wurzelová, J., Metastable zone-width of some aqueous solutions. *Journal of Crystal Growth* **1970**, *6* (2), 151-162.
- 3. Ulrich, J.; Strege, C., Some aspects of the importance of metastable zone width and nucleation in industrial crystallizers. *Journal of Crystal Growth* **2002**, 237-239 (Part 3), 2130-2135.
- 4. Garside, J. M., A.; Nyvlt, J., *Growth and Nucleation Rates*. 2nd ed.; Institution of Chemical Engineers (IChemE): Rugby, UK, 2002.
- 5. Omar, W.; Ulrich, J., Solid Liquid Equilibrium, Metastable Zone, and Nucleation Parameters of the Oxalic Acid-Water System. *Crystal Growth & Design* **2006**, *6* (8), 1927-1930.
- 6. Mullin, J. W., Crystallization. Butterworth-Heinemann: Oxford, 2001.
- 7. Kashchiev, D.; van Rosmalen, G. M., Review: Nucleation in solutions revisited. *Crystal Research and Technology* **2003**, *38* (7-8), 555-574.
- 8. Simon, L. L.; Nagy, Z. K.; Hungerbuhler, K., Comparison of external bulk video imaging with focused beam reflectance measurement and ultra-violet visible spectroscopy for metastable zone identification in food and pharmaceutical crystallization processes. *Chemical Engineering Science* **2009**, *64* (14), 3344-3351.
- 9. Tavare, N. S., Batch Crystallizers: A Review. *Chemical Engineering Communications* **1987**, *61* (1), 259 318.
- 10. Groen, H.; Roberts, K. J., An Examination of the Crystallization of Urea from Supersaturated Aqueous and Aqueous-Methanol Solutions as Monitored In-Process Using ATR FTIR Spectroscopy. *Crystal Growth & Design* **2004**, *4* (5), 930-936.
- 11. Alvarez Rodrigo, A.; Lorenz, H.; Seidel-Morgenstern, A., Online monitoring of preferential crystallization of enantiomers. *Chirality* **2004**, *16* (8), 499-508.
- 12. Grant, D. J. W.; Mehdizadeh, M.; Chow, A. H. L.; Fairbrother, J. E., Non-linear van't Hoff solubility-temperature plots and their pharmaceutical interpretation. *International Journal of Pharmaceutics* **1984**, *18* (1-2), 25-38.
- 13. Toschev, S.; Milchev, A.; Stoyanov, S., On some probabilistic aspects of the nucleation process. *Journal of Crystal Growth* **1972**, *13-14*, 123-127.
- 14. Melia, T. P.; Moffitt, W. P., Crystallization from aqueous solution. *Journal of Colloid Science* **1964**, *19* (5), 433-447.

- 15. Jiang, S. ter Horst, J. H., Crystal Nucleation Rate from Probability Distributions of Induction Times. *Crystal Growth and Design* **2011**, 11(1), 256-261.
- 16. ter Horst, J. H.; Kashchiev, D., Determination of the nucleus size from the growth probability of clusters. *The Journal of Chemical Physics* **2003**, *119* (4), 2241-2246.
- 17. Mersmann, A.; Sangl, R.; Kind, M.; Pohlisch, J., Attrition and secondary nucleation in crystallizers. *Chemical Engineering & Technology* **1988**, *11* (1), 80-88.
- 18. Virone, C.; ter Horst, J. H.; Kramer, H. J. M.; Jansens, P. J., Growth rate dispersion of ammonium sulphate attrition fragments. *Journal of Crystal Growth* **2005**, 275 (1-2), e1397-e1401.
- 19. Gahn, C.; Mersmann, A., Brittle fracture in crystallization processes Part B. Growth of fragments and scale-up of suspension cyrstallizers. *Chemical Engineering Science* **1999**, *54* (9), 1283-1292.
- 20. Kondepudi, D. K.; Kaufman, R. J.; Singh, N., Chiral Symmetry Breaking in Sodium Chlorate Crystallizaton. *Science* **1990**, *250* (4983), 975-976.
- 21. Kramer, H.; Jansens, P., Tools for Design and Control of Industrial Crystallizers State of Art and Future Needs. *Chemical Engineering & Technology* **2003**, *26* (3), 247-255.
- 22. Urbanus, J.; Laven, J.; Roelands, C. P. M.; ter Horst, J. H.; Verdoes, D.; Jansens, P. J., Template Induced Crystallization: A Relation between Template Properties and Template Performance. *Crystal Growth & Design* **2009**, *9* (6), 2762-2769.

Chapter 3

A New View on the Metastable Zone Width

This chapter is published as:

Kadam, S. S., Kulkarni, S. A., Ribera, R. C., Stankiewicz, A. I., ter Horst, J. H., Kramer, H. J. M."A New View on the Metastable Zone Width during Cooling Crystallization." Chem. Eng. Sci., 2012, 72, 10-19.

The Metastable Zone Width (MSZW) is the difference between the saturation temperature and the temperature at which crystals are detected under constant cooling rate. The MSZW is conventionally treated as a reproducible, deterministic, volume independent property and is commonly used to characterize crystal nucleation and to determine the crystallization process operation window. In this study we investigate the volume dependency of the MSZW both experimentally and theoretically. MSZW measurements were performed for paracetamol-water and isonicotinamide-ethanol model systems at four different volumes between 500 mL and 1 L. A stochastic model developed based on the single nucleus mechanism and a deterministic population balance were used to theoretically study the effect of volume on MSZW. It was experimentally observed that the MSZW is not a reproducible point at small volumes but a spread which increases roughly inversely proportional to the volume. The dependency on volume of the MSZW cannot be explained by the deterministic population balance model but can be explained by the stochastic model based on the single nucleus mechanism. The knowledge of the MSZW behaviour at a certain volume and nucleation rate would help in identifying a process operating window limited by the saturation temperature on one side and the smallest MSZ limit on the other for a particular concentration. The knowledge of the process window at given conditions of volume and concentration would lead to better crystalline product quality as controlled seeding can be performed without the influence of crystals appearing as a result of a primary nucleation event.

3.1 Introduction

Metastable Zone Width (MSZW) measurements have been commonly employed to characterize nucleation and to determine the crystallization process operating window.¹⁻⁴ MSZW is the difference between the saturation temperature of a solution and the temperature at which the crystals are first detected, the MSZ limit, during cooling of a clear solution at a constant rate.⁵ Conventionally, the crystals detected at the MSZ limit are thought to be the result of multiple nuclei born simultaneously (termed as the conventional mechanism henceforth) and grown to detectable size.⁵ Due to the simultaneous formation of a large number of nuclei, reproducibility of MSZW is considered inherent and the MSZW is treated as a reproducible property under identical experimental conditions.^{1-3, 6} It is therefore common to represent the MSZ limit as a curve within the solubility graph to represent the operating window.

We have shown recently⁷ that the MSZW is not a fixed quantity. In fact, for paracetamol in water at 1 mL scale,⁷ the MSZW is a distribution of values differing approximately 25 °C at a cooling rate of 0.5 °C/min. This dramatic deviation from the theory could not be explained by the classical interpretation of the MSZW based on the Conventional Mechanism. Instead we postulated the Single Nucleus Mechanism (SNM), which assumes that only a single nucleus is formed in the clear supersaturated solution, which after growing to a certain size undergoes secondary nucleation. The MSZW distribution arises since the formation of this single nucleus is a stochastic process. Secondary nucleation occurs in the supersaturated solutions in presence of the solute in crystalline form. Presence of crystalline material has a catalytic effect on nucleation and hence secondary nucleation can occur at much lower supersaturations compared to primary nucleation.⁴

The single nucleus mechanism has strong implications industrially as well as scientifically. Industrially, the occurrence of the SNM implies that one crystal is the origin of all crystals in the final suspension. Hence to obtain better product quality, the control strategies should be focused not only on primary nucleation but also on secondary nucleation. Scientifically, the occurrence of the SNM in 1 mL scale implies that the primary nucleation rates are relatively low compared to those postulated by the Classical Nucleation Theory (CNT).8 The low primary nucleation rates are responsible for the fluctuations in the MSZW. On the other hand if a sufficiently accurate model is developed, primary nucleation rates can be obtained from the

measured fluctuations in the MSZW. In order to validate such a model the effect of volume on fluctuations in MSZW should be investigated experimentally.

In this chapter a stochastic model is presented based on the SNM and the Poisson's law which is used not only to determine nucleation kinetics from MSZW measurements but also to predict the transition volume at which the MSZW would become practically-deterministic. The effect of volume on the MSZW determined by the stochastic model is compared with the conventional population balance model. The MSZW measurements are described at different volumes to identify if such a transition volume exists and compare the experimental results with those obtained by the stochastic and population balance model.

3.2 Model structures

A stochastic model based on the Poisson's law and on the SNM was developed which gives probability of detecting MSZW within a certain value. When combined with the experimentally determined values of the MSZW, the stochastic model can be used for determining nucleation kinetics. With the knowledge of the kinetic parameters, the stochastic model and conventional population balance model can be compared to predict the effect of volume on the MSZW. In both the models, the stationary state nucleation is considered and the nucleation rate expression (eq. 3.1) from classical nucleation theory is used.⁸

$$J(t) = A \exp\left(\frac{-B}{\ln^2 S(t)}\right) \tag{3.1}$$

where A is the kinetic pre-exponential factor which is weakly dependent on supersaturation and B is the strongly supersaturation dependent exponential factor. S is supersaturation expressed as the ratio of initial concentration of solute in the solution c_0 to the saturated concentration at a particular temperature c^* . For the sake of simplicity we have neglected the effect of temperature on the factors A and B.

The details of the models are listed in sections 3.2.1 and 3.2.2.

3.2.1 Stochastic model

The appearance of a nucleus in a supersaturated solution can be considered to be a random process and also to be independent both from other nuclei formed in the same volume at constant supersaturation as well as independent from parallel experiments. The stochastic process of nucleation can therefore be described by the Poisson's law which then expresses the probability of finding m nuclei at a constant supersaturation as

$$P_{m} = \frac{N^{m} \exp(-N)}{m!} \tag{3.2}$$

where *N* is the average number of expected nuclei.

The probability P_0 of finding zero nuclei (no nucleation event) is therefore

$$P_0 = \exp(-N) \tag{3.3}.$$

Based on eq. 3.3, the probability of finding at least one nucleus within metastable zone width of ΔT after time t is

$$P_{>1}(t) = 1 - \exp[-N(t)]$$
 (3.4).

The average number N(t) of expected nuclei within a certain volume V is a function of the primary heterogeneous nucleation rate J (eq. 3.1)

$$N(t) = V \int_{t|_{\Delta T = 0}}^{t|_{\Delta T = \Delta T}} J(t)dt$$
(3.5)

where the nucleation rate is depending on the prevailing supersaturation which in turn is a function of the prevailing temperature. $\Delta T'$ is the undercooling when the nuclei are formed.

Commonly it is assumed that the growth time, which is the time between the formation of nuclei and their detection in form of crystals, is negligible in order to overcome the difficulty of uncoupling nucleation and growth.^{10, 11}

During the single nucleus mechanism, a single nucleus is formed in a supersaturated solution at nucleation time t_n . This single nucleus grows to a certain size in growth time t_g and then undergoes extensive secondary nucleation. The nucleation event is detected after the secondary nucleation of the single crystal. Attrition by crystal impeller collision has been recognized by many researchers as the most common secondary nucleation mechanism. Following are the assumptions made about secondary nucleation during the development of the stochastic model based on the single nucleus mechanism

- Secondary nucleation occurs after the crystal reaches a certain minimum size.
 This minimum size is constant at different concentrations, supersaturations and volumes.
- 2. Secondary nucleation occurs via attrition
- 3. One secondary nucleation event is enough to generate detectable crystal volume fraction in negligible amount of time.

The knowledge of the attrition size r_a and the supersaturation dependent growth rate G, leads to the supersaturation dependent growth time. The supersaturation dependent growth time allows uncoupling of nucleation and growth.

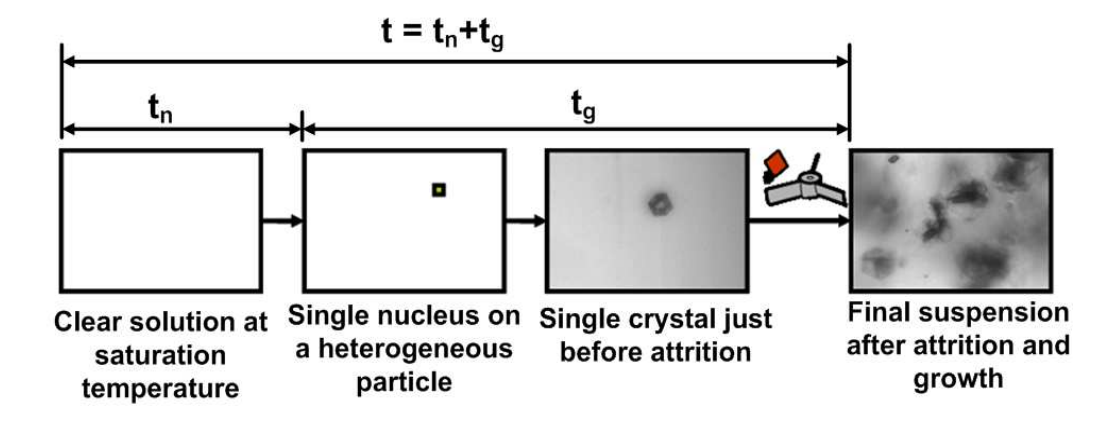


Figure 3.1: Schematics of the single nucleus mechanism. Detection time t consists of nucleation time t_n and growth time t_g .

Empirical power law kinetics is generally used to describe the growth rate.

$$G = k_{g} (S - 1)^{g} \tag{3.6}$$

where k_g is the growth rate constant while g is the growth rate exponent. The growth time t_g is therefore expressed as,

$$t_g = \frac{r_a}{G} \tag{3.7}$$

Combining eq. 3.4 and 3.5 and taking into account the growth time until MSZW is detected, we get the probability of detecting crystals within the temperature range ΔT at time $t'=t-t_3$ as

$$P(\Delta T) = 1 - \exp[-V \int_{0}^{t'} J(t')dt']$$
(3.8)

The probability distribution function in eq. 3.4 considers nuclei while the probability distribution function in eq. 3.8 considers crystals. The change from time (eq. 3.4) to temperature (eq. 3.8) for probability distribution is valid when the SNM occurs as only a single nucleus grows into a single crystal.

For N_t isolated experiments, the experimental probability of detecting crystals within the metastable zone width ΔT is given as

$$P(\Delta T) = \frac{N^{+}(\Delta T)}{N_{t}} \tag{3.9}$$

where $N^{+}(\Delta T)$ is the number of experiments in which crystals are detected within the temperature range ΔT .

The growth time of the crystal to attrition size will reduce as the supersaturation at which crystallization is detected goes on increasing. With the knowledge of the growth kinetics and the largest experimental growth time, which is time required to reach smallest measured MSZW during constant cooling, it becomes possible to obtain the supersaturation dependent growth time. It is assumed that the instance of nucleation when the largest growth time is measured, takes place at time zero i.e. at the instance of

crossing the solubility curve during cooling. The parameters for the CNT nucleation rate expression can be obtained by making a fit of analytical and experimental probability of detecting crystals within the metastable zone width ΔT . Once the nucleation kinetics are known, the model can be used for predicting the effects of volume on MSZW.

3.2.2 Conventional population balance model

For linear cooling crystallization experiments, the nucleation is detected when a certain minimum volume fraction of solids ε_t is reached.^{1, 3, 6} The nuclei are formed at a high rate as predicted by the classical nucleation theory and simultaneously growth of the formed crystals occurs. The subsequent secondary nucleation of crystals after they reach a certain critical size will speed up the detection process but is not strictly necessary to occur. The difference between the temperature at which the initial solution is saturated and the temperature at which the volume fraction ε_t is reached is taken as the MSZW. This nucleation mechanism is termed as conventional mechanism in this chapter.

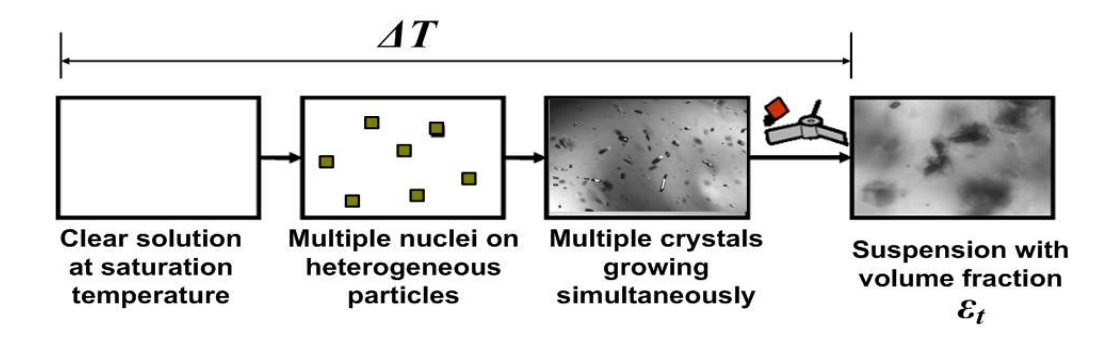


Figure 3.2: Schematics of the conventional mechanism.

The conventional mathematical model used to describe a batch crystallization process is generally developed based on the dynamic population balance, the conservation laws and the kinetic expressions. For a well-mixed batch crystallizer the one dimensional population balance equation¹⁵ can be written as

$$\frac{\partial n(L,t)}{\partial t} = -\frac{\partial (G(L,t)n(L,t))}{\partial L} - B$$
(3.10)

where n(L,t) is the number density function, t is the time, L is the characteristic crystal size, G(L,t) is the crystal growth rate and B' is the total nucleation rate. B' is expressed as sum of primary nucleation rate (eq. 3.1) and the secondary nucleation rate B_s ¹⁶ expressed empirically as

$$B_{s} = k_{b} \mu_{3}^{\beta} \sigma^{\alpha} P_{sp}^{\Phi} \tag{3.11}$$

where k_b is the nucleation rate constant, μ_3 is the third moment of the crystal size distribution, σ is the relative supersaturation, P_{sp} is the specific impeller power, β is the moment exponent, α is the supersaturation exponent and Φ is the specific power exponent.

One of the computationally efficient methods of solving population balances is to perform a moment transformation. ¹⁸ The details of the model structure and the moment transformations for batch cooling crystallization are described in the literature.²

The stochastic nature of nucleation is not considered in the population balance model and therefore the model considers that the nucleation detection temperature and hence the MSZW is reproducible under identical experimental conditions.

3.3 Experimental

Paracetamol (>99.0% pure, Sigma Aldrich) in demineralized water and isonicotinamide (>99.0% pure Aldrich) in ethanol (>99.8% pure, Sigma-Aldrich) were used as model systems for performing the experiments. The experiments were performed to determine the attrition size and the threshold crystal volume fraction required for crystallization detection by light beam (section 3.3.1). The attrition size and threshold volume fraction are necessary in the stochastic and the population balance models respectively. Experiments were also performed for MSZW measurements at different volumes.

3.3.1 Attrition size and threshold crystal volume fraction determination

The critical attrition size after which the single crystal undergoes secondary nucleation and the threshold crystal volume fraction after which the crystallization is detected by obscuration of the light beam were determined from the same experiments.

This attrition size is necessary in the stochastic model in order to determine the growth time. Instead of assuming a certain value for the critical attrition size, measuring of this value was preferred. Batch cooling crystallization experiments were performed at 3 mL scale for paracetamol in water (0.0220 g/mL) with a magnetic stirrer (PTFE, 10×3 mm) at 700 rpm in another multiple reactor setup (Crystalline, Avantium Technologies). The setup consists of 8 glass reactors which can be stirred by both magnetic and overhead stirrers. Experiments in four of the reactors could be followed with a particle visualization module (Avantium Technologies) consisting of in-situ cameras with resolution of 5-11 μ m/pixel. In order to determine the attrition size, images were taken every second during the process. The size of the single crystal before undergoing attrition was measured with built in image analysis software.

The threshold volume fraction ε_t is necessary in the population balance model. When the volume fraction of the crystalline material is equal to the threshold fraction ε_t , crystallization is detected. The same experiments used for the attrition size determination were continued further to determine the threshold volume fraction. The visualization module coupled with image analysis software (Avantium technologies) were used to determine the crystal size distribution and hence the volume fraction at the instance when light obscuration occurred.

3.3.2 MSZW measurements

MSZW measurements for paracetamol in water and isonicotinamide in ethanol were performed on 1 L, 900 mL, 700 mL and 500 mL scales per concentration at a cooling rate of 0.5 °C/min. Two different concentrations for both paracetamol-water (0.0150 g/mL and 0.0470 g/mL) and isonicotinamide-ethanol (0.0807 g/mL and 0.1619 g/mL) crystallization systems were used. The temperature dependent solubility of paracetamol in demineralized water⁷ and for isonicotinamide in ethanol¹⁹ was taken from the literature.

The measurements were performed using a jacketed glass crystallizer connected to a RK8KP Lauda thermostatic bath. The solution was stirred at 350 rpm using a magnetic stirrer (PTFE, 40 x 8 mm) and an IKA RET basic C stirring hotplate. The presence of crystals was detected with visual observations. The measurements were started at 1 L and the solution was successively removed to create volumes for subsequent experiments. At least 8 measurements were performed per volume except for

paracetamol in water at 1 L scale where only 4 measurements were considered sufficient.

For comparison, the MSZW measurements performed earlier at 1 mL with a magnetic stirrer (PTFE, 7 x 2 mm) at 700 rpm are also reported.⁷

3.4 Results and discussions

Kinetic parameters for nucleation and growth are estimated by making a fit of the analytical probability distribution from the stochastic model with the experimental probability distribution. An educated guess of the kinetic parameters is made for the conventional population balance model. Both models are compared qualitatively in analyzing the effect of volume on MSZW. With the knowledge of the kinetic parameters, the stochastic model enables determination of the volume lower limit at which the MSZW will be practically-deterministic. That transition volume is determined in section 3.4.4. Experimental measurements of MSZW at different volumes were performed to verify if such a transition volume exists.

3.4.1 Attrition size and threshold crystal volume fraction determination

In order to determine the attrition size of a single crystal, images were collected every second with Crystalline (Avantium Technologies). As the attrition occurs rapidly with a magnetic stirrer, the detection of the single crystal just before attrition required several experiments. Attrition fragments started appearing after approximately 10 sec of spotting of the single crystal.

In one of the experiments the single crystal was successfully captured right before (approximately 10 sec) the outburst of secondary nuclei. The size of this crystal was found to be approximately 200 μ m and this was taken as the estimate for the attrition size. For the sake of simplicity, the attrition size has been assumed constant at different concentrations, supersaturations and volumes.

The detectable volume fraction by light obscuration was determined based on the image analysis software supplied with Crystalline. The particle sizes, the number of particles with those sizes and the volume shape factor of 0.61 20 were used to determine the total volume of the crystalline phase. The determined crystal volume was divided with the volume within the view of the camera to obtain the threshold volume fraction

of approximately 0.0001. It was assumed during the calculation that the crystals are uniformly distributed throughout the crystallization volume in the vial.

3.4.2 Parameter estimation

Stochastic model

The growth rate constant was determined based on the experimental value of the largest growth time and by assuming volume diffusion controlled growth (growth rate exponent, *g*=1). The time at which the experimental probability distribution becomes non-zero is considered as the largest growth time. The experimental data for four different concentrations reported previously were used.⁷ The obtained values of the growth rate constant are presented in Table 3.1.

Table 3.1: Determined growth rate constant at various concentrations for paracetamolwater system, attrition size 200 µm.

Concentration [g/mL]	Saturation temperature [°C]	Largest experimental t_g [s]	k _s x 10 ⁶ [m/s]
0.0150	25.8	972	0.79
0.0220	38.6	827	0.95
0.0320	49.2	720	1.14
0.0470	59.1	601	1.55

Based on the experiments reported in chapter 2 for four different concentrations of paracetamol in water, a trial and error fit between analytical (equation 3.8) and the experimental (equation 3.9) probability of crystal detection within the metastable zone width ΔT at 1 mL, was made to estimate the classical nucleation theory parameters. The fits for different concentrations and the Root Mean Square Errors (RMSE) associated with them are shown in Figure 3.3 and the estimated parameters are listed in Table 3.2.

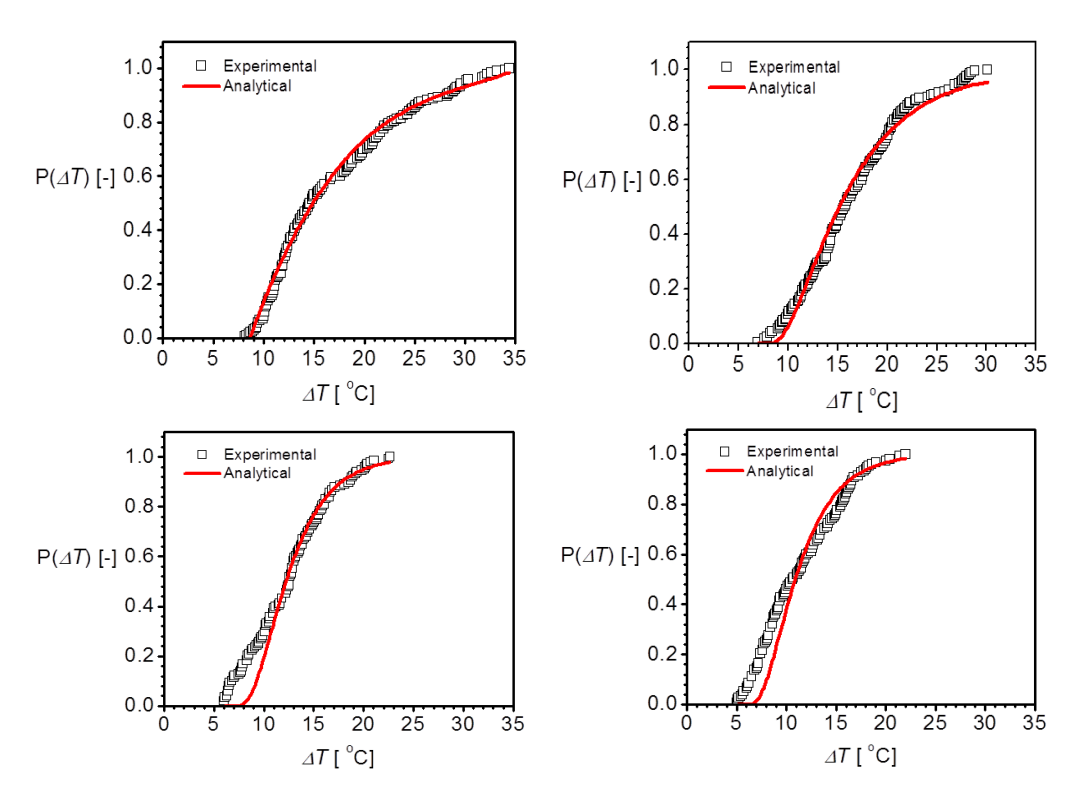


Figure 3.3: Fit between analytical and experimental probability distributions at 1 mL for paracetamol-water system a.) 0.0150 g/mL, Root Mean Square Error (RMSE) = 0.025, b.) 0.0220 g/mL, RMSE = 0.035, c.) 0.0320 g/mL, RMSE = 0.073 d.) 0.0470 g/mL, RMSE = 0.084.

Table 3.2: Estimated classical nucleation theory kinetic parameter A, thermodynamic parameter B, and the effective interfacial energy⁸ γ_{eff} for paracetamol-water system.

Concentration	A	В	$\gamma_{\it eff}$ [mJ/m²]
[g/mL]	[m ⁻³ s ⁻¹]	[-]	(at 25 °C)
0.0150	1000	0.001	0.48
0.0220	1480	0.029	1.47
0.0320	2900	0.029	1.47
0.0470	2800	0.022	1.34

The thermodynamic parameter B (dimensionless) for heterogeneous nucleation is expressed as⁸

$$B = \frac{4}{27} \frac{c^3 v^2 \gamma_{eff}^3}{k^3 T^3} \tag{3.12}$$

where c is the shape factor⁸ ($c = (36\pi)^{1/3}$ for spheres, c = 6 for cubes), v is the molecular volume of the paracetamol crystalline phase (19.4 x 10^{-27} m³) calculated using molecular weight, density and Avogadro's number, v is the effective interfacial energy, v is the Boltzmann constant and v is the temperature in K. The values of effective interfacial energies were determined with help of equation 3.12 using shape factor for spheres and are reported in Table 3.2. These values (except for concentration of 0.0150 g/mL) agree reasonably with the previously determined values of effective interfacial energies. The model is sensitive to measurement errors and these errors might have resulted in a smaller value of v for 0.015 g/mL. For the sake of simplicity, the effect of temperature on parameters v and v has been neglected in the model which could also have contributed to the error.

The value of the kinetic parameter A postulated in literature is in the order of 10^{15} to 10^{25} m⁻³s⁻¹. ²¹ With respect to the literature values, the values obtained for A in this work are relatively low. On the other hand, low values of the kinetic factor A have been previously reported in literature indicating either a two-step nucleation mechanism or a single nucleus mechanism.²³⁻²⁵ The value of A determined here indicates that either the concentration of the active nucleation sites in the solution is very low or the attachment frequency of molecules to the nucleus is low.

Conventional population balance model

The incentive for using the population balance model was to investigate qualitatively if the experimental trends in MSZW could be reproduced with this model. Due to lack of information for the conventional model, the parameters for primary nucleation rate and growth rate were chosen similar for both the conventional population balance model and the stochastic models. The threshold volume fraction ε_t at which nucleation was detected by light beam obscuration (section 3.4.1) was determined experimentally to be approximately 0.0001. For other parameters an educated guess was made. The list of used parameters is in Table 3.3.

Table 3.3: Parameters used in the population balance model for paracetamol-water system.

Symbol	Parameter	Value	Unit
kь	Secondary nucleation rate	1.0×10^{14}	#m-4
P_{sp}	Specific power input of the impeller	1.5	W/kg
ρ_w	Density of water	1000	kg/m³
$ ho_c$	Density of the crystals	1300	kg/m³
Cp_c	Specific heat of the crystals	2.9	kW/kg.K
Cp_w	Specific heat of water	4.1	kW/kg.K
A	Pre-exponential factor in CNT	2000	m ⁻³ s ⁻¹
В	Exponential factor in CNT	0.02	-
Φ	Specific power input exponent	1	-

3.4.3 Effect of volume on MSZW

The effect of volume on the probability distribution $P(\Delta T)$ was investigated with both the population balance and the stochastic model at 1 L, 900 mL, 700 mL, 500 mL, 100 mL, 10 mL and 1 mL. The results of the simulations are presented in Figure 3.4.

The population balance model indicates that the volume has no effect on the MSZW while the stochastic model indicates that the MSZW is a spread. For the stochastic model, as the volume is increased, the spread in MSZW reduces and probability distribution rises more sharply. The reduction in spread of the MSZW occurs exponentially with increase in volume indicating that the MSZW would be deterministic as the volume approaches infinity. The volume dependence indicates that for the stochastic model a transition volume exists above which the MSZW is reproducible within 0.5 °C. The MSZW above the transition volume can be considered practically-deterministic. When crystallization kinetics are known, it is possible to determine the transition volume with the help of the stochastic model.

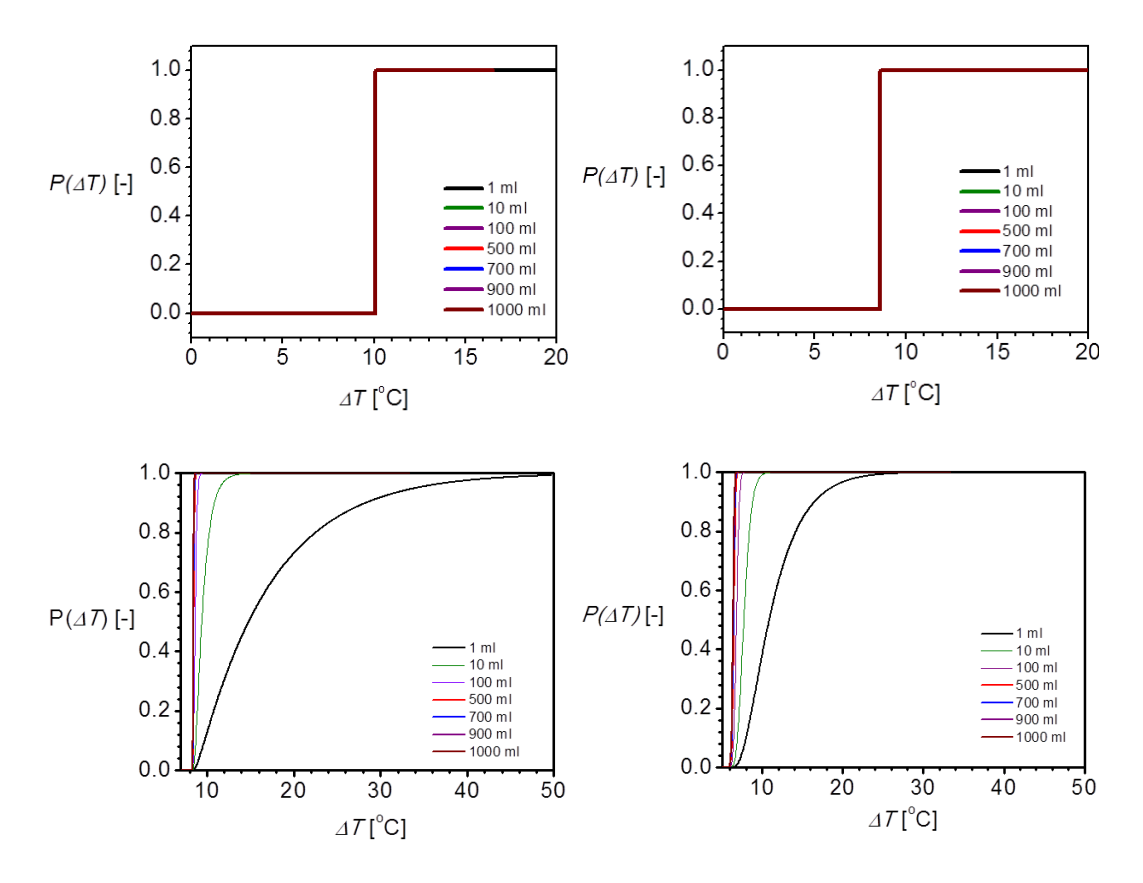


Figure 3.4: Effect of volume on probability distributions for paracetamol-water system a.) 0.0150 g/mL population balance model b.) 0.0470 g/mL population balance model c.) 0.0150 g/mL stochastic model d.) 0.0470 g/mL stochastic model.

3.4.4 Transition volume determination as function of nucleation rate

The transition volumes for paracetamol concentration of 0.0470 g/mL at different nucleation rates is shown in Figure 3.5. The variations in the nucleation rate are represented in the form of variations in the CNT kinetic parameter *A* while the CNT thermodynamic parameter *B* is kept constant at 0.022. Those transition volumes are represented by the solid line in Figure 3.5. Above the solid line MSZW becomes practically-deterministic. But at higher volumes, inhomogeneties in mixing might arise. These inhomogeneties can lead to locally higher supersaturations in a small sub volume that is responsible for the single nucleus within that sub volume . The volume at which the inhomogeneous mixing would occur will be dependent on several factors including the design of vessel, agitation type and frequency etc. Hence it is represented by dashed line in Figure 3.5.

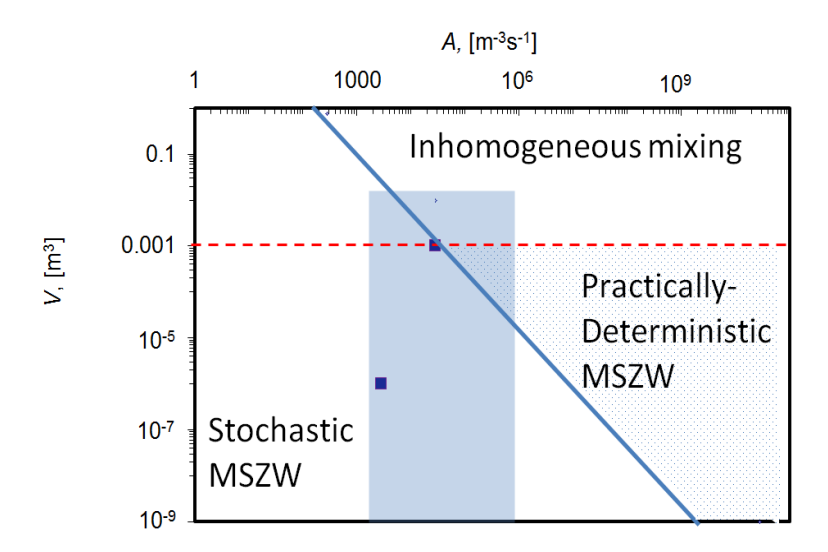


Figure 3.5: Volumes (m^3) at which the MSZW becomes practically-deterministic for paracetamol concentration of 0.0470 g/mL as a function of CNT kinetic parameter $A(m^{-3}s^{-1})$. CNT thermodynamic parameter B was kept constant at 0.022. MSZW would be practically-deterministic above the solid line. Inhomogeneties in mixing would start appearing above the dashed line. Solid squares are the experiments at 1 mL and 1 L scale and the shaded area represents experimental region commonly encountered in laboratory.

Actual experiments would provide answer if the MSZW is practically-deterministic in the region above both the solid and dashed lines. Under the experimental conditions in this work for paracetamol concentration of 0.0470 g/mL at 1 mL, the experimental data points lie in the region of the stochastic MSZWs while that for 1 L lie at the transition point above which the MSZW is practically-deterministic. Although Figure 3.5 is made for paracetamol-water model system, it can be easily adjusted to other systems if the nucleation and growth kinetics are known. As can be seen from Figure 3.5, only a small operating region encountered in laboratory leads to practically-deterministic MSZWs and caution must be exercised when using the MSZW determined at different scales for determining process operating window.

3.4.5 MSZW measurements

The stochastic model indicates that the variability in MSZW goes on reducing with the increase in the volume and after a certain transition volume, MSZW becomes practically-deterministic (Section 3.4.3). In order to verify this result, MSZW

measurements were performed for two different concentrations at different volumes for paracetamol in water and isonicotinamide in ethanol. The concentrations used and the corresponding saturation temperatures are listed in Table 3.4.

Table 3.4: Saturation temperatures for various concentrations of paracetamol in water⁷ and isonicotinamide in ethanol.¹⁹

Model system	Concentration [g/mL]	Saturation temperature [°C]
paracetamol-water	0.0150	25.8
paracetamol-water	0.0470	59.1
isonicotinamide-ethanol	0.0807	27.9
isonicotinamide-ethanol	0.1619	51.1

At least 8 measurements per concentration are reported per volume between 500 mL and 1 L scales while at least 150 experiments per concentration are presented at 1 mL scale except for paracetamol-water at 1 L scale for which 4 experiments were considered sufficient. There was no substantial effect of mixing on the MSZW measurements.

Figure 3.6a shows that the MSZW measured at 1 L scale is reproducible within 0.5 °C for paracetamol concentration of 0.015 g/mL. At 1 mL scale, on the contrary, the MSZW displays variations up to 26 °C. At intermediate volumes the variations are lower than that on a 1 mL scale. Similar trends are seen in Figure 3.6b. For both concentrations the variations in the MSZW increase gradually as the volume is decreased.

Comparing both graphs in Figure 3.6 it can be seen that the MSZWs at 0.0470 g/mL at each volume are smaller than the MSZWs for corresponding volumes at 0.0150 g/mL. This is because of the exponential rise of solubility with temperature which results in higher supersaturations at the same MSZWs for the concentration of 0.0470 g/mL. There is a small offset of approximately 1 °C between the smallest measured MSZW at 1 mL and other volumes due to the difference in the detection technique. The solid line in Figure 3.6 a and b indicates the smallest MSZW detected with light obscuration at 1 mL while the dashed line indicates the smallest MSZW detected by visual observation at volumes between 500 mL and 1 L.

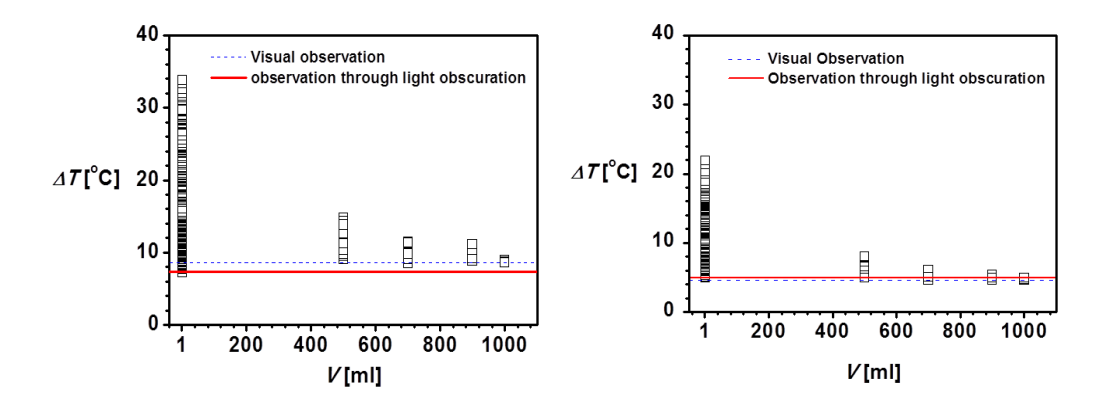


Figure 3.6: MSZW (ΔT) for paracetamol concentration of 0.0150 g/mL (a) and 0.0470 g/mL (b) at a cooling rate of 0.5 °C/min for different volumes. The solid line indicates the smallest MSZW detected with light obscuration at 1 mL while the dashed line indicates the smallest MSZW detected by visual observation at volumes between 500 mL and 1 L.

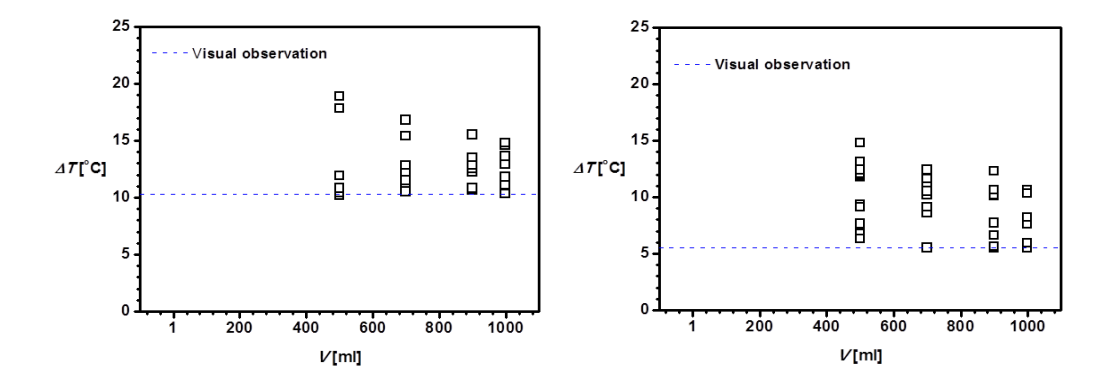


Figure 3.7: MSZW (ΔT) for isonicotinamide concentration of 0.0807 g/mL (a) and 0.1619 g/mL (b) at a cooling rate of 0.5°C/min for different volumes. The dashed line indicates the smallest MSZW detected by visual observation at volumes between 500 mL and 1 L.

For the MSZW of isonicotinamide in ethanol shown in Figure 3.7 similar trends were observed. As seen in Figure 3.7a and 3.7b the spread in MSZW increases with the decrease in volume.

In spite of the similar trend, there was one distinguishing feature for isonicotinamide-ethanol system compared to the paracetamol-water system. i.e. unlike

paracetamol, the MSZW at 1 L was not reproducible (within $0.5~^{\circ}$ C) and displayed a spread of more than $5~^{\circ}$ C. This indicates that the volume at which the MSZW becomes reproducible within $0.5~^{\circ}$ C is higher for the isonicotinamide model system.

An interesting feature seen in Figures 3.6 and 3.7 for both paracetamol in water and isonicotinamide in ethanol is that the smallest measured MSZW is the same (within approximately 1 °C, taking the differences in detection technique into account). The same result was obtained earlier during MSZW measurements for paracetamol in water at 1 mL to 1 L scale.⁷ A scale-up rule for MSZW was formulated as the smallest measured MSZW at 1 mL scale is equal to MSZW at 1 L scale. Considering Figures 3.6 and 3.7, the scale up rule can be extended as the smallest measured MSZW at any volume between 1 mL and 1 L is the same.

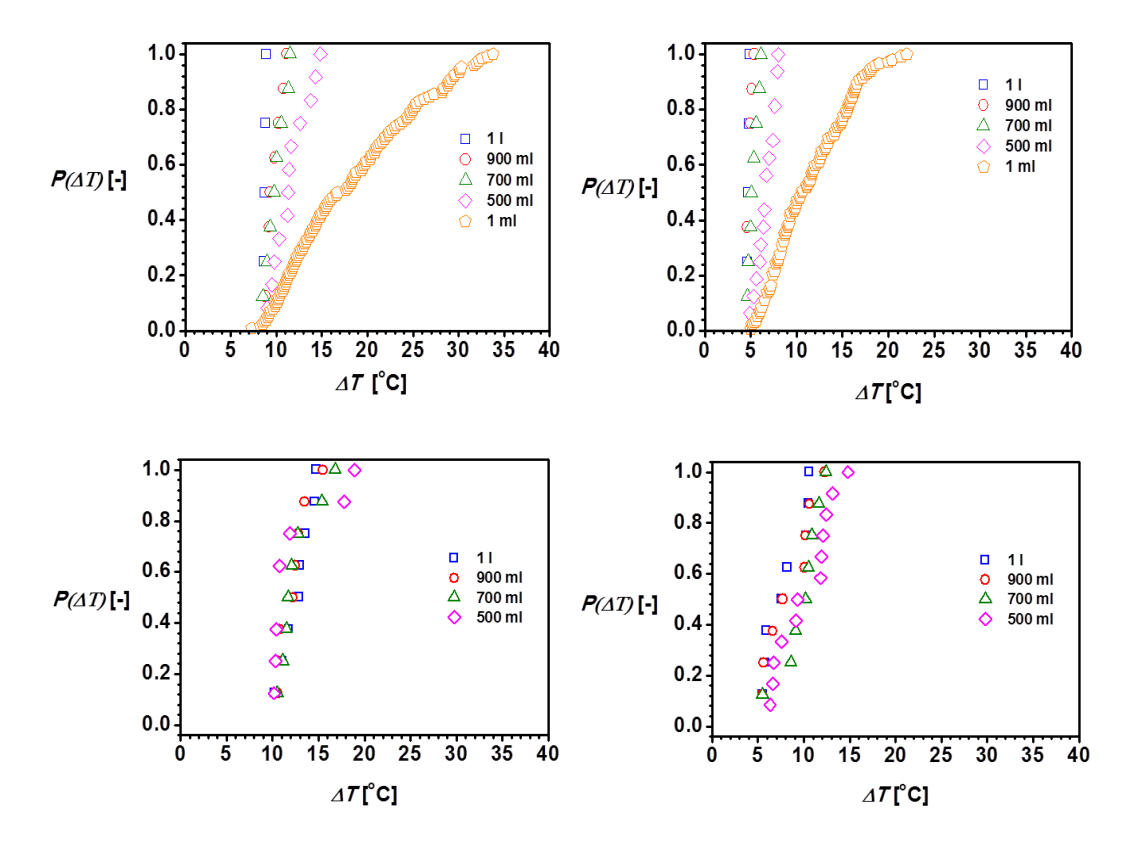


Figure 3.8: Experimental probability distributions (eq. 3.9) for paracetamol-water concentration of a.) 0.0150 g/mL, b.) 0.0470 g/mL and isonicotinamide-ethanol concentration of c.) 0.0807 g/mL and d.) 0.1619 g/mL.

The MSZW spread can be analyzed in terms of the probability of detecting a MSZW of ΔT or smaller, $P(\Delta T)$, given by eq. 3.9. As seen in Figure 3.8a for paracetamol concentration of 0.015 g/mL, the $P(\Delta T)$ shows a large spread at 1 mL scale. The spread in $P(\Delta T)$ decreases with increasing volume. As the smallest MSZW is the same at all volumes between 1 mL and 1 L for paracetamol in water, the $P(\Delta T)$ becomes non-zero for all volumes simultaneously. A similar trend is seen in Figure 3.8b for paracetamol concentration of 0.0470 g/mL. On the other hand as seen in Figure 3.8c and d for isonicotinamide-ethanol, the $P(\Delta T)$ becomes non-zero at the same MSZW for all volumes but there is no clear trend with volume. A clear trend may appear if more experiments per volume are performed for the isonicotinamide-ethanol system.

The MSZW has been traditionally treated as a volume independent reproducible property. 1-3, 6 Contrary to the conventional understanding of the MSZW, Figures 3.6 and 3.7 show that the MSZW is a volume dependent stochastic property. This nature of MSZWs at different volumes and their inter-relationship can be explained based on the Single Nucleus Mechanism (SNM).7 Nucleation can result in the formation of just a single nucleus. This single nucleus might be formed at different time instances in isolated experiments due to the stochastic nature of nucleation. The stochastic nature expresses itself strongly at smaller volumes during MSZW measurements because the probability of forming the single nucleus then is smaller. Larger volumes can be considered to be made up of large number of smaller compartments. An instance of nucleation in one of the smaller compartments followed by secondary nucleation would lead to crystallization of the entire volume. Hence nucleation should gradually become a deterministic property as the volume, and hence the number of smaller compartments comprising the volume, is increased. The variations in the MSZW should gradually disappear as the volume is increased. The volume at which the experimental variations in the MSZW would reduce to within 0.5 °C would be dependent on crystallization system as seen in Figures 3.6 and 3.7. Under non-ideal mixing conditions at higher volumes, the stochastic nature may well appear again due to regions of high local supersaturations.

3.4.6 Nucleation mechanism above the transition volume

The MSZW gets deterministic when measured under equal experimental conditions but at increasing volumes. This behaviour of MSZW has been observed experimentally and is also predicted by the stochastic model. The stochastic model predicts a sharp rise in the probability distribution function for volumes above 700 mL (approximately 1 L) while experiments show a sharp rise at 1 L for paracetamol in water. The sharp increase in probability distribution function obtained by the stochastic model above 1 L is similar to that obtained from the population balance model which is based on conventional mechanism. The similarity in probability distribution at volumes above 1 L for paracetamol in water for both stochastic model and population balance model prompts to following two issues.

- a.) Is there a transition to the conventional mechanism above 1 L for paracetamol in water?
- b.) Would temperature and supersaturation fluctuations in industrial scale crystallizers lead to the single nucleus mechanism?

One of the following methods could be used to identify the mechanism above the transition volume.

- 1. Experiments at volumes above the transition volume with model systems like sodium chlorate in water ²⁶ or isonicotinamide in mixture of solvents ²⁷ would help in determining the mechanisms. If crystals of same handedness are obtained in case of sodium chlorate and if only a single polymorph of isonicotinamide is obtained in a mixture of solvents, the single nucleus mechanism holds.
- 2. Computational Fluid Dynamics (CFD) calculations to identify local cold spots and volumes of those cold spots.
- 3. Pre-exponential kinetic parameters obtained from stochastic modeling could also help in identifying the mechanism at volumes well above transition volume (assuming ideal mixing conditions). But for the volumes close to the transition volumes, experimental methods must be employed to identify the nucleation mechanism.

If the single nucleus mechanism also occurs above the transition volumes, the efforts on control of nucleation on industrial scale should be focused on controlling secondary nucleation and not primary nucleation.

3.5 Conclusion

Unlike conventional interpretation of MSZW experiments which treats MSZW as volume independent deterministic property, it is shown that the MSZW is a volume dependent stochastic property. Instead of reproducible MSZWs, a spread in MSZW values is obtained at various volumes for paracetamol-water and isonicotinamide-ethanol model systems. The spread in the MSZW values increases at decreasing volumes due to the stochastic nature of nucleation. This behaviour of MSZWs cannot be explained either by the conventional interpretation of these experiments nor by deterministic population balance modeling but can be explained by a new interpretation based on the Single Nucleus Mechanism and stochastic modeling. The stochastic modeling can predict the effect of volume on the MSZW with reasonable accuracy and can be used to identify the transition volume at which the MSZW becomes reproducible. The stochastic model also acts as a tool for rapid and efficient determination of primary nucleation rates from solutions. With the knowledge of the transition volume, experiments can be performed in future to identify the nucleation mechanism occurring above the transition volumes.

3.6 Nomenclature

Α kinetic pre-exponential factor in Classical Nucleation Theory, [m⁻³s⁻¹] В exponential factor in Classical Nucleation Theory, [-] B_s secondary nucleation rate, [#/m⁴.s] B'total nucleation rate, [#/m⁴.s] Cp_c specific heat of the crystals, [kW/kg.K] Cp_w specific heat of water, [kW/kg.K] shape factor, [-] C initial concentration of solute in the solution, [g/mL] actual concentration of solute in the solution, [g/mL] saturated concentration, [g/mL] G growth rate, [m/s] primary nucleation rate, [m⁻³s⁻¹] k_b secondary nucleation rate constant, [#/m4] k Boltzmann constant, [J/K] k_g growth rate constant, [m/s] L crystal characteristic size, [m]

m number of nuclei, [#]

N average number of expected nuclei, [#] N_t total number of isolated experiments, [#]

 $N^+(\Delta T)$ number of experiments in which crystals are detected within metastable

zone width ΔT , [#]

n(L,t) crystal number density, [#/m⁴] n growth rate exponent, [-]

 P_m probability of finding m nuclei, [-]

 P_{sp} specific power input of the impeller, [W/kg]

Po probability of finding 0 nuclei, [-]

 $P(\Delta T)$ Probability of detecting crystals within metastable zone width ΔT , [-]

 $P_{\geq 1}$ probability of finding at least one nucleus, [-]

ra Attrition size, [m]

S supersaturation ratio, [-]

T temperature, [K]

 ΔT , $\Delta T'$ metastable zone width, [K]

t,t' time, [s]

 t_g growth time, [s] t_n nucleation time, [s]

V volume of the vessel, [m³] v molecular volume, [m³]

 α supersaturation exponent, [-]

 β moment exponent, [-]

 γ_{eff} effective interfacial energy, [mJ/m²]

 ε_t minimum detectable crystal volume fraction, [-] μ_3 third moment of crystal size distribution, [-]

 ho_c density of crystals, [kg/m³] ho_w density of water, [kg/m³] σ relative supersaturation, [-] Φ specific power exponent, [-]

3.7 References

- (1) Nyvlt, J., Kinetics of nucleation in solutions. *Journal of Crystal Growth* 1968, 3-4, (C), 377-383.
- (2) Nagy, Z. K.; Fujiwara, M.; Woo, X. Y.; Braatz, R. D., Determination of the Kinetic Parameters for the Crystallization of Paracetamol from Water Using Metastable Zone Width Experiments. *Industrial & Engineering Chemistry Research* 2008, 47, (4), 1245-1252.
- (3) Kubota, N., A new interpretation of metastable zone widths measured for unseeded solutions. *Journal of Crystal Growth* 2008, 310, (3), 629-634.
- (4) Myerson, A. S., *Handbook of Industrial Crystallization*. 2nd ed.; Butterworth-Heinemann: Woburn, MA, 2002.
- (5) Mullin, J. W., *Crystallization*. Fourth ed.; Butterworth-Heinemann: Oxford, 2001.
- (6) Mersmann, A.; Bartosch, K., How to predict the metastable zone width. *Journal of Crystal Growth* 1998, 183, (1-2), 240-250.
- (7) Kadam, S. S.; Kramer, H. J. M.; ter Horst, J. H., Combination of a Single Primary Nucleation Event and Secondary Nucleation in Crystallization Processes. *Crystal Growth & Design* 2011, 11, (4), 1271-1277.
- (8) Kashchiev, D., *Nucleation: Basic Theory with Application*. ed.; Butterworth-Heinemann: Oxford, 2000.
- (9) Krishnan, V., *Probability and Random Processes*. ed.; John Wiley and Sons: Hoboken, NJ, 2006.
- (10) Goh, L.; Chen, K.; Bhamidi, V.; He, G.; Kee, N. C. S.; Kenis, P. J. A.; Zukoski, C. F.; Braatz, R. D., A Stochastic Model for Nucleation Kinetics Determination in Droplet-Based Microfluidic Systems. *Crystal Growth & Design* 2010, 10, (6), 2515-2521.
- (11) Nielsen, A. E., Homogeneous Nucleation in Barium Sulfate Precipitation. *Acta Chem. Scand.* 1961, 15, 441-442.
- (12) Virone, C.; ter Horst, J. H.; Kramer, H. J. M.; Jansens, P. J., Growth rate dispersion of ammonium sulphate attrition fragments. *Journal of Crystal Growth* 2005, 275, (1-2), e1397-e1401.
- (13) Gahn, C.; Mersmann, A., Brittle fracture in crystallization processes Part B. Growth of fragments and scale-up of suspension crystallizers. *Chemical Engineering Science* 1999, 54, (9), 1283-1292.
- (14) Mersmann, A.; Sangl, R.; Kind, M.; Pohlisch, J., Attrition and secondary nucleation in crystallizers. *Chemical Engineering & Technology* 1988, 11, (1), 80-88.

- (15) Hulburt, H. M.; Katz, S., Some problems in particle technology: A statistical mechanical formulation. *Chemical Engineering Science* 1964, 19, (8), 555-574.
- (16) Kadam, S. S.; Mesbah, A.; van der Windt, E.; Kramer, H. J. M., Rapid online calibration for ATR-FTIR spectroscopy during batch crystallization of ammonium sulphate in a semi-industrial scale crystallizer. *Chemical Engineering Research and Design* 2011, 89, (7), 995-1005.
- (17) Daudey, P. J.; van Rosmalen, G. M.; de Jong, E. J., Secondary nucleation kinetcs of ammonium sulfate in a CMSMPR crystallizer. *Journal of Crystal Growth* 1990, 99, (1-4, Part 2), 1076-1081.
- (18) Randolph, A. D., Larson, M. A., *Theory of Particulate Processes*. 2nd ed.; Academic Press: San Diego, California, 1988.
- (19) ter Horst, J. H.; Cains, P. W., Co-Crystal Polymorphs from a Solvent-Mediated Transformation. *Crystal Growth & Design* 2008, 8, (7), 2537-2542.
- (20) Granberg, R. A.; Rasmuson, Å. C., Crystal growth rates of paracetamol in mixtures of water + acetone + toluene. *AIChE Journal* 2005, 51, (9), 2441-2456.
- (21) Kashchiev, D.; van Rosmalen, G. M., Review: Nucleation in solutions revisited. *Crystal Research and Technology* 2003, 38, (7-8), 555-574.
- (22) Omar, W.; Mohnicke, M.; Ulrich, J., Determination of the solid liquid interfacial energy and thereby the critical nucleus size of paracetamol in different solvents. *Crystal Research and Technology* 2006, 41, (4), 337-343.
- (23) Jiang, S.; ter Horst, J. H., Crystal Nucleation Rates from Probability Distributions of Induction Times. *Crystal Growth & Design* 2011, 11, (1), 256-261.
- (24) Vekilov, P. G., Nucleation. *Crystal Growth & Design* 2010, 10, (12), 5007-5019.
- (25) Erdemir, D.; Lee, A. Y.; Myerson, A. S., Nucleation of Crystals from Solution: Classical and Two-Step Models. *Accounts of Chemical Research* 2009, 42, (5), 621-629.
- (26) Kondepudi, D. K.; Kaufman, R. J.; Singh, N., Chiral Symmetry Breaking in Sodium Chlorate Crystallizaton. *Science* 1990, 250, (4983), 975-976.
- (27) Kulkarni, S. A., Kadam S. S., Stankiewicz, A. I., Meekes, H., ter Horst, J. H. In *Validation of the Single Nucleus Mechanism by Polymorphism*, 18th International Workshop on Industrial Crystallization, Delft, The Netherlands, 7-9 September, 2011; Kadam, S. S., Kulkarni, S. A., ter Horst, J. H., Ed. Delft, The Netherlands, 7-9 September, 2011; pp 75-80.

Chapter 4

A Comparative Study of ATR-FTIR and FT-NIR spectroscopy

This chapter is published as:

Kadam S. S., van der Windt, E., Daudey, P. J., Kramer, H. J. M. "A Comparative Study of ATR-FTIR and FT-NIR Spectroscopy for In situ Concentration Monitoring during Batch Cooling Crystallization Processes." Cryst. Growth Des., 2010, (10)6, 2629-2640.

Crystallization is a widely used separation and purification process in the chemical industry. The final product properties such as the crystal size distribution and the morphology are largely defined during this process. In order to achieve proper control over the crystallization process, accurate in situ measurements are necessary. This study presents the assessment of in situ infrared spectroscopic techniques for solute concentration measurements. It presents a comparative study of attenuated total reflectance (ATR) Fourier transform infrared (FTIR) and Fourier transform (FT) near infrared (NIR) spectroscopy for batch cooling crystallization of four different crystallization systems. These two techniques were compared based on the partial least square models developed by extensive calibration in the laboratory, the independent data sets generated while determining saturation concentrations in presence of crystals and for monitoring the batch cooling crystallization processes. The ATR-FTIR spectroscopy was found to perform better statistically and also in the presence of crystals. The FT-NIR spectroscopy was less reliable as the probe head was more susceptible to scaling. The average relative error in predicting the solubilities in the presence of crystals was sensitive to the crystallizing system and was in the order of 2% for ATR-FTIR while it was much higher for FT-NIR.

4.1 Introduction

The batch cooling crystallization is one of the important steps in pharmaceutical, fine and specialty chemicals industry which dictates the final product quality. The crystal quality is generally defined in terms of the crystal size, shape, polymorphic fraction, purity, product filterability, etc., and it is to a large extent dependent on the driving force for crystallization. The driving force for crystallization is the difference between the chemical potentials of the solute in the crystal and in the solution phase. However, it is common to express the driving force as supersaturation which is based on the concentration. The supersaturation can be expressed as the difference between the solute concentration in the solution and the saturation concentration at the given temperature. Since the birth and the growth of a new crystal phase and subsequently its properties are directly affected by the supersaturation in the crystallizer, control of the supersaturation is very essential. In order to control supersaturation, accurate in situ concentration measurements would be necessary which could also perform efficiently in presence of crystals. Apart from this classical approach of supersaturation control, in situ concentration measurements would also be necessary in the approach based on the control of growth rates. This approach based on the knowledge of concentration gradient in time, surface area, and density of the crystalline phase can be directly linked to the production rate. In this case, accurate concentration measurements would be necessary not only for monitoring concentration gradient but also to define the start of the process (seeding point, for instance).

4.1.1 Available concentration measurement techniques

Several techniques have been reported in the past to monitor the concentration and hence the supersaturation. They are based on measurement of a wide range of properties such as the refractive index,² the conductivity of the solution,³ the density of the liquid phase,⁴ the heat flux accompanying crystallization,⁵ the pH of the solution,⁶ the absorbance of the electromagnetic light by the solution etc.⁷⁻¹⁰ The limitations of some of these techniques are presented briefly below.

The accurate measurement of the refractive index has been done classically by using differential measurements with a reference material.² A differential refractometer consists of cells for the sample and for the reference material. It measures the deflection of the light resulting from the differences between the refractive indices of the reference material and the sample. These measurements require strict regulation of the

conditions in the experimental set up. This might become very tedious when done in the presence of crystals. Commercial process refractometers (K-Patents, Finland, www.kpatents.com) do exist, but only limited information about their applicability can be found in recent scientific literature.¹¹ The measurement of the conductivity³ as a means to determine the concentration is restricted to conducting solvents. Unfortunately, most of the organic solvents are non-conducting. Although the technique has potential to compensate for temperature fluctuations during the process, the application of this technique is difficult because the conductivity cell is susceptible to fouling and may pose operational difficulties. The measurement of the density⁴ offers a reasonably good means on the lab scale when pure solutions are employed and the conditions are controlled. Its application on industrial scale is still not widely accepted as it is sensitive to unknown impurities and the temperature changes. Also it needs crystal free liquid for measurements, making the set up complicated with a solidliquid separation unit. The heat generation accompanying crystallization⁵ could be used to determine the crystallization rate and hence indirectly to determine concentration, but the results are reliable and accurate only when done offline. This could be because of the low enthalpy of crystallization for most crystallizing systems. The majority of the problems associated with pH measurements are related to the sensor especially on the reference side. They include junction plugging, poisoning, and depletion of the electrolyte.6 Separate pressurized reference electrodes are available nowadays which would reduce the junction plugging and poisoning problem, but the problem with electrolyte depletion still persists. Furthermore, obtaining a reasonably good relationship between the concentration and pH values is often a formidable task as it depends on the solution under consideration. The applicability of the above techniques is qualitatively summarized in Table 4.1.

Table 4.1: Qualitative summary of the applicability of concentration measurement techniques.

Sr.No.	Technique based	Offline, in presence of		In situ, for
	on	Only liquid	Liquid and	crystallization control
			Crystals	
1	refractive Index	++	+	+
2	conductivity	+	-	-
3	density	++	-	-
4	heat effects	+	-	-
5	рН	++	-	-

Most of the problems mentioned above can be circumvented effectively by the techniques based on spectroscopy. The attenuated total reflectance (ATR) Fourier transform infrared (FTIR), the Fourier transform (FT) near infrared (NIR) and ultraviolet visible (UV-vis) are the most common spectroscopic techniques employed for online, inline or in situ concentration measurements. Dunuwila and Berglund¹² demonstrated the use of the ATR-FTIR spectroscopy for online concentration measurements during the crystallization of maleic acid from water. Thereafter, this technique has been used by many researchers for concentration monitoring during crystallization.¹³⁻¹⁷ The use of NIR for in-line concentration measurement of a drug during crystallization has been reported by Zhou et al.¹⁸ Howard et al.¹⁹ have reported the use of ATR UV-vis for concentration measurements during the polymorphic transformation of sodium benzoate from IPA/water mixture while the details of the calibration process for ATR UV-vis were reported by Abu Bakar et al.²⁰ The comparison of UV-vis for metastable zone width determination with focused beam reflectance measurement (FBRM) and bulk video imaging (BVI) has been performed by Simon et al.21 while the application of ATR UV-vis coupled with robust chemometrics for online model based control has been demonstrated by Nagy.²² In comparison with ATR-FTIR, relatively fewer studies are done for other spectroscopic techniques. The above mentioned studies have concluded that the online spectroscopic techniques show potential for concentration monitoring during the crystallization process.

The spectroscopic techniques are fast and nondestructive. They do not need an external sampling loop as they can be used in situ.²³⁻²⁴ With the spectroscopic techniques, the effects of the impurities and the temperature variations during the process can be appropriately incorporated.²⁵

Of the above-mentioned techniques, ATR-FTIR and FT-NIR were chosen for comparison in this work. Attenuated total reflectance (ATR) probe enables collecting spectra in situ without any sample preparation. A beam of infrared light is passed through the ATR crystal located at the tip of the probe in such a way that attenuated total internal reflection occurs and evanescent wave is generated which extends into the sample by a few micrometers. ²⁶ The depth of penetration in the sample depends on the wavelength. The reflected light is sent to the detector and is later analyzed with chemometrics ^{25, 27-28} to derive relation between concentration of solute and the spectral features. FT-NIR spectroscopy on the other hand uses a transflection probe which can work in both transmission and reflection mode. The probe consists of a slit of 1 mm through which the sample passes while being illuminated by the NIR radiations. The

radiations are either reflected back to the detecting fiber optic guide present in the same probe (in case of opaque samples) or are transmitted through (in case of transparent samples) after which they are reflected back with the help of a mirror.

4.1.2 Incentive for the work and the approach

Although some comparative studies have been carried out for above techniques, they are mainly for single phase systems (liquids) in the petrochemical industry.²⁹⁻³¹ To the best of our knowledge, a comparison between any two spectroscopic techniques for in situ concentration monitoring during crystallization processes for multiple crystallizing systems has never been carried out.

This work presents the comparison between ATR-FTIR spectroscopy based on mid infrared (MIR) region of the electromagnetic spectrum (termed MIR henceforth) and FT-NIR spectroscopy based on near infrared (NIR) region of the electromagnetic spectrum (termed NIR henceforth) during the crystallization of different crystallization systems viz. α -lactose monohydrate in water, ammonium sulfate in water, ibuprofen in hexane and L-glutamic acid in water. These two techniques were compared based on the PLS models developed by extensive calibration in the laboratory and also based on the independent data sets generated while determining saturation concentrations in the presence of the crystals. Furthermore, the batch cooling experiments of the above crystallizing systems were carried out wherein undersaturated solution was cooled at a specific cooling rate until the nucleation point. The two techniques were further compared based on their ability to monitor concentration and to detect nucleation points.

Multiple crystallizing systems were chosen during comparison to analyze systemwise sensitivities of the techniques and to get a broader understanding of their application in crystallization.

4.2 Experimental

4.2.1 Set up

Two different set ups were constructed to carry out the calibration, the subsequent validation, and the crystallization experiments. First set up, termed as the makeup was

used to make saturated solution, and it consisted of a 2 L jacketed and insulated glass vessel. The vessel was maintained at a constant temperature by using E300 thermostatic bath by Lauda GmbH and was agitated by a pitch blade impeller connected to Janke and Kunkel IKA Werk mixer. A Watson Marlow peristaltic pump was used to pump the slurry through a filter to get saturated crystal free solution. The second set up termed as the measurement set up, consisted of 1 L jacketed glass crystallizer as shown in Figures 4.1a and 4.1b.

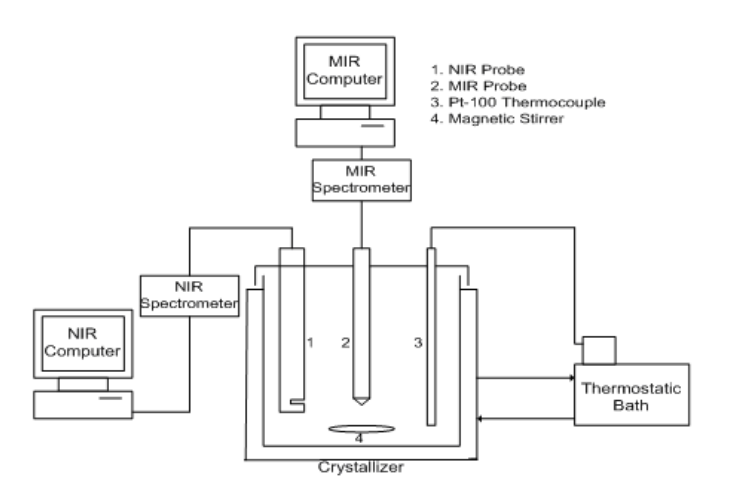


Figure 4.1 a: Measurement set up schematics.

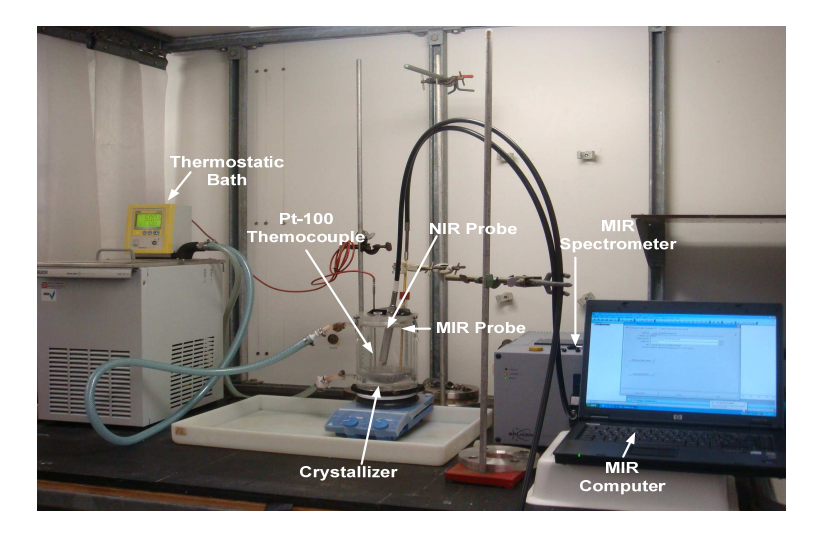


Figure 4.1 b: Measurement set up.

It was connected to a Lauda RK8KP thermostatic bath which maintained and controlled the temperature inside the crystallizer with the help of an external platinum resistance thermocouple Pt-100. Both MIR and NIR probes were inserted through the lid as seen in Figure 4.1b. The crystallizer was maintained well mixed by an IKA RET basic C magnetic stirrer. Care was taken that the agitation was not too vigorous and that no vortex was formed.

4.2.2 Instruments

The MIR and the NIR spectrometers were supplied by Bruker Optics GmbH, Germany, along with the fiber optics probes. The MIR spectrometer MATRIX-MF was connected to the IN-350T fiber optics probe. The probe head was made of gold plated hastelloy and had a diamond prism at the end. It was approximately 300 mm in length and 6 mm in diameter as shown in Figure 4.2a. The MIR spectra were collected over 4000-400 cm⁻¹ with a resolution of 8 cm⁻¹. The effective region for this probe was 3500-560 cm⁻¹. The optical path length is not constant but depends on the penetration depth at each wavelength. Each spectrum consisted of 16 co-added scans.

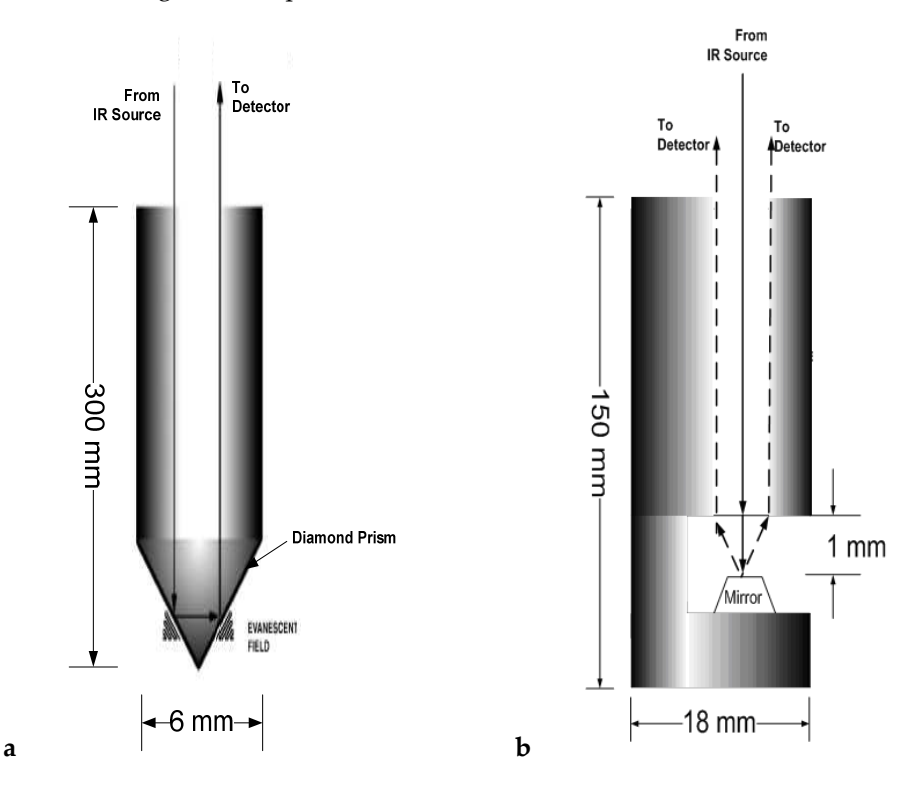


Figure 4.2: Schematics of MIR (a) and NIR probe (b) (Figure not to scale).

The NIR spectrometer MATRIX-F was connected to the IN-271P transflection probe. The probe was 18 mm in diameter, 150 mm in length as shown in Figure 4.2b and was made of SS316. The transflection probe consisted of a central fiber optics guide coming from the source surrounded by six fiber optics guides toward the periphery of the probe to collect the reflected light. It also consisted of a reflecting mirror which was separated by 1 mm from the optical fibers. Hence, the actual path length for the radiations was 2 mm. The NIR spectra were collected over 12000-4000 cm⁻¹ with resolution of 8 cm⁻¹. Each spectrum consisted of 16 co-added scans.

4.2.3 Materials

Table 4.2 shows the solutes and solvents used for the experiments.

Table 4.2: Solutes and solvents used

Compound	Chemical	M. Wt.	Purity
α -lactose monohydrate	C12H22O11. H2O	360.31	pharmaceutical grade
ibuprofen	C13H18O2	206.28	99.9% pure
ammonium sulfate	(NH ₄) ₂ SO ₄	132.14	technical pure, 21% N
L-glutamic acid	C5H9NO4	147.13	99.5% pure
n-hexane	C6H14	086.18	95% pure, HPLC grade
water	H ₂ O	018.00	demineralized

4.2.4. Procedures

Calibration

Calibration of the MIR and the NIR probes was carried out in the same vessel. Saturated solutions were prepared at four different temperatures which were then diluted successively by the addition of known amounts of solvent as shown in Figure 4.3. In principle, another calibration approach can be used wherein the spectra are collected in both undersaturated and supersaturated regions.²⁰ However, this approach may not be effective for the crystallizing systems with small metastable zone widths and for the systems which tend to nucleate on the crystallizer wall.

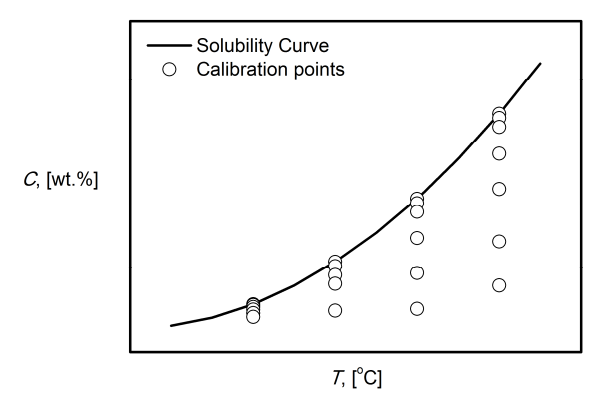


Figure 4.3: Schematics representing the calibration procedure.

In the current approach, approximately 100 spectra were collected for each crystallizing system. Out of the total collected spectra, 70% of the spectra were used as a training set to build a partial least square (PLS)^{25,27-28} model, while the remaining 30% were used as a test set. The PLS model was validated statistically based on the test set.

Solubility curve determination

The developed and statistically validated PLS models were tested in the presence of the crystals. Excess amounts of solute were equilibrated at the highest temperature in the range with the solvent for one and a half hours to make sure that the equilibrium was reached. The temperature was then lowered and the slurry was allowed to come to equilibrium at that temperature. A set of three spectra was collected at each temperature. The spectra were then analyzed with the developed PLS model to determine the saturation concentration. The concentration determined by both MIR and NIR probes was compared with either literature or experimentally determined saturation concentrations.

Batch experiment

Undersaturated solutions were prepared at the conditions mentioned in Table 4.3. These solutions were then cooled at rate of 0.5 °C/minute until the nucleation point was detected by visual inspection. Once the nucleation point was detected, the cooling was stopped and the temperature was maintained constant. Spectra were collected throughout the process after every 30 seconds.

Table 4.3: Starting temperatures and concentrations for batch cooling crystallization experiments.

Test System	T, [°C]	<i>C</i> , [wt.%]
ammonium sulfate-water	45	43.24
ibuprofen-hexane	45	36.01
L- glutamic acid-Water	55	02.34

The primary nucleation of α - lactose monohydrate is an extremely slow process and nucleation times of several hours are not uncommon. It is further inhibited by the presence of α - lactose, an anomer of α - lactose monohydrate which acts as an impurity during the process. ³²⁻³³ Hence, due to the long experimental times, the batch cooling experiment for α - lactose monohydrate was not performed.

4.3 Results and discussions

4.3.1 Spectral features

Representative spectra of each crystallizing system collected during the experiments by MIR and NIR probe are shown in Figures 4.4 and 4.5, respectively. The spectra are shifted vertically from their original position for more clarity.

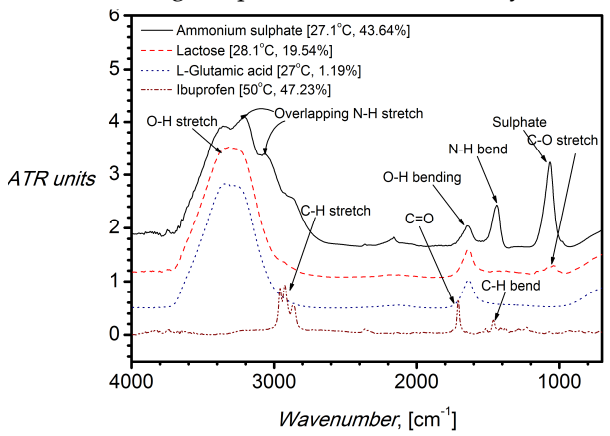


Figure 4.4: MIR spectra.

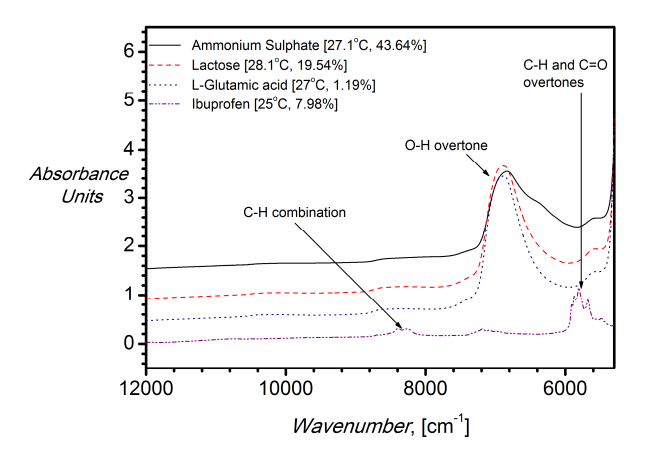


Figure 4.5: NIR spectra.

In this study with MIR, all spectra were collected in ATR absorption units. As can be seen from the Figure 4.4, the three water-based systems stand out distinctly from the hexane-based system. For the ammonium sulfate in water system, a broad absorbance region is observed at approximately 3500-2700 cm⁻¹ which consists of an O-H stretch absorption at approximately 3500-3000 cm⁻¹ along with an overlapping band for the N-H stretch at 3300-2700 cm⁻¹. The shoulders on this broad absorption band are due to the solute-solvent interactions. At approximately 1640 cm⁻¹ a band due to water bending is observed. The bands at 1450 and 1000 cm⁻¹ are due to N-H bending and Sulfate.

L-Glutamic acid exists mainly as zwitterion (internal salt), and hence its spectra exhibits combination of carboxylate and the primary amine salt. The spectrum is dominated by the absorptions of water in form of a broad band at 3400 cm⁻¹ for O-H stretching vibrations and a band at 1640 cm⁻¹ for the O-H bending vibrations. Apart from these bands, a very broad NH³⁺ band at approximately 3400 cm⁻¹ should exist, but the solubility of L-glutamic acid in water is too low for visual inspection. For the same reason N-H bend (symmetric/asymmetric) is not observed at approximately 1640-1560 cm⁻¹.

Although the band for carboxylate ions COO cannot be seen in ATR spectrum due to the low concentration of L-glutamic acid, it is observed in the absorption spectrum at approximately 1400 cm⁻¹ as shown in Figure 4.6. The PLS model was based around this peak.

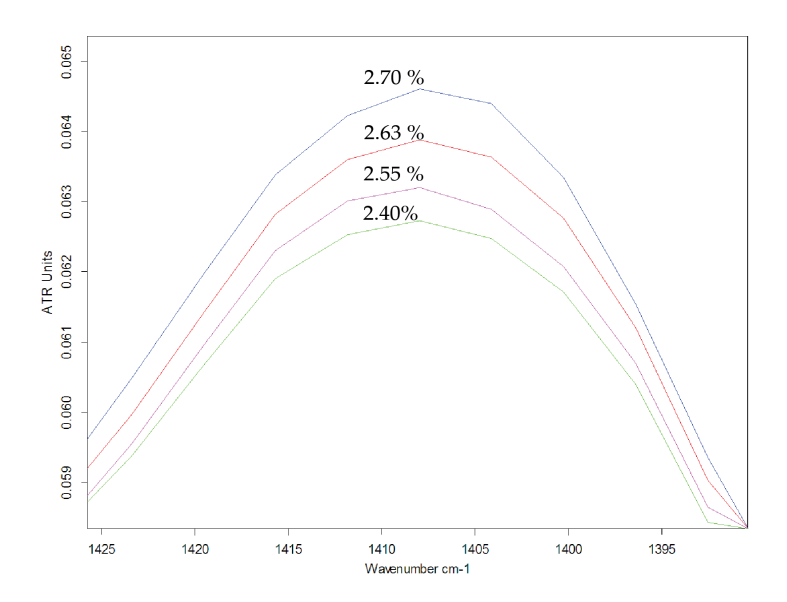


Figure 4.6: L-glutamic acid peaks in absorption mode at 55 °C.

The main absorptions for the α - lactose monohydrate spectrum are quite similar to the L-glutamic acid spectrum (water predominantly) except for a band at around 1300-1000 cm⁻¹ related to C-O stretching vibrations. The ibuprofen spectrum stands out discretely due to presence of a carbonyl peak at 1715 cm⁻¹. Small bands in the region of 1600-1500 cm⁻¹ indicate presence of an aromatic ring. Absorption bands due to C-H stretching vibrations in the region between 3000 and 2800 cm⁻¹ and the absorption band due to C-H bending vibration at 1450 cm⁻¹ are from the aliphatic chain of hexane.

Where MIR spectral region consists of the fundamental stretching and bending vibrations of the molecular groups, the NIR spectral region shows the combination bands of these fundamental vibrations and their first, second and third overtone. NIR spectra do not contain readily interpretable peaks as in the MIR spectra. A glance at spectra provides relatively less amount of information like the nature of solvent. But they are in general more reproducible and appear to suffer less from base line shifts. For water based systems of ammonium sulfate, α-lactose monohydrate and L-glutamic acid a band due to vibration of O-H group is present in the first overtone region around approximately 6800 cm⁻¹. For the hexane based ibuprofen system, the absorption bands are present between approximately 6000 to 5000 cm⁻¹ due to the first overtone of the stretching vibrations of C-H and C=O (carbonyl group of ibuprofen) in the second overtone region. The ibuprofen spectra also contain bands due to C-H combination vibration (hexane) around approximately 7500-7000 cm⁻¹. Due to relatively

less amount of evident information from the spectra, robust chemometrics is required to extract useful information from the NIR spectra.

4.3.2 Partial least square (PLS) modeling

For both MIR and NIR spectra the Bruker OPUS software was used to generate the prediction models. Within the program, the spectra are manipulated by selection of specific spectral regions and by preprocessing steps like the first derivative, normalization, etc. In principle, the software was used to select the spectral regions based on the principal component analysis and the partial least squares. The details of these treatments can be found elsewhere. ^{25,27-28} The selected regions coincide with the region where absorption bands of interest for the given solute should be.

In quantitative analysis, it is assumed that the layer thickness (i.e. the effective path length of the infrared light in the sample) is identical in all measurements. A lack of reproducibility in the samples can easily cause variations in the layer thickness. The effect of variable layer thickness can be effectively eliminated by normalization of the spectra. Hence, normalization, which is a part of preprocessing, is done to ensure a good correlation between the spectral data and the concentration values.

The benefits of preprocessing are explained for the α -lactose monohydrate-water system. The Figure 4.7a shows the raw data as it was obtained under the laboratory conditions. The Figure 4.7b shows the same spectra after the min-max normalization pretreatment. Min-max normalization performs a linear transformation on the original data values. It first subtracts a linear offset and then sets the y maximum to a value of 2 (in this case) by multiplication with a constant. $^{34-37}$

As can be seen in Figure 4.7b, the normalization provides us a more clear view of the relation between the lactose C-O stretching absorptions at 1300-1000 cm⁻¹ for different concentrations. The advantage of using min-max normalization is that it preserves the relationships among the original data and it does not introduce any bias. Similar effects from preprocessing were derived for other systems. The regions and preprocessing steps used for developing the PLS model for all crystallizing systems are presented in Tables 4.4-4.5.

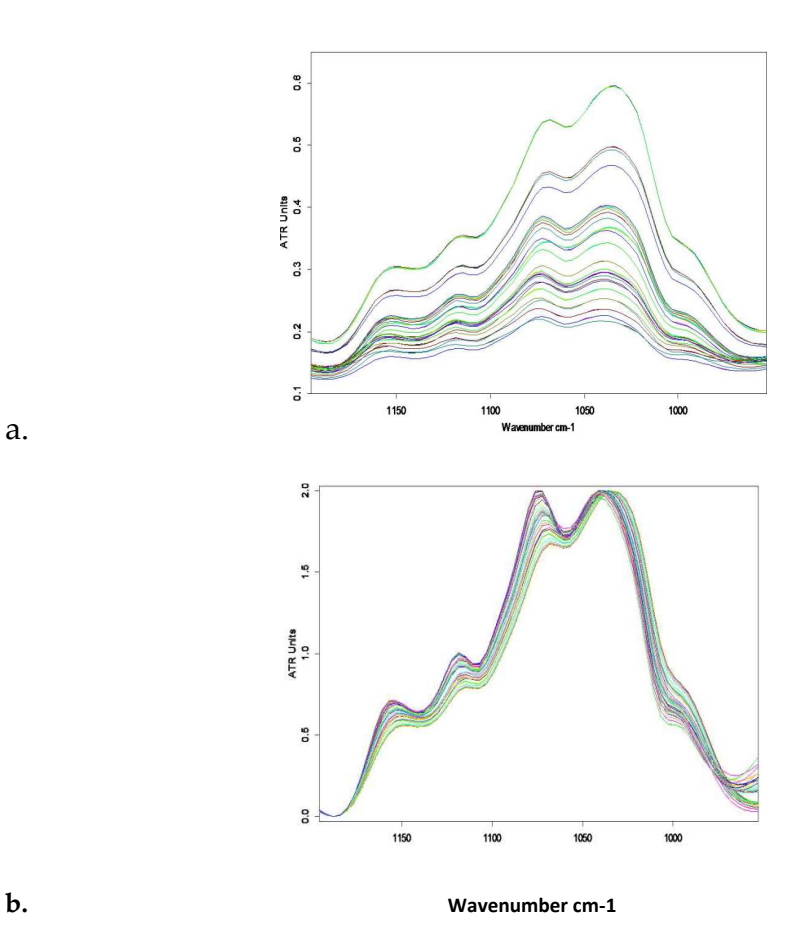


Figure 4.7: Raw spectra for α - lactose monohydrate-water under laboratory conditions (a) and after preprocessing (b).

The PLS models developed as above were evaluated based on the coefficient of determination (R^2) values which is an indication of the goodness of the fit between the actual concentration values and those predicted by the model. It is expressed as follows

$$R^{2} = \left[1 - \frac{\sum_{i=1}^{n} (y_{i} - y_{pi})^{2}}{\sum_{i=1}^{n} (y_{i} - y_{m})^{2}} \right] \times 100$$
(4.1)

where y = true value

 y_p = predicted value

*y*_m= mean value

n = Number of samples in training set.

Table 4.4: Regions and preprocessing steps for MIF	Table 4.4:	Regions and	preprocessing	steps for MIR
---	-------------------	-------------	---------------	---------------

Test system	Regions	Preprocessing step ³⁴⁻³⁷	
lpha - lactose monohydrate-	1195.8-0952.8 cm ⁻¹	min-max normalization	
ammonium sulfate -water	3633.7-3271.1 cm ⁻¹	first derivative + vector	
	2916.2-2194.9 cm ⁻¹	normalization	
	1836.1-1114.8 cm ⁻¹		
ibuprofen-hexane	2920.0-2349.2 cm ⁻¹	first derivative	
	2071.4-933.5 cm ⁻¹		
L- glutamic acid-water	1828.4-1404.1 cm ⁻¹	straight line subtraction	

Table 4.5: Regions and preprocessing steps for NIR

Test system	Regions	Preprocessing step ³⁴⁻³⁷
lpha - lactose monohydrate-	5851.5-5446.5 cm ⁻¹	first derivative + straight line
water		subtraction
ammonium sulfate-water	7510.1-7274.8 cm ⁻¹	first derivative
	7043.4-6804.2 cm ⁻¹	
	6576.6-5870.8 cm ⁻¹	
	5639.3-5400.2 cm ⁻¹	
ibuprofen-hexane	6102.2-5446.5 cm ⁻¹	first derivative + vector
		normalization
	4601.7-4424.3 cm ⁻¹	
L- glutamic acid-water	9384.7-8401.1 cm ⁻¹	constant offset elimination

The other criteria used for evaluation was the Root Mean Square Error in Prediction (RMSEP). It is an indication of how well the model predicts the concentration values of the test set spectra. It is expressed as follows

$$RMSEP = \sqrt{\frac{1}{n} \sum_{i=1}^{n} (y_i - y_{pi})^2}$$
 (4.2)

The model is better if the RMSEP value is as low as possible and within the standard deviation of the reference values. The prediction vs true graphs (weight fractions) with the R^2 and RMSEP values are presented in Figures 4.8 and 4.9.

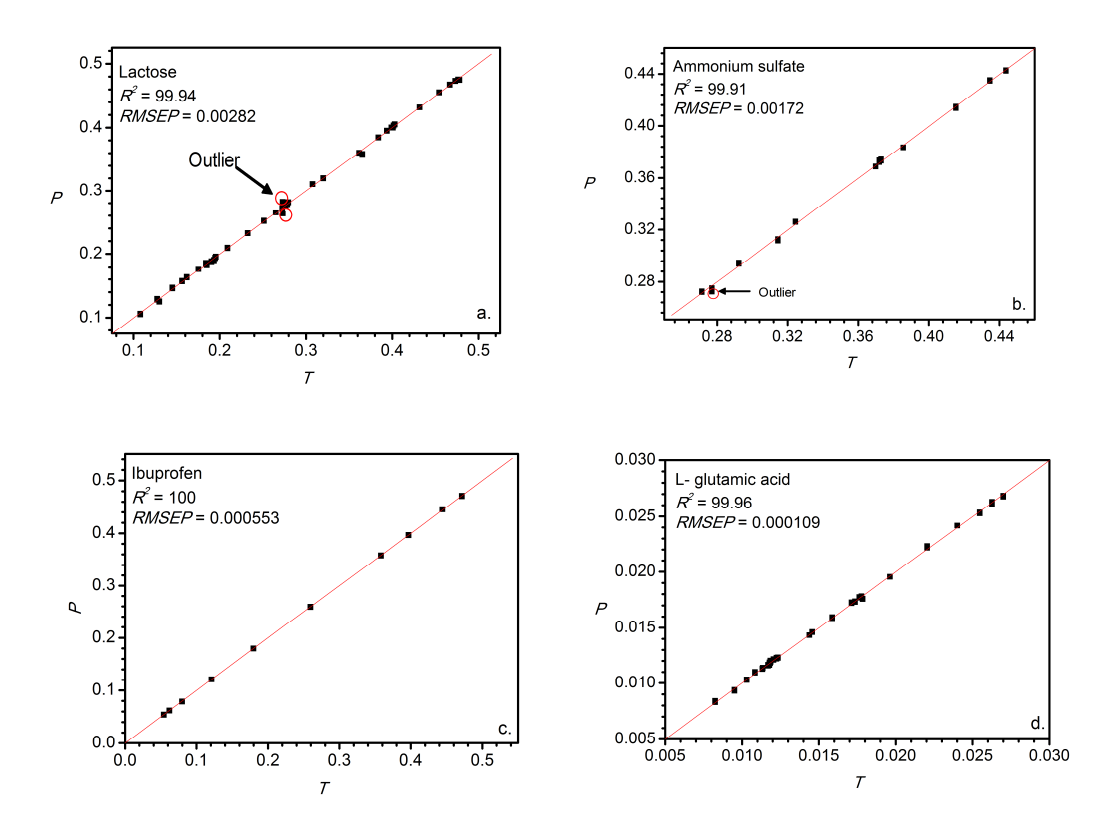


Figure 4.8: Prediction (*P*) vs True (*T*) graphs (wt.frac.) for MIR.

The predictions for the sample marked with circle in Figure 4.8 are the outliers as their concentration prediction differs from actual concentration by more than 2.5 times the *RMSEP*. The outliers represent the advantage that multivariate data analysis brings. Multivariate data analysis not only marks the sample carrying unexpected component as outliers but also allows modeling of the presence of potential interference. This helps in accurate predictions of the solute concentration.³⁸

As can be seen from Figures 4.8 and 4.9, the PLS model displayed extremely good prediction vs true fits with the R^2 value more than 99.8 % (except for NIR L-glutamic acid). Most of the studies carried out for MIR and NIR in which calibration data was collected in homogeneous liquid phase ^{15, 29-31, 39-41} have reported R^2 values of less than 99% (typically in the range of 70-95%).

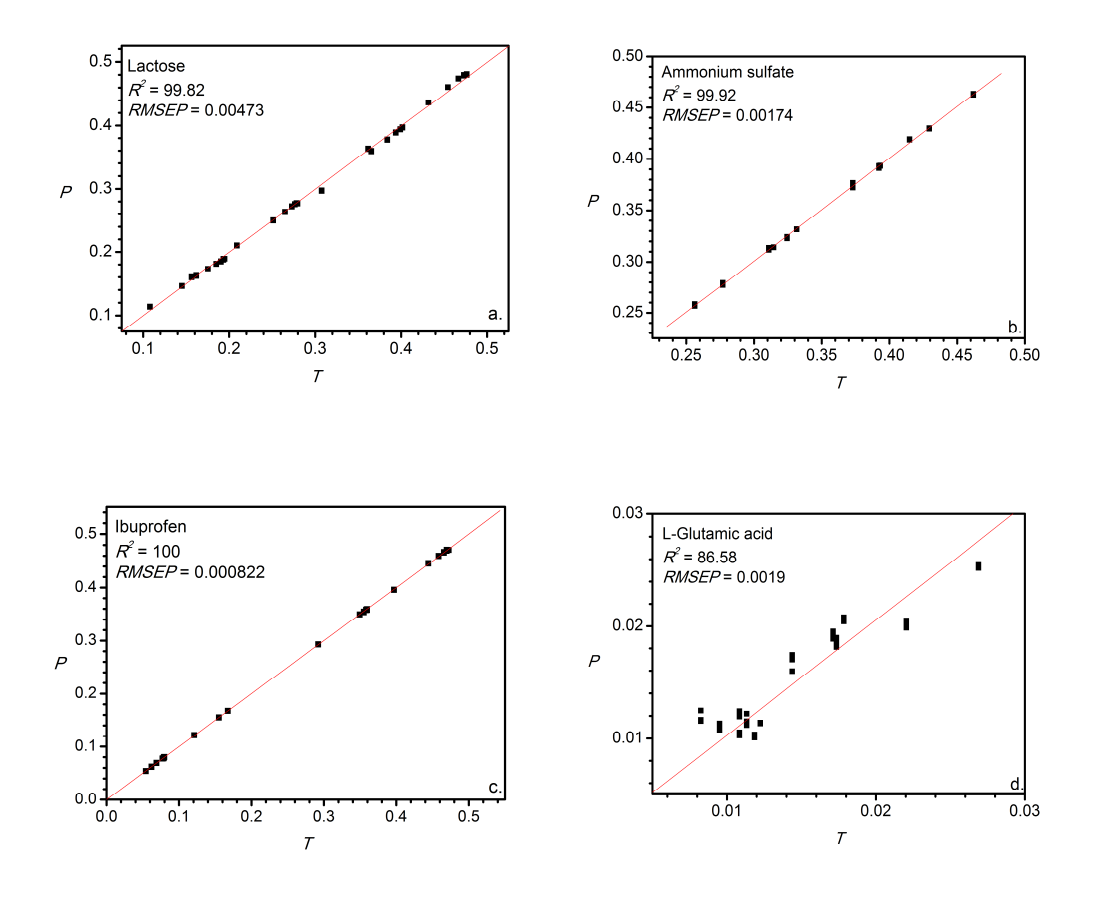


Figure 4.9: Prediction (*P*) vs True (*T*) graphs (wt.frac.) for NIR.

4.3.3 Solubility curve determination

As can be seen in Figure 4.10 the solubility curve determined for α -lactose monohydrate by the MIR model is in excellent agreement with the one reported in the literature.

The average relative error observed for the MIR was 1.9%. On the other hand, the NIR was not as good as the MIR and had an average relative error of 10%. The high deviation of the NIR model could be attributed to the fouling of the NIR probe as shown in Figure 4.11.

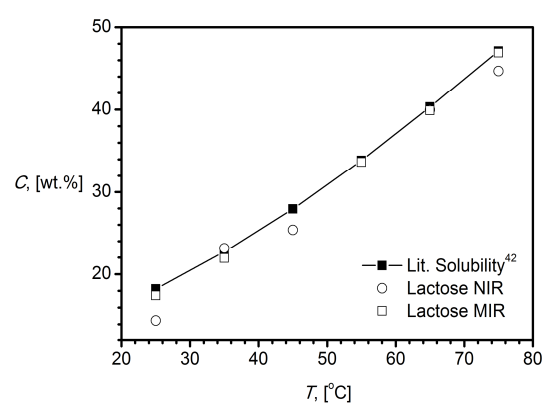


Figure 4.10: α - lactose monohydrate (Lactose) solubility curve.

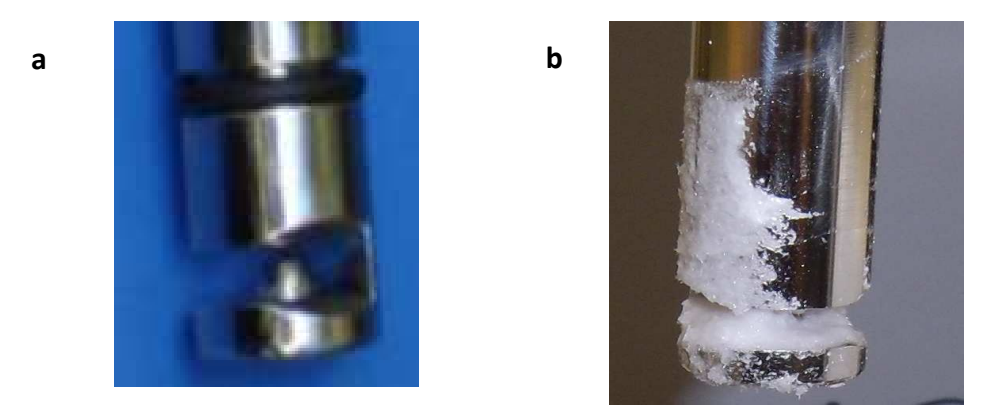


Figure 4.11: Unfouled NIR probe (a) and fouled NIR probe (b)

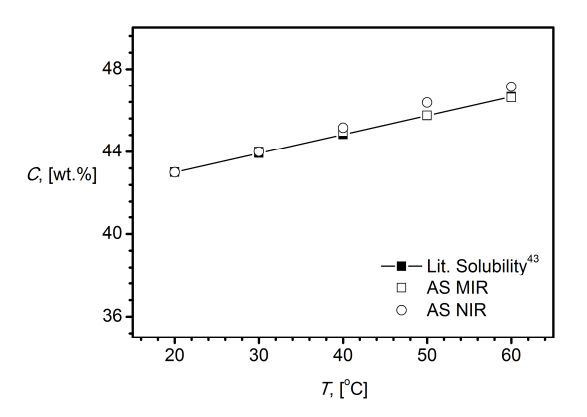


Figure 4.12: Ammonium sulfate (AS) solubility curve.

For ammonium sulfate, both the MIR and the NIR models displayed tremendously improved accuracy compared to α - lactose monohydrate as shown in the Figure 4.12. Compared to the solubility values reported in literature⁴³ the maximum relative error for MIR model was 0.28% and that for NIR model was 1.38%.

Fouling with the ammonium sulfate crystals was not as pronounced as for lpha -lactose monohydrate crystals.

For ibuprofen, the solubility curve determined by MIR model is in good agreement with the solubility values determined experimentally by using the Crystal16 multiple reactor setup (Avantium Technologies). The Crystal16 uses turbidity measurements to determine the phase change. The average relative error for the MIR was 2.18% while that for the NIR was 11.1%

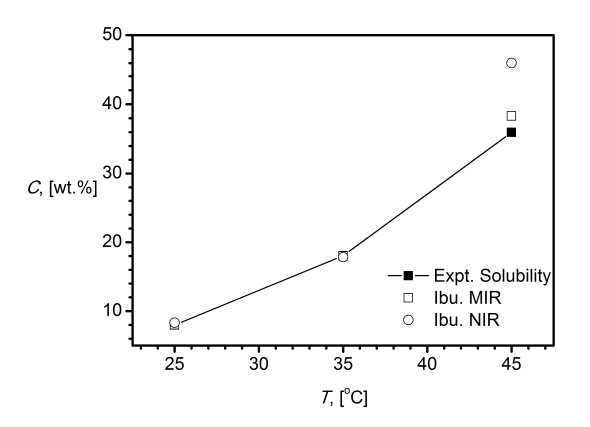


Figure 4.13: Ibuprofen (Ibu.) solubility curve

Fouling of the NIR probe was pronounced with Ibuprofen as well.

The solubility values of L-glutamic acid in literature vary a lot. Models were prepared based on reference 44. The average relative error in the solubility values was 1% for the MIR while for the NIR it was 38.33%.

The reason for a large average relative error for NIR with L-glutamic acid could again be the fouling of the probe. Normally, NIR spectra do not have distinct peaks in the spectrum. But with L-glutamic acid, those peaks were very distinctly seen during the solubility measurements because of the fouling. They are presented in Figure 4.15.

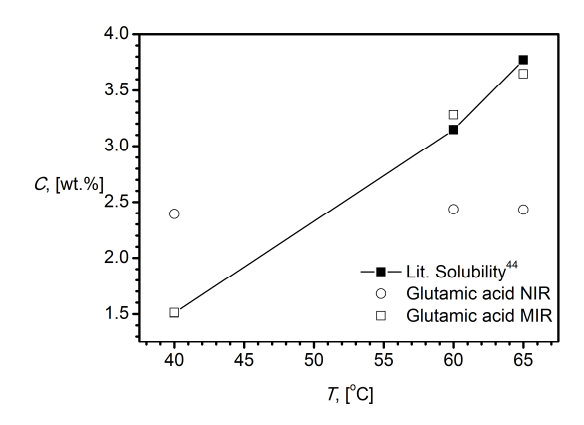


Figure 4.14: L-glutamic acid (Glutamic acid) solubility curve

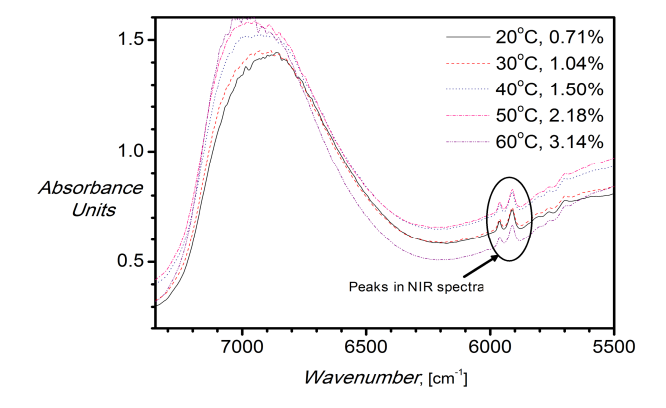


Figure 4.15: Peaks in L-glutamic acid NIR spectra.

The presence of these peaks indicated that the spectra collection was severely affected in presence of crystals. Usage of these spectra in determining solubility concentrations led to an error.

4.3.4 Batch experiments

An undersaturated solution of ammonium sulfate under the conditions mentioned in Table 4.3 was cooled linearly at cooling rate of 0.5 °C/min. During the process, both MIR and NIR were used to predict the concentration values. It was observed that the concentration stayed constant while the crystallizer was being cooled until the nucleation detection. In this time the supersaturation kept on building until 62 minutes after which it dropped sharply due to nucleation. This characteristic event was captured precisely by both the instruments as seen in Figure 4.16 as was verified by visual observations as well.

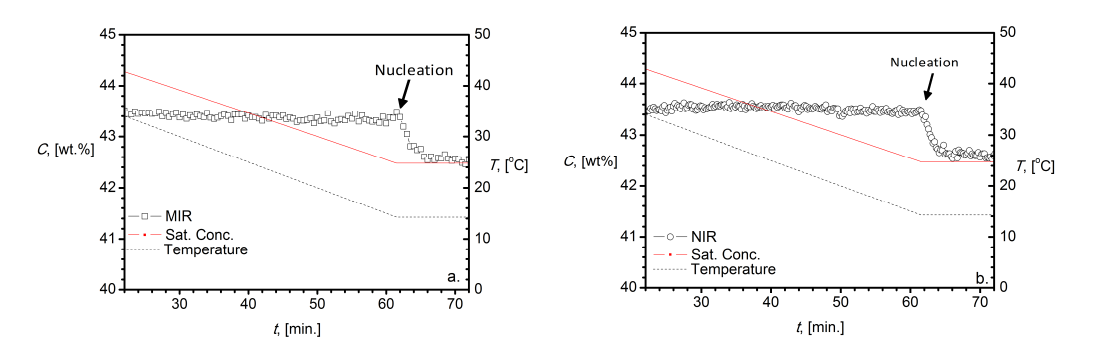


Figure 4.16: Ammonium sulfate batch experiment MIR (a) and NIR (b).

Similar cooling conditions were imposed on ibuprofen in hexane. Both probes were able to detect correct initial concentration and also the nucleation point as seen in Figure 4.17. This was confirmed with visual observation. Solubility of ibuprofen has exponential relation with temperature and increases very rapidly with it. So when the solution was cooled, large amounts of ibuprofen crystallized resulting into the solidification of most of the crystallizer content. The stirrer was not able to stir anymore. At this condition, collection of spectra was terminated.

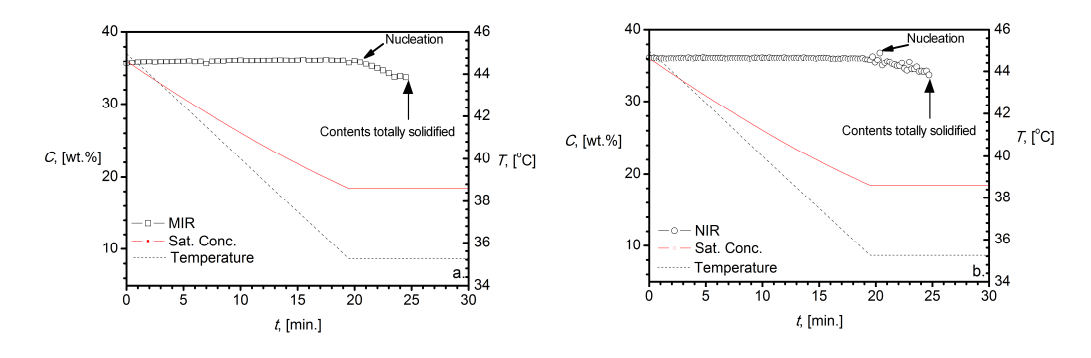


Figure 4.17: Ibuprofen batch experiment MIR (a) and NIR (b).

For L-glutamic acid, the initial concentration was predicted well by both the MIR and the NIR as can be seen in Figure 4.18. The solution was cooled to 35 °C and was allowed to stay at this temperature. After approximately 90 minutes, there was a nucleation event after which the concentration decreased rapidly. The nucleation event was detected by both the probes simultaneously. The concentration values predicted by both MIR and NIR where within the error range specified in Figures 4.8 and 4.9 until the nucleation point.

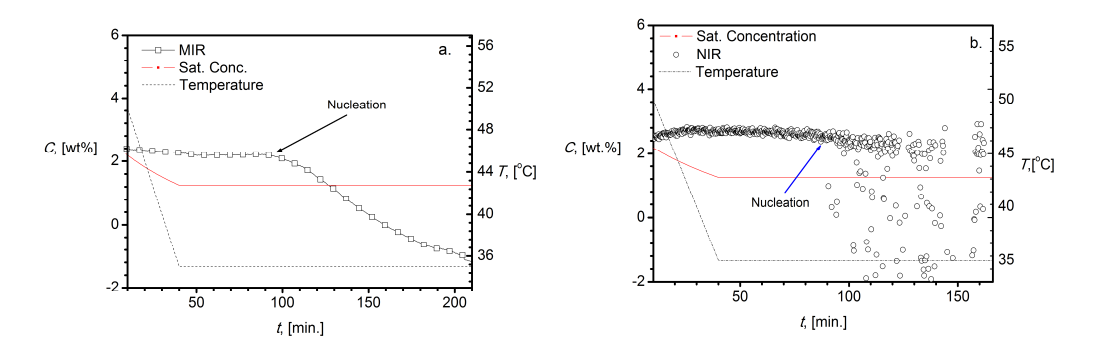


Figure 4.18: L-Glutamic acid batch experiment MIR (a) and NIR (b).

But surprisingly after nucleation, the concentration did not stabilize along the saturation concentration. The measured concentration went on decreasing even beyond 0%. This might be due to the crystallization of L-glutamic acid on the probe surface which leads to the shifting of the spectra in upward direction as shown in Figure 4.19. The distributed nature of NIR predictions after nucleation could be due to the solids interfering in the optical path length of the radiation.

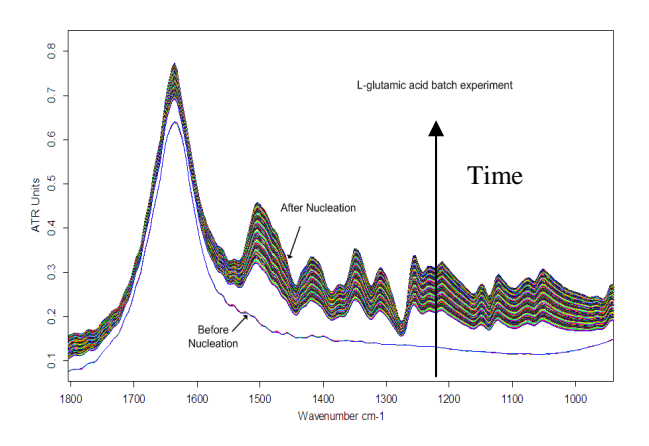


Figure 4.19a: Shifting of MIR spectra after nucleation.

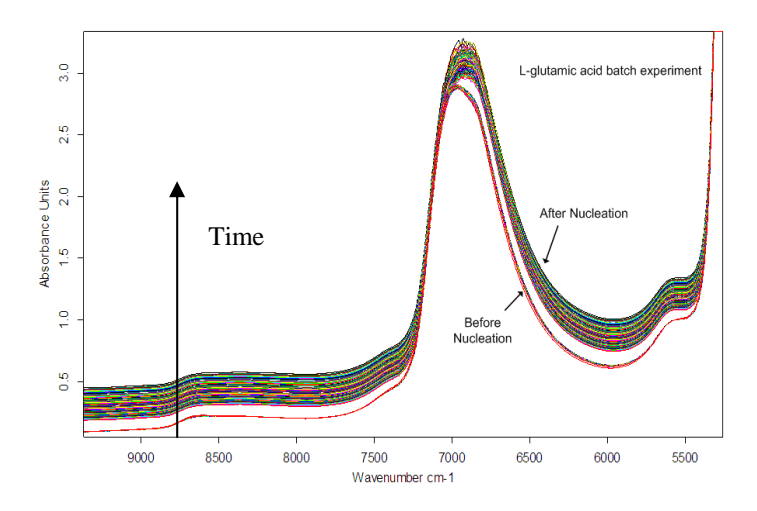


Figure 4.19b: Shifting of NIR spectra after nucleation.

4.3.5 Associated problems

Both the MIR and the NIR are quite sophisticated techniques. They can provide a lot of valuable information if implemented correctly. But their proper implementation in crystallization experiments is not an easy task. The final spectra for both the techniques are obtained by dividing the sample channel scan by the background channel scan. These scans, especially the background scan for MIR is sensitive to the temperature at which it is collected and the stresses in the fiber optics during collection. This implies that if the position of the probe is changed during the experiment or if the temperature changes along the length of the fiber optics, a shift in spectra may occur. The extent of the error caused in final prediction may depend on the intensity of these changes. However, it must be noted that most of these changes can be taken care of by applying suitable preprocessing steps.

4.4 Conclusions

The comparison of MIR and NIR for four different crystallizing systems viz. α -lactose monohydrate in water, ammonium sulfate in water, ibuprofen in hexane, and L-glutamic acid in water has been successfully performed. It was found that MIR performs better in pure liquid as well as in vicinity of crystals and is more accurate. On the other hand, it is more sensitive to the stresses in the fiber optics. Although NIR has comparable performance in pure liquid, it suffers in the presence of crystals as it is

more susceptible to fouling. Also the spectra collection for NIR is affected due to the crystals in the path of the radiations. The performance of both techniques is dependent on the crystallizing systems.

As MIR spectrum consists of distinct peaks, it provides a distinct advantage in selecting regions of interest while developing the PLS models. The NIR spectrum consists of broad bands resulting from the overtones and the combination vibrations and hence chemometrics must be relied on in selecting regions of interest.

During the experiments of determining solubilities in the presence of crystals, the average relative errors for MIR were around 2% while they were considerably higher for NIR due to crystals in path of the radiations. Hence, in order to use the NIR probe appropriately, more care must be taken to create ideal hydrodynamic conditions. During batch cooling experiments, both probes are susceptible to fouling due to primary nucleation on the probe surface. The extent of scaling depends on the crystallizing system. In all cases, it was observed that the MIR is less prone to fouling than the NIR.

Hence based on this study, it can be concluded that the MIR shows higher potential than NIR to monitor concentration during crystallization processes.

4.5 References

- (1) Tavare, N.S. In *Industrial Crystallization-Process Simulation Analysis and Design*; Eds.; Plenum Publishing Corporation: New York, 1995.
- (2) Helt, J.E.; Larson, M.A., Effects of temperature on the crystallization of potassium nitrate by direct measurement of supersaturation. *AIChE Journal*. 1977, 23, 822-830.
- (3) Hlozny, L.; Sato, A; Kubota, N. *J.*, On-Line Measurement of Supersaturation during Batch Cooling Crystallization of Ammonium Alum. *Journal of Chemical Engineering of Japan* 1992, 25, 604-606.
- (4) Gutwald, T.; Mersmann, A. Batch cooling crystallization at constant supersaturation: Technique and experimental results. *Chemical Engineering & Technology* 1990, 13, 229-237.
- (5) Lewiner, F.; Klein, J.P.; Puel, F.; Fevotte, G. On-line ATR FTIR measurement of supersaturation during solution crystallization processes. Calibration and

- applications on three solute/solvent systems. *Chemical Engineering Science* **2001**, 56, 2069-2084.
- (6) Perry, R.H.; Green, D.W. In Chemical Engineers Handbook; McGraw Hill: 2007.
- (7) Doki, N.; Kubota, N.; Sato, A.; Yokota, M. Effect of cooling mode on product crystal size in seeded batch crystallization of potassium alum. *Journal of Chemical Engineering of Japan* 2001, *81*, 313-316.
- (8) Moscosa-Santilla'n, M.; Bals, O.; Fauduet, H.; Porte, C.; Delacroix, A., Study of batch crystallization and determination of an alternative temperature-time profile by on-line turbidity analysis application to glycine crystallization. *Chemical Engineering Science* 2000, 55, 3759-3770.
- (9) Wang, F.; Berglund, K. A., Monitoring pH Swing Crystallization of Nicotinic Acid by the Use of Attenuated Total Reflection Fourier Transform Infrared Spectrometry. *Industrial & Engineering Chemistry Research* 2000, 39, 2101-2104.
- (10) Monnier, O.; Fevotte, G.; Hoff, C.; Klein, J. P., Model identification of batch cooling crystallizations through calorimetry and image analysis. *Chemical Engineering Science* 1997, 52, 1125-1139.
- (11) Rozsa, L., Sugar crystallization: look for the devil in the details Part 2. *International Sugar Journal* 2008, 110, 729-739.
- (12) Dunuwila, D. D.; Berglund, K. A., ATR FTIR spectroscopy for in situ measurement of supersaturation. *Journal of Crystal Growth* 1997, 179, 185-193.
- (13) Togkalidou, T.; Fujiwara, M.; Patel, S.; Braatz, R.D., Solute concentration prediction using chemometrics and ATR-FTIR spectroscopy. *Journal of Crystal Growth* 2001, 231, 534-543.
- (14) Derdour, L.; Fe'votte, G.; Puel F.; Carvin, Real-time evaluation of the concentration of impurities during organic solution crystallization. *Powder Technology*, 2003, 129, 1-7.
- (15) Borissova, A.; Khan, S.; Mahmud, T.; Roberts, K. J.; Andrews, J.; Dallin, P.; Chen, Z.-P.; Morris, In Situ Measurement of Solution Concentration during the Batch Cooling Crystallization of l-Glutamic Acid using ATR-FTIR Spectroscopy Coupled with Chemometrics. *Crystal Growth & Design* 2009, 9, 692–706
- (16) Hojjati, H.; Rohani, S., Measurement and Prediction of Solubility of Paracetamol in Water–Isopropanol Solution. Part 1. Measurement and Data Analysis. *Organic Process Research & Development*, 2006, 10, 1101-1109.
- (17) O'Sullivan, B.; Glennon, B, Application of in Situ FBRM and ATR-FTIR to the Monitoring of the Polymorphic Transformation of d-Mannitol. *Organic Process Research & Development* 2005, 9, 884-889.

- (18) Zhou, G.X.; Crocker, L.; Xu, J.; Tabora, J.; Zhihong, G., In-line measurement of a drug substance via near infrared spectroscopy to ensure a robust crystallization process. *Journal of Pharmaceutical Sciences* 2006, 95, 2337-2347.
- (19) Howard K.S.; Nagy, Z.K.; Saha, B.; Robertson, A.L.; Steele, G.; Martin, D., A Process Analytical Technology Based Investigation of the Polymorphic Transformations during the Antisolvent Crystallization of Sodium Benzoate from IPA/Water Mixture. *Crystal Growth & Design* 2009, 9,3964–3975.
- (20) Bakar, M. R. A.; Nagy, Z. K.; Rielly, C.D., Seeded Batch Cooling Crystallization with Temperature Cycling for the Control of Size Uniformity and Polymorphic Purity of Sulfathiazole Crystals. *Organic Process Research & Development* 2009, 13(6), 1343-1356.
- (21) Simon, L.L.; Nagy, Z.K.; Hungerbuhler, K., Comparison of external bulk video imaging with focused beam reflectance measurement and ultra-violet visible spectroscopy for metastable zone identification in food and pharmaceutical crystallization processes. *Chemical Engineering Science* 2009, 64(14), 3344-3351.
- (22) Nagy, Z. K., Model based robust control approach for batch crystallization product design. *Computer & Chemical Engineering* 2009, 33(10), 1685-1691.
- (23) Fujiwara, M.; Chow, D.L.; Braatz, R.D., Paracetamol Crystallization Using Laser Backscattering and ATR-FTIR Spectroscopy: Metastability, Agglomeration, and Control. *Crystal Growth & Design* 2002, 2 363–370.
- (24) Thompson, D.R.; Kougoulos, E.; Jones, A.G.; Wood-Kaczmar, M.W., Solute concentration measurement of an important organic compound using ATR-UV spectroscopy. *Journal of Crystal Growth* 2004, 276, 230-236.
- (25) Bjørsvik, H.R., Online Spectroscopy and Multivariate Data Analysis as a Combined Tool for Process Monitoring and Reaction Optimization. *Organic Process Research & Development* 2004, 8, 495-503.
- (26) Settle, F.A. *Handbook of Instrumental Techniques for Analytical Chemistry*, Prentice Hall: New Jersey,1997
- (27) Geladi, P.; Kowalski, B.R., Partial least-squares regression: a tutorial *Analytica Chimica Acta* 1986, 186, 1-17.
- (28) Brown, S.D.; Sum, S.T.; Despagne, F.; Lavine, B.K., Chemometrics. *Analytical Chemistry*, 1996, 68, 21-62.
- (29) Chung. H.; Ku, M.; Lee, J., Comparison of near-infrared and mid-infrared spectroscopy for the determination of distillation property of kerosene. *Vibrational Spectroscopy* 1999, 20, 155-163.
- (30) Cooper, J.B.; Wise, K.L.; Welch, W.T.; Sumner, M. B., Wilt, B.K.; Bledsoe, R.R., Comparison of Near-IR, Raman, and Mid-IR Spectroscopies for the

- Determination of BTEX in Petroleum Fuels. *Applied Spectroscopy* 1997, 51, 1613-1620.
- (31) Felicio, C.C., Comparison of PLS algorithms in gasoline and gas oil parameter monitoring with MIR and NIR. *Chemometrics & Intelligent Laboratory Systems* 2005, 78, 74-80.
- (32) Vissers, R. A. *Crystal Growth Kinetics of Alpha Lactose Hydrate*, PhD Thesis, University of Nijmegen, The Netherlands, 1983.
- (33) Raghavan, S.L.; Ristic, R.I.; Sheen, D.B.; Sherwood, J.N., The bulk crystallization of α -lactose monohydrate from aqueous solution. *Journal of Pharmaceutical Science* 2001, 90, 823-832
- (34) Quant, User Manual, OPUS Spectroscopy Software Version 6, 2006, Bruker Optik, GmbH.
- (35) Priddy, K. L.; Keller, P. E. *Artificial Neural Networks: An introduction*, SPIE- The International Society for Optical Engineering, Washington, 2005.
- (36) Griffiths, P. R.; de Haseth, J. A. Fourier Transform Infrared Spectroscopy, 2nd Edition, John Wiley and Sons Inc., Hoboken, New Jersey, 2007.
- (37) Larote D.T. *Discovering knowledge in data: An Introduction to Data Mining, John Wiley and Sons Inc., Hoboken, New Jersey, 2005.*
- (38) Olivieri, A.C., Analytical Advantages of Multivariate Data Processing. One, Two, Three, Infinity? *Analytical Chemistry* 2008, 80, 5713-5720.
- (39) Karoui, R.; Mounem, A.; Dufour, E.; Pillonel, L.; Shcaller, E.; Picque, D.; De Baerdemaeker, J.; Bosset, A comparison and joint use of NIR and MIR spectroscopic methods for the determination of some parameters in European Emmental cheese. *European Food Research & Technology* 2006, 223, 44-50.
- (40) Reid, L. M.; Woodcock, T.; Donnell, C. P. O.; Kelly, J. D.; G. Downey, Differentiation of apple juice samples on the basis of heat treatment and variety using chemometric analysis of MIR and NIR data. *Food Research International* 2005, 38, 1109-1115.
- (41) Bras, L.P.; Bernardino, S.A.; Lopes, J.A.; Menezes, J.C., Multiblock PLS as an approach to compare and combine NIR and MIR spectra in calibrations of soybean flour. *Chemometrics & Intelligent Laboratory Systems* 2005, 75, 91-99.
- (42) Rajah, K.K. et. al. *The Alm Guide lactose Properties and Uses*, Association of Lactose Manufacturers, 1988.
- (43) Daudey, P.J. Crystallization of Ammonium Sulphate- Secondary Nucleation and Growth Kinetics in Suspension, PhD Thesis, Technical University of Delft, The Netherlands, 1987.

(44) Sembira-Nahum, Y.; Apelblat, A.; Manzurola, E., Volumetric Properties of Aqueous Solutions of L-Glutamic Acid and Magnesium-L-Glutamate. *Journal of Solution Chemistry* 2008, 37, 391-401.

Chapter 5

Rapid Online Calibration for ATR-FTIR spectroscopy

This chapter is published as:

Kadam, S. S., Mesbah, A., van der Windt, E., Kramer, H. J. M. "Rapid Online Calibration for ATR-FTIR Spectroscopy during Batch Crystallization of Ammonium Sulfate in a Semi-Industrial Scale Crystallizer." Chem. Eng. Res. Des., 2011, 89, 995-1005.

The knowledge of solute concentration throughout a batch crystallization process is essential from process control perspective. Despite the progress in Process Analytical Technology (PAT), there still exist several challenges for online measurement of solute concentration at industrial scale. In this study, concentration monitoring was realized using attenuated total reflectance Fourier transform infrared (ATR-FTIR) spectroscopy at lab as well as semi-industrial scale. Applications of the calibration model developed at lab scale for the measurements at the semi-industrial scale however resulted into strongly biased concentration predictions, caused by the differences in the curvature of fiber optics and the uneven thermal expansion of the probe. Therefore an alternative rapid online calibration method was developed during the start-up phase of the process. With this method, the time required for developing a working calibration model for concentration monitoring during crystallization of ammonium sulfate in a semi-industrial scale draft tube crystallizer has been reduced approximately by 90%. With the help of simultaneous concentration and crystal size distribution measurements at semi-industrial scale, the descriptive capability of the model was improved due to better kinetic parameters.

5.1 Introduction

Crystallization is an important unit operation which determines the product quality in the pharmaceutical, specialty, fine and agrochemicals industry. Generally, the crystal quality is defined in terms of the purity, size and shape distribution, polymorphic fraction, etc.¹ These properties are highly dependent on the operating conditions in the crystallizer. A small variation in these properties may affect the efficiency of the downstream processing units and the product performance.^{2, 3} Hence, an effective control over these properties and in turn the crystallization process is essential.

In recent years, with the developments in the computing power and the in situ monitoring of the process variables like crystal size distribution (CSD) and concentration, two distinct control approaches have evolved. One of these approaches (model-free) requires determination of a supersaturation profile (generally experimental) which seeks a trade-off between crystal quality and process productivity. The supersaturation profile determined in this way is always near-optimal. Once the supersaturation profile has been determined, a control strategy is devised which maintains the desired relation between the system states, viz. concentration and temperature, along the predefined supersaturation profile.⁴⁶ The other approach (model-based) relies on the model developed with the population balance,⁷ conservation laws and kinetic expressions.^{2, 8, 9} This model is used in an optimization framework wherein the objective function, generally related to the CSD, is used to obtain a desired supersaturation profile.¹⁰ The performance of the model based controller depends on the model structure and the precise determination of the kinetic parameters which in turn is dependent on the CSD and the concentration profile.

Accurate measurement of the process variables is a pre-requisite for employing advanced control strategies. Several techniques exist for monitoring of concentration and CSD during a crystallization process. Their relative merits and demerits are summarized in the literature.^{11, 12} In recent years, techniques based on imaging are finding increased applications in monitoring process conditions during crystallization. The real-time images of the crystal slurry provide not only quantitative information like CSD for spherical¹³ and non-spherical particles^{13, 14} but also qualitative information like change in morphological form during crystal growth¹⁵ and onset of nucleation.¹⁶⁻¹⁸ The information obtained by imaging can also be integrated in the supersaturation control strategies to obtain better product quality.¹⁹

As a first step towards better product quality, it is essential to monitor concentration accurately at industrial scale. Many researchers have already confirmed that the attenuated total reflectance (ATR) Fourier transform infrared (FTIR) spectroscopy is well suited for concentration monitoring during crystallization.^{11, 20-23} However, its proper implementation requires time consuming calibration work.^{24, 25}

Calibration of ATR-FTIR for concentration monitoring during crystallization process is generally performed by collecting several spectra methodically at different concentrations and temperatures. The spectra are collected either by varying temperatures while keeping the concentration constant²⁶ or vice versa²². Based on these spectra, a Partial Least Square (PLS)²⁷ calibration model is developed that can predict concentration. As the spectra collection is usually done at lab scale, it would be of great interest for the industrial community to verify if the PLS model developed in the lab performs as expected at the industrial scale.

In this contribution we examine the feasibility of the ATR-FTIR spectroscopy for concentration monitoring at semi-industrial scale. In sections 5.4.1-5.4.3, we first present the feasibility of ATR-FTIR spectroscopy for concentration monitoring at lab scale during the batch crystallization process of ammonium sulfate from its aqueous solution. Having done that, we discuss the problems associated with the use of the PLS model developed at the laboratory scale on a semi-industrial scale set-up for the same instrument in section 5.4.4 and then present a method for rapid online calibration which avoids these problems in section 5.4.5. To the best of our knowledge, the attempt was made for the first time to demonstrate this technique on a semi-industrial scale crystallizer. Finally in section 5.4.6, we demonstrate the solute concentration monitoring at pilot plant with ATR-FTIR and show that this process information together with the on-line CSD measurements can lead to better kinetic parameter estimates and enhanced process understanding.

5.2 Experimental details

5.2.1 Set ups

Experiments were performed both on lab and semi-industrial scales.

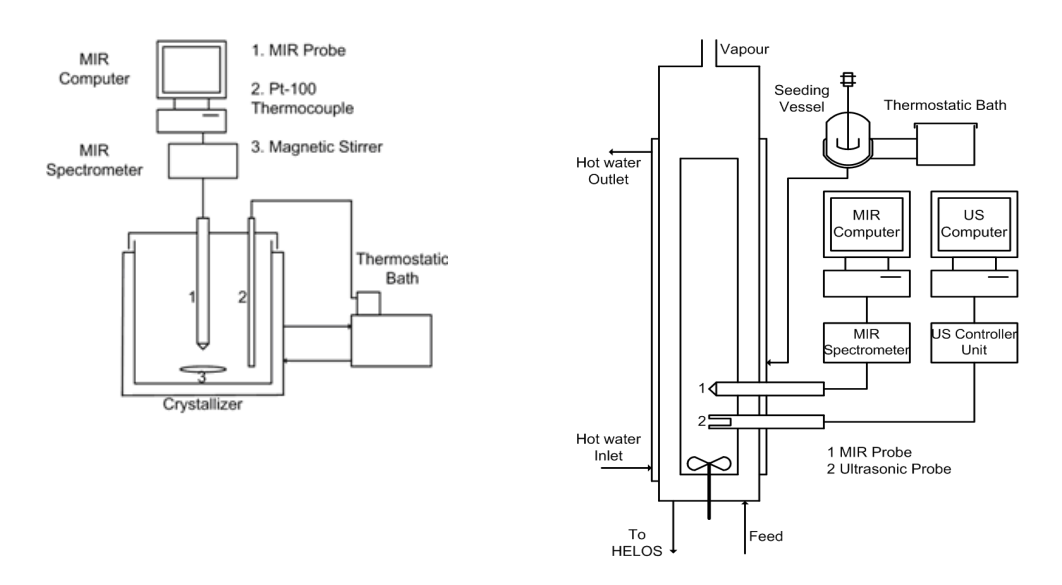


Figure 5.1a: Lab scale set-up.

Figure 5.1b: Semi-industrial scale set-up.

Lab scale

The set-up at lab scale was used to carry out the calibration of ATR-FTIR, the subsequent validation of the developed calibration model in the presence of crystals and the batch cooling crystallization experiments. It consisted of a 1 L jacketed glass crystallizer as shown in Figure 5.1a, connected to a Lauda RK8KP thermostatic bath which maintained and controlled the temperature inside the crystallizer with the help of an external platinum resistance thermocouple Pt-100. The crystallizer was maintained well mixed by an IKA RET basic C magnetic stirrer. The gold plated hastelloy ATR probe with diamond internal reflection element (IN 350 T) connected to MATRIX-MF spectrometer from Bruker Optics GmbH was inserted from the lid. The spectrometer has tightly controlled environment with very minimal effect of water vapor in the path length of the beam. Hence, nitrogen flushing of the spectrometer was not performed.

Semi-industrial scale

The experiments at semi-industrial scale were carried out isothermally at 50 °C in a 75 L seeded fed-batch evaporative draft tube crystallizer shown in Figure 5.1b. The fed-batch operation was implemented to compensate for the losses of the crystallization volume by evaporation of the solvent and sampling of the slurry. Hence the crystallizer was continuously fed with the crystal free feed stream containing saturated ammonium sulfate solution at 50 °C. The crystallizer was equipped with an on-line laser diffraction instrument (HELOS-Vario, Sympatec) to measure evolution of the product CSD during the batch. A small product flow was withdrawn from the crystallizer at regular time intervals and was diluted with saturated feed solution to facilitate the CSD measurements. The in situ concentration monitoring was done simultaneously by an ultrasonic (US) probe (LiquiSonic 20, SensoTech) and the same ATR-FTIR instrument used during the lab experiments. The US probe can monitor the concentration till the seeding point only as it cannot work in the presence of crystals.

5.2.2 Procedures

Lab scale calibration

Two common calibration approaches are described in the literature. In one of the approaches the temperature is kept constant while the concentration is changed by dilution with known amount of solvent.²² In the other approach, the concentration is kept constant while the temperature is changed till nucleation is detected.²⁶ The constant concentration approach allows collection of the spectra in undersaturated as well as supersaturated regions. But care must be exercised in using this approach as it might be difficult to apply for the crystallizing systems which have narrow metastable zone widths and for systems which tend to nucleate on the crystallizer walls and the in situ probes. If the solute nucleates on the wall of the crystallizer or the probe, the nucleation would not be detected even by a sensitive in situ particle size measurement instrument resulting in a faulty calibration. In order to avoid the complexities associated with the second calibration approach, a simple dilution based calibration²² was used during this work. The details of the temperatures and concentrations used in the calibration experiment are given in appendix.

The background scan was collected in air at room temperature for the calibration process. Air was chosen over crystal free solvent as the spectrum of the solvent is

extremely sensitive to temperature variations. Details regarding motivation for using background spectrum in air can be found in the appendix. The spectra were collected over 4000-650 cm⁻¹ with resolution of 8 cm⁻¹. Each spectrum consisted of 16 co-added scans. Based on 114 spectra at four different temperatures, a single partial least square (PLS)²⁷ model was developed using the software OPUS provided by Bruker Optik GmbH. 70% of the spectra collected during calibration were used as a training set while the remaining 30% were used as a test set. The model was constructed by selecting the following three spectral regions, 3633.7-3271.1 cm⁻¹, 2916.2-2194.9 cm⁻¹ and 1836.1-1114.8 cm⁻¹. The spectra were preprocessed by using first derivative and vector normalization.²⁸ The Root Mean Square Error in Prediction (*RMSEP*)²⁹ value was used to assess the quality of the model statistically. It is calculated as

$$RMSEP = \sqrt{\frac{1}{n} \sum_{i=1}^{n} (y_i - y_f)^2}$$
 (5.1)

where y_i is the true concentration value , y_f is the fitted concentration value and n is the number of data points.

Validation of calibration model

Independent data set validation of the developed PLS model was performed by measuring solubility in the presence of crystals at 20, 30, 40, 50 and 60 °C. The concentration values predicted by the PLS model were compared with the values in the literature.³⁰

Batch cooling crystallization

The validated PLS model was used for concentration monitoring in a batch cooling experiment in which, the undersaturated solution at 45 °C with concentration of 43.24 wt% was cooled at 0.5 °C/min. till the cloud point was detected by visual inspection. Once the cloud point was detected, the cooling was stopped and the temperature was maintained constant. Spectra were collected throughout the process after every 30 seconds.

Semi- industrial scale fed-batch evaporative crystallization

The PLS model validated based on the test set and the independent data set was applied for concentration monitoring on the semi-industrial scale set-up. Concentration was also monitored by an US probe. Background spectrum for ATR-FTIR was collected in the empty crystallizer. The motivation for using air as background spectrum is explained in details in the appendix section. Two experiments, viz., Batch 1 and Batch 2 were performed. During Batch 1, the crystallizer was brought to 50 °C and was maintained under vacuum. Saturated crystal free solution prepared in tap water (not in DM water as for the lab scale experiments) at 50 °C was then pumped in the crystallizer. In mean the time 600 g of seeds with size range 90 to 125 µm were aged for 57 minutes in the saturated solution.31 The crystallizer was then brought to a predetermined supersaturation of 0.01443 and seeding was carried out. To control the supersaturation around this predetermined limit, rinse water at 60 °C was added at regular intervals. The heat input to the crystallizer was raised from 4.5 kW to 6 kW after 2000 s, there after the system was excited further by increasing the heat input by 1 kW every 20 minutes till 13 kW. Similar procedure was applied during Batch 2, except for the heat input profile which was constant at 9 kW throughout the experiments and the initial supersaturation which was 0.01627. The ATR-FTIR spectroscope was not available during the Batch 2.

5.3 Process model development and parameter estimation

The mathematical models that describe a batch crystallization process are generally developed based on the dynamic population balance, the conservation laws and the kinetic expressions. For a well-mixed semi-batch crystallizer the one dimensional population balance equation can be written as³²

$$\frac{\partial n(L,t)}{\partial t} + \frac{\partial (G(L,t)n(L,t))}{\partial L} = -\frac{Q_P}{V}n(L,t)$$
(5.2)

with the following boundary and initial conditions

$$n(L_0, t) = \frac{B_0(t)}{G(L_0, t)}, n(L, 0) = n_{seed}$$
(5.3)

where n(L,t) is the number density function (# m⁻³m⁻¹), t is the time (s), L is the characteristic crystal size (m), G(L,t) is the crystal growth rate (ms⁻¹) , Q_P is the unclassified product flow-rate (m³s⁻¹), V is the volume of the crystallizer (m³) and B_0 is the total nucleation rate (#m⁻³s⁻¹).

To complete the model, constitutive equations are necessary for the nucleation and the growth rates. The most commonly used expressions for describing the total secondary nucleation rate and the size independent crystal growth rate of ammonium sulfate are empirical power laws³³

$$B_0 = k_b \mu_3 S^b \tag{5.4}$$

$$G = k_{\scriptscriptstyle g} S^{\scriptscriptstyle g} . \tag{5.5}$$

In the expressions above, $S = C - C_{sat}$ represents the supersaturation, where C is the solute concentration (kg solute/kg solution), C_{sat} is the saturation concentration (kg solute/kg solution) at a given temperature, k_b is the nucleation rate constant (#m⁻⁴), k_g is the growth rate constant (ms⁻¹), b is the nucleation rate exponent and g is the growth rate exponent.

The solute concentration expression for the case of the semi-industrial scale isothermal evaporative crystallizer under consideration was taken from the literature.³⁴

In order to determine the initial crystal size distribution, a log normal volume size distribution is fitted to the first CSD measurement given in equation 5.6

$$v(L,0) = \frac{1}{\ln(\sigma_{g,1})\sqrt{2\pi L}} \exp\left(\frac{\left(\ln\left(\frac{L}{L_{0,g1}}\right)\right)^2}{2\left(\ln\left(\sigma_{g,1}\right)\right)^2}\right). \tag{5.6}$$

The parameter L_{0,g_1} (m) defines the median crystal size and the parameter $\sigma_{g,1}$ (-) is the geometrical standard deviation defining the spread of CSD. It should be noted that the CSD measurements are obtained as the volume density distribution

 $(m_{crystal}^3 m^{-1} m^{-3})$. They are converted to number density distribution before further use.³⁴

The solution of the set of equations 5.2-5.5 and that for the solute concentration would result into the description of the temporal evolution of the crystal size distribution and the solute concentration. As the high order finite volume method in combination with flux-limiting functions³⁵ is able to capture sharp discontinuities and steep moving fronts commonly encountered in the simulation of seeded batch crystallization processes, it was used as the numerical solution technique to solve the population balance equation.³⁶

5.4 Results and Discussions

5.4.1 Spectral features

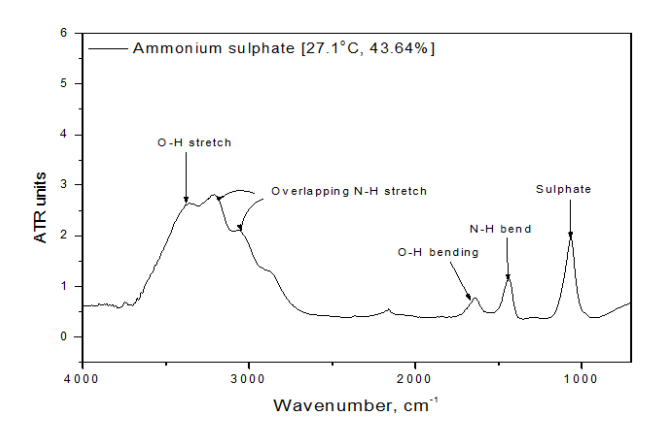


Figure 5.2: Ammonium sulfate-water spectrum.

The representative spectrum collected in aqueous solution of ammonium sulfate by the ATR probe is as shown in Figure 5.2. A broad absorbance region is observed at approximately 3500-2700 cm⁻¹ which consists of an O-H stretch absorption at approximately 3500-3000 cm⁻¹ along with an overlapping band for the N-H stretch at 3300-2700 cm⁻¹. The shoulders on this broad absorption band are due to the solute-solvent interactions. At approximately 1640 cm⁻¹ a band due to water bending is observed. The bands at 1450 and 1000 cm⁻¹ are due to N-H bending and sulfate.

5.4.2 Validation of the PLS model

The developed PLS model was analyzed for possible over-fitting by considering the increase in the co-efficient of determination (R^2) ²⁹ and the decrease in the *RMSEP* with the model rank.³⁷ The variations in these two parameters are plotted in Figure 5.3. Four loadings were used in making the PLS model. As seen from Figure 5.3, rank above four would lead to over-fitting.

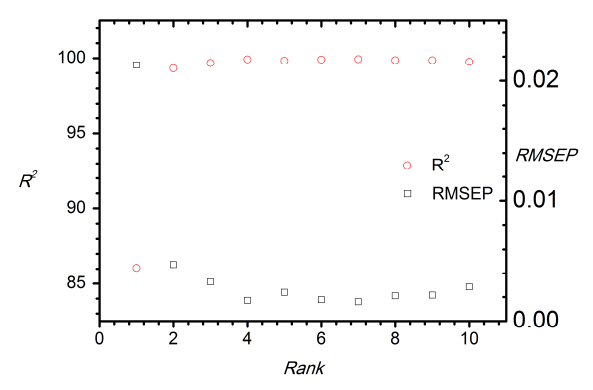
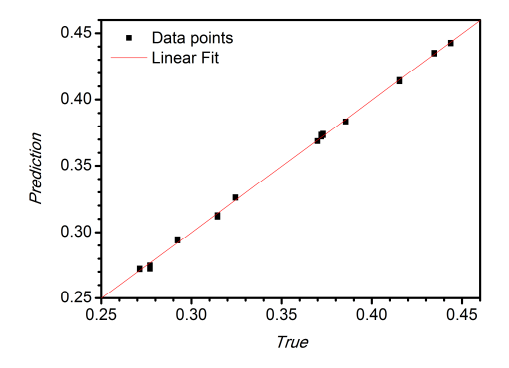


Figure 5.3: Variations in R^2 and RMSEP with model rank.

The results of the statistical and independent data set validation are presented in Figures 5.4a and 5.4b respectively. The units in Figure 5.4a are weight fractions (wt. frac.). The developed PLS model had a *RMSEP* value of 0.00172. It predicted saturation concentration during independent data set validation in the presence of crystals with a maximum relative error of 0.28% compared to the literature.³⁰ This model was used for monitoring concentration during batch cooling crystallization.

5.4.3 Batch cooling crystallization

The concentration profile during the cooling of the undersaturated solution mentioned in section 5.2.2, is depicted in Figure 5.5. As can be seen from Figure 5.5, the PLS model and the ATR probe were able to predict the starting concentration value of 43.24% with good accuracy. The constant concentration trend till nucleation was also successfully captured by the probe and the PLS model.



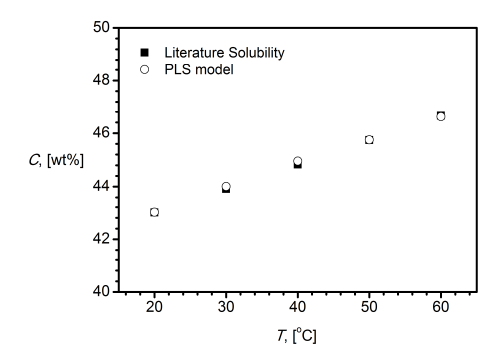


Figure 5.4a: Statistical validation, **Figure 5.4b:** Independent data set *RMSEP*=0.00172. validation.

Furthermore, the nucleation event was detected by the probe and was also confirmed by visual observation. After the nucleation event, there was an exponential drop in the concentration due to crystal growth till the solubility curve. As expected, the concentration stabilized at the saturation concentration for further part of the

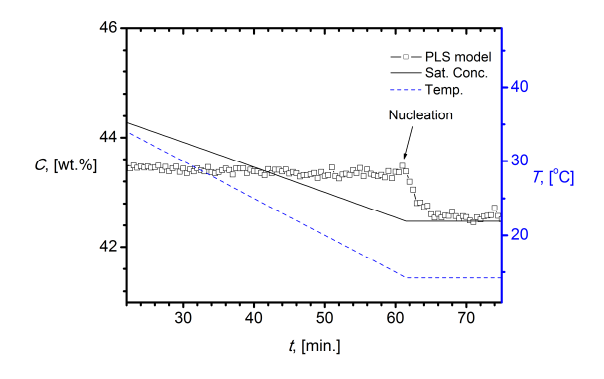


Figure 5.5: Batch cooling experiment at lab scale.

experiment as shown in Figure 5.5.

5.4.4 Semi-industrial experiments

The applicability of the PLS model developed under laboratory conditions was examined for concentration monitoring on semi-industrial scale by comparing the concentration profiles measured by the ATR-FTIR and the US probe till the seeding point. The feasibility of the US probe for concentration monitoring of ammonium sulfate has been established earlier³⁸ and hence it was used as a reference.

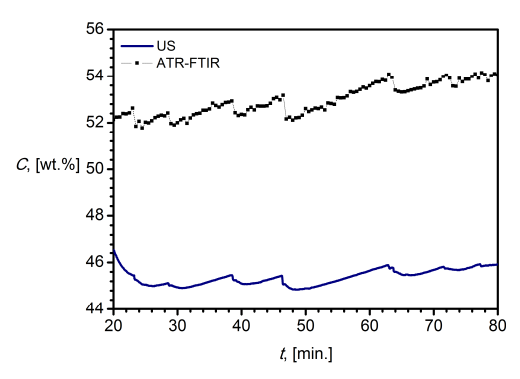


Figure 5.6: ATR-FTIR and US concentration predictions during Batch 1 prior to seeding.

As can be seen from Figure 6, the concentration profile measured by the ATR-FTIR has a similar trend as the one measured by the US probe but the deviation in actual concentration values is as high as 16%. The rises and falls in the concentration values seen in Figure 5.6 are due to the addition of rinse water at regular intervals to control the concentration increase by evaporation.

Three possible reasons for the large deviation of the calculated concentrations by the ATR-FTIR instrument compared to that of the reference profile^{24, 25} have been identified in literature. They are, change in the composition of the samples, change in the instrument response function or the change in the instrument's environment over time. If the spectra collected on lab and pilot plant scale for the same composition and temperature are compared as shown in Figure 5.7, the first possibility, a change in composition of the sample, could be ruled out as there are no extra peaks seen in the spectrum of the liquid phase. Small peaks are seen around 2400 cm⁻¹ due to CO₂ and around 3700 cm⁻¹ due to water vapor but this part of the spectrum has not been used for the PLS model. It must be noted that these peaks do not arise due to background measurement in air, but due to the presence of small amounts of water vapor and CO₂ in the beam path while collecting the sample spectrum.

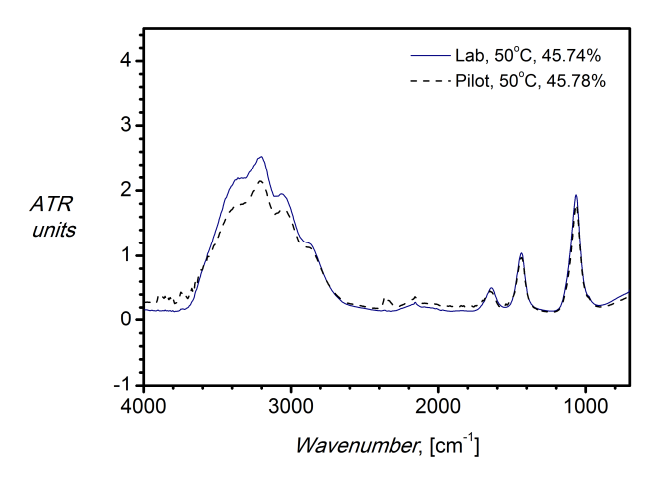


Figure 5.7: Ammonium sulfate - water spectra on lab and semi-industrial scale.

The second possible reason, a change in the instrument response function, is not likely as the same instrument was used in the lab and semi-industrial scale set-up. The third possibility, a change in instrument's environment while using on semi-industrial crystallizer, is more likely. Almost 60% of the ATR probe head was inside the crystallizer which was at 50 °C while the remaining 40% was outside at room temperature. This uneven temperature distribution along the length of the probe induces changes in the characteristic absorptions as the alignment of the optical component is disturbed by the uneven thermal expansion. Furthermore, the intensity can also be altered due to the differences in the curvature of the fiber optics. With the increase in the curve of the fiber optics, the absorption of the radiation inside the fiber increases. This leads to the reduction in the intensity of the radiations available for the measurement. It should be noted that the change in intensity is also in the region of liquid water and N-H bend (not to be confused with water vapor) which has been used in the calibration. Considering these effects, it is obvious that the calibration performed in one set-up may not always be applicable for the concentration monitoring in the other set up.

5.4.5 Online Calibration

One of the proposed alternatives for this would be to do online calibration. Online calibration is referred to the calibration which is performed by collecting spectra during the initial part of the process. This type of calibration ensures that the differences in temperature gradient along the length of the ATR probe and the curvature in the fiber

optics are minimal during calibration and monitoring phase. In this work, online calibration was performed by monitoring the concentration simultaneously by the US probe and the ATR-FTIR. For experimental conditions under consideration, 52 spectra collected in the first 26 minutes (which spanned the concentration and temperature ranges to be encountered during process) of the process were found to be enough to make an entirely new PLS model. The preprocessing of the spectra wasn't necessary and the PLS model based on the spectral range 1836.1 cm⁻¹ to 1473.5 cm⁻¹ was ready within the next 30 minutes. With this approach, the time required to achieve a working calibration model on semi-industrial scale can be reduced substantially by almost 90%. As seen in Figure 5.8 for variation in R^2 and RMSECV, the number of loadings required to achieve this model increased by just one to five, as compared with the lab calibration model. Using more than five loadings would lead to over-fitting for this PLS mode.³⁷

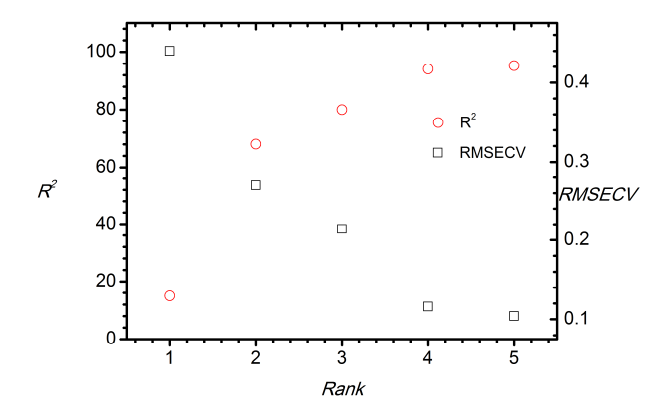


Figure 5.8: Variations in R² and RMSECV with the model rank.

The prediction versus fit data in weight percent is shown in Figure 5.9. The rapidly prepared PLS model had Root Mean Square Error in Cross Validation (*RMSECV*)²⁹ of 0.1%. This error is comparable to the one typically achieved on the lab scale¹¹ and hence for semi-industrial scale it can be termed as reasonably well. The model was validated directly online, by comparing its predictions with the US concentration measurements from 26th minute till the 80th minute (seeding point). It should be noted that the PLS model was developed based on the spectra collected in first 26 minutes only. Thus, the on-line calibration technique is not only efficient but also easy and simple in implementation.

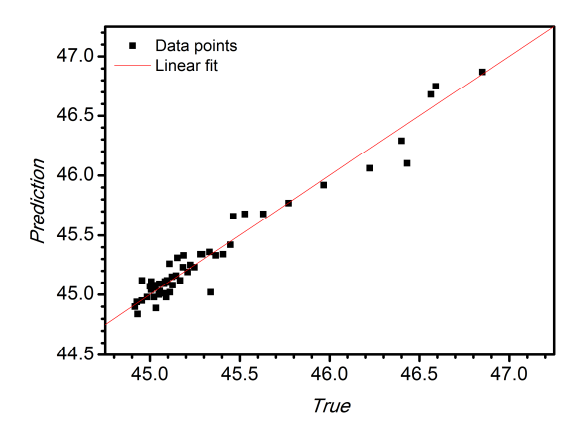


Figure 5.9: PLS model by online calibration, RMSECV=0.10.

The capability of this PLS model to monitor the concentration is shown in Figure 5.10. As can be seen, the concentration profiles predicted by both the ATR and the US probes are in good agreement until the seeding point. After seeding, the concentration measurements by the US failed as expected due to the presence of a second phase. The sharp dips observed in the concentration are due to the addition of rinse water at regular intervals. In spite of the failure of the US probe, ATR probe continued to measure concentration successfully till the end of the process when the concentration stabilized close to the saturation concentration as expected. It should be recalled that there is no effect of the crystals on the concentration measurements by the ATR-FTIR as shown in Figure 5.4b. The peaks seen in the temperature profile are due to the increase in the heat input at regular time intervals.

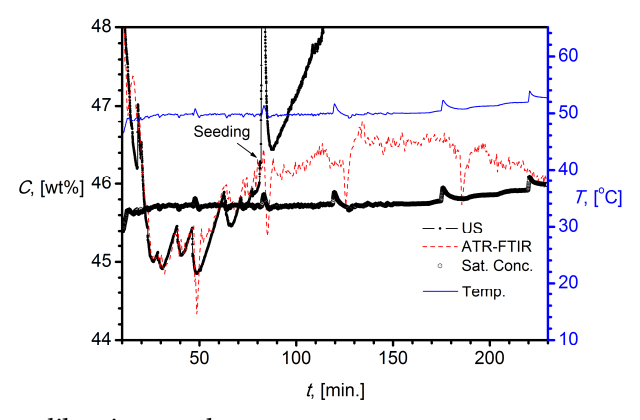


Figure 5.10: Online calibration results.

Based on the good agreement in the concentration predictions between the US probe and the ATR-FTIR until the seeding point, it can be concluded that the online calibration method can be an attractive alternative for calibration in the lab. It avoids the aforementioned calibration problems and the tedious and time consuming calibration procedure.

5.4.6 Parameter estimation and model validation

Precise determination of the kinetic parameters is essential for successful use of the process model for advanced control applications. The parameters were estimated with the help of the online CSD measurements by laser diffraction and the in-situ concentration measurements with the ATR-FTIR spectroscopy during Batch 1. The system was excited by increasing the heat input as shown in Figure 5.11.

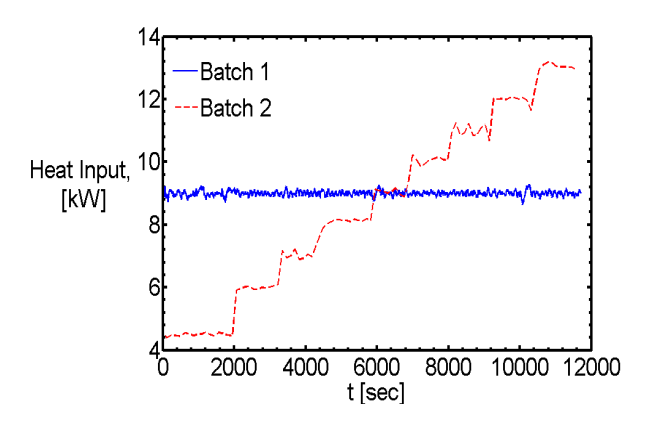


Figure 5.11: Heat input profiles for Batch 1 and 2.

The estimated kinetic parameters were used to arrive at a process model with sufficient descriptive capabilities. The model has been validated by comparing the experimental and the simulated time evolution of the crystal size distribution during Batch 2. The heat input during Batch 2 was kept constant throughout the process as shown in Figure 5.11.

Before estimating the kinetic parameters, the parameters L_{0,g^1} and $\sigma_{g,1}$ of the log normal distribution had to be estimated. They were estimated by fitting the first CSD measurement to the log normal distribution in equation 5.6. As can be seen from the Figure 5.12, there is a good agreement between the experimental and the predicted size

distribution. The estimated values of the parameters for log-normal distribution are given in Table 5.1.

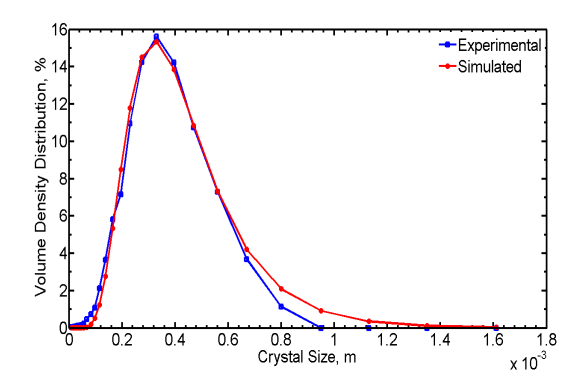


Figure 5.12: Experimental and simulated initial size distributions (immediately after seeding) during Batch 1.

The estimation of the kinetic parameters was carried out from the data collected in Batch 1. The crystallizer was excited by increasing the heat input in a step wise fashion as shown in Figure 5.11. The batch performed in this manner is expected to produce the data that contains more information of the crystallization dynamics compared to the data produced in the batch with constant heat input. The kinetic parameters were estimated by the weighted least squares³⁹ fitting of the experimentally measured concentration and the second, third and fourth moments of CSD to the predicted ones. The zeroth and the first moments of the CSD were not used due to the limitations of the laser diffraction technique. It has low sensitivity towards small crystals. Hence the determination of the zeroth moment, which represents the number of crystals and the first moment, which is directly related to the number of crystals could be erroneous.^{8,40} The estimated parameters are listed in the Table 5.2. The 95% confidence intervals of the estimated parameters are calculated by specifying the asymptotic probability density function of the weighted least square estimator.⁴¹ These estimated kinetic parameters are lower in value compared to the ones previously obtained.³⁴

Symbol	Parameter	Value	Unit
b	Nucleation rate exponent	1	-
C*	Saturation concentration	0.46	kg solute/kg solution
H_c	Specific enthalpy of crystals	60.75	kJ/kg
H_L	Specific enthalpy of liquid	69.86	kJ/kg
Hv	Specific enthalpy of vapor	2.59×10^3	kJ/kg
Kv	Volumetric shape factor	0.43	-
$L_{0,g1}$	Estimated location parameter for distribution	395.7 x 10 ⁻⁶	m
Q_p	Product flow rate	1.73 x 10 ⁻⁶	m³/s
V	Crystallizer volume	7.5 x 10 ⁻²	m^3
$ ho_c$	Density of crystals	1767.35	kg/ m³
ρι	Density of saturated solution	1248.93	kg/ m³
$\sigma_{g,1}$	Estimated spread parameter of distribution	1.58	-

Table 5.1: Model parameters and physical properties of the crystallization system.

Table 5.2: Estimated kinetic parameters (95% confidence interval)

Symbol	Parameter	Value	Relative	Unit
8	Growth rate exponent	(9.11±0.27).10 ⁻¹	2.96%	-
k_b	Nucleation rate constant	(1.13±0.19). 10 ⁸	16.81%	#/m³.s
k_g	Growth rate constant	(4.37±0.08). 10 ⁻⁶	1.83%	m/s

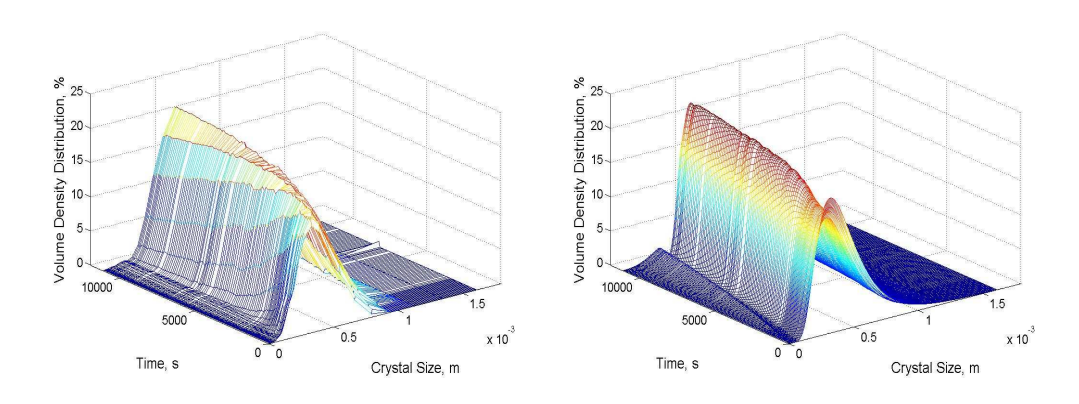


Figure 5.13: Experimental (a) and simulated (b) CSDs for Batch 1

The simulated CSD and the solute concentration based on the model with estimated parameters are shown in Figure 5.13 and Figure 5.14 respectively. A close agreement is obtained between the measured and simulated values of the CSD. Also a reasonable agreement is obtained for concentration values with maximum deviation of the predicted concentration values from the reference values of about 1.7%. As can be seen from Figure 5.14, the experimental values are higher than the simulated values. This might be due to the partial dissolution of the seeds. As the process model does not incorporate dissolution kinetics, it predicts a lower concentration value.

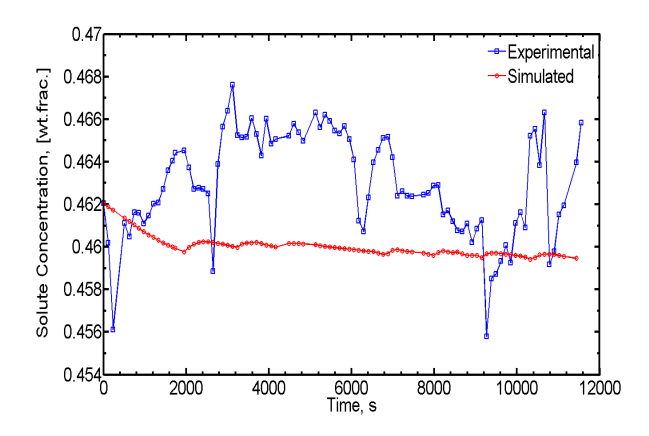


Figure 5.14: Experimental and simulated solute concentration for Batch 1.

The model was validated by evaluating it for its descriptive capability in the second Batch. The estimated kinetic parameters along with the other relevant model parameters listed in Table 5.1 and 5.2 were used to simulate the process at hand. Figure 5.15 shows the experimental and the predicted CSDs for Batch 2. The experimental CSD shows bimodal distribution in the first few measurements. This could be attributed to the plugging in the product flow line of the set-up, where the crystals stick to each other. During rinsing, these crystals were transferred to the laser diffraction instrument and resulted into a bimodal distribution. Apart from those measurements, there is a good agreement between the experimental and simulated distributions.

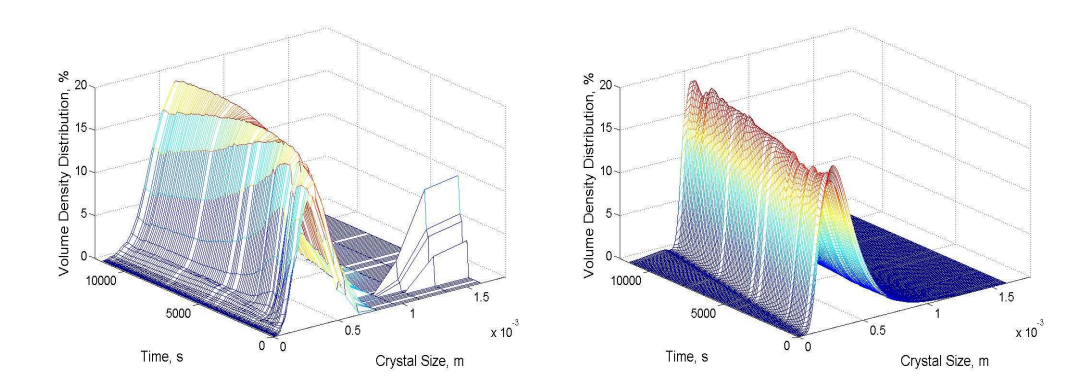


Figure 5.15: Experimental (a) and simulated (b) CSDs of Batch 2.

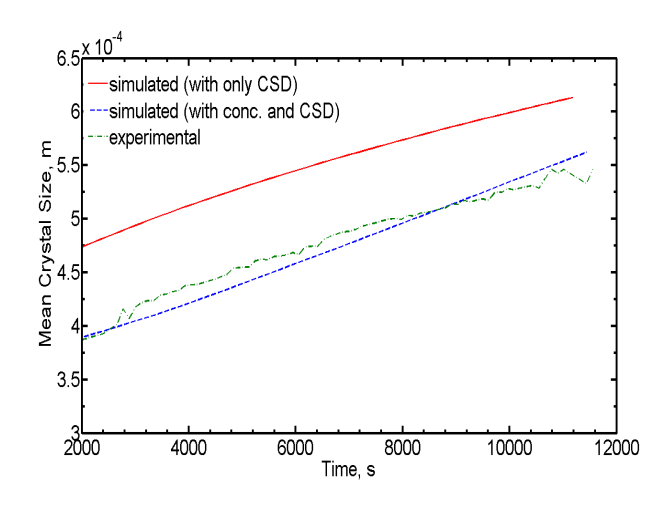


Figure 5.16: Experimental and simulated mean crystal size for Batch 2.

A better understanding of the comparison is obtained by considering the experimental and the predicted evolution of the mean crystal size as shown in Figure 5.16. It has been plotted by leaving out the initial bimodal size distributions. It consists of two simulated curves for mean crystal size, one with the old parameters estimated based only on CSD measurements³⁴ and the other with new parameters estimated based on the CSD and concentration measurements. These two curves are compared with the measured mean crystal size. As can be seen, the simulated curve with old parameters deviates considerably from the measured values. This is mainly due to the overestimation of the growth rate constant k_g . With the incorporation of concentration measurements for parameter estimation, the estimate of the growth rate constant has

been revised from 7.5×10^{-5} m/s to 4.47×10^{-6} m/s. This results into a very good agreement between the experimental and simulated values with the new parameters.

In most parts of the batch, the experimental values of the mean crystal size are slightly higher than the predicted values. This trend changes towards the end when larger crystals are formed. This could be attributed to improper mixing in the vessel. When the crystal fraction increases and the crystals grow larger, it becomes difficult for the impeller to keep the crystals in suspension.

5.5 Conclusions

The application of ATR-FTIR spectroscopy for concentration monitoring of ammonium sulfate on semi-industrial scale crystallizer has been demonstrated. In situ concentration monitoring is essential to have better understanding of the process and also to obtain accurate kinetic parameter estimates for model based control. It is shown that the use of the PLS model developed at lab scale may lead to biased concentration measurements on semi-industrial scale due to the differences in the curvature of fiber optics and the uneven thermal expansion of the probe. As there are problems associated with use of lab calibration model on industrial scale, a method that would allow calibration model to be ready without consuming significant industrial time is necessary. A method for rapid online calibration has been proposed and demonstrated. It has the potential to reduce the time required to achieve a working semi-industrial scale calibration model by almost 90%. With the help of these results it would be possible to easily circumvent the problems associated with calibration transfer from lab to industrial scale set ups and use the concentration measurements for advanced control strategies. The availability of the concentration measurements along with the CSD measurements can give better insights in the process and the model equipped with the revised parameter estimates can better describe the system dynamics.

5.6 Appendix

5.6.1 Concentrations and Temperatures used for Lab Calibration model

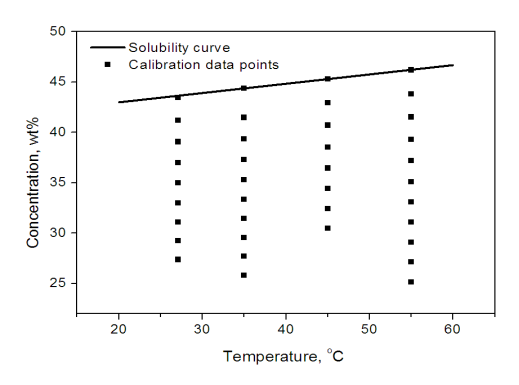


Figure 5.17: Concentrations and temperatures used for lab calibration model.

5.6.2 Motivation for using background spectrum in air instead of in solvent:

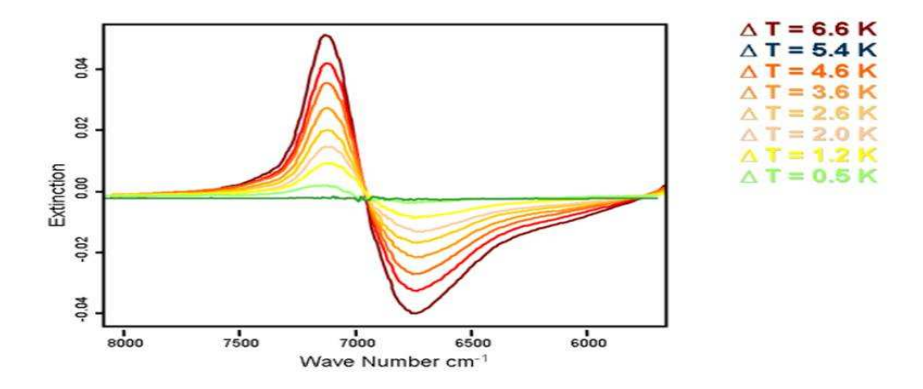


Figure 5.18: Extinction in solvent as function of temperature for near infrared radiations

The use of solvent for background measurement in a semi-industrial set-up is not advisable. It is not very easy to control the temperature in a semi-industrial set-up at a given set-point with a good accuracy. A slight shift of even 0.5 K in the temperature may lead to the change in extinction of the radiations in solvent which results in shifting of the absorption bands. Figure 18 represents the change in extinction for near infrared in a solvent with the change in temperature. As the change in temperature

increases from 0.5 K to 6.6 K, a dramatic change is observed in extinction. Use of background in solvent collected at one temperature, may therefore result in unwanted spectral features when used as background for other temperature. The effects on extinction with change in temperature will be same for mid infrared radiations.

One of the possible ways to avoid above problems would be to leave out spectral ranges associated with solvent. This approach is not suitable for the crystallizing system of ammonium sulfate-water as shoulders due to N-H interactions are seen on water band itself as seen in the Figure 5.2 of the chapter.

The use of background spectrum in air will have deficiencies due to variations in humidity and CO₂ levels. But leaving out regions of water vapor and CO₂ will result in good PLS model without loss of information. Hence, background spectrum in air was used in this research.

5.7 References

- (1) Mersmann, A., Crystallization Technology Handbook. Second ed.; Marcel Dekker, Inc.: New York, 2001.
- (2) Braatz, R. D., Advanced control of crystallization processes. *Annual Reviews in Control* **2002**, 26, (1), 87-99.
- (3) Wibowo, C.; Chang, W.-C.; Ng, K. M., Design of integrated crystallization systems. *AIChE Journal* **2001**, 47, (11), 2474-2492.
- (4) Fujiwara, M.; Nagy, Z. K.; Chew, J. W.; Braatz, R. D., First-principles and direct design approaches for the control of pharmaceutical crystallization. *Journal of Process Control* **2005**, 15, (5), 493-504.
- (5) Nagy, Z. K.; Chew, J. W.; Fujiwara, M.; Braatz, R. D., Comparative performance of concentration and temperature controlled batch crystallizations. *Journal of Process Control* **2008**, 18, (3-4), 399-407.
- (6) Zhou, G. X.; Fujiwara, M.; Woo, X. Y.; Rusli, E.; Tung, H.-H.; Starbuck, C.; Davidson, O.; Ge, Z.; Braatz, R. D., Direct Design of Pharmaceutical Antisolvent Crystallization through Concentration Control. *Crystal Growth & Design* **2006**, 6, (4), 892-898.
- (7) Hulburt, H. M.; Katz, S., Some problems in particle technology: A statistical mechanical formulation. *Chemical Engineering Science* **1964**, 19, (8), 555-574.

- (8) Mesbah, A.; Landlust, J.; Huesman, A. E. M.; Kramer, H. J. M.; Jansens, P. J.; Van den Hof, P. M. J., A model-based control framework for industrial batch crystallization processes. *Chemical Engineering Research and Design* **2010**, 88, 1223-1233.
- (9) Nagy, Z. K., Model based robust control approach for batch crystallization product design. *Computers & Chemical Engineering* **2009**, 33, (10), 1685-1691.
- (10) Rawlings, J. B.; Miller, S. M.; Witkowski, W. R., Model identification and control of solution crystallization processes: a review. *Industrial & Engineering Chemistry Research* **1993**, 32, (7), 1275-1296.
- (11) Kadam, S. S.; van der Windt, E.; Daudey, P. J.; Kramer, H. J. M., A Comparative Study of ATR-FTIR and FT-NIR Spectroscopy for In-Situ Concentration Monitoring during Batch Cooling Crystallization Processes. *Crystal Growth & Design* **2010**, 10, (6), 2629-2640.
- (12) Neumann, Andreas M.; Kramer, Herman J. M., A Comparative Study of Various Size Distribution. *Particle & Particle Systems Characterization* **2002**, 19, (1), 17-27.
- (13) Darakis, E.; Khanam, T.; Rajendran, A.; Kariwala, V.; Naughton, T. J.; Asundi, A. K., Microparticle characterization using digital holography. *Chemical Engineering Science* **2010**, 65, (2), 1037-1044.
- (14) Larsen, P. A.; Rawlings, J. B., The potential of current high-resolution imaging-based particle size distribution measurements for crystallization monitoring. *AIChE Journal* **2009**, 55, (4), 896-905.
- (15) Calderon De Anda, J.; Wang, X. Z.; Roberts, K. J., Multi-scale segmentation image analysis for the in-process monitoring of particle shape with batch crystallisers. *Chemical Engineering Science* **2005**, 60, (4), 1053-1065.
- (16) Simon, L. L.; Nagy, Z. K.; Hungerbuhler, K., Comparison of external bulk video imaging with focused beam reflectance measurement and ultra-violet visible spectroscopy for metastable zone identification in food and pharmaceutical crystallization processes. *Chemical Engineering Science* **2009a**, 64, (14), 3344-3351.
- (17) Simon, L. L.; Abbou Oucherif, K.; Nagy, Z. K.; Hungerbuhler, K., Bulk video imaging based multivariate image analysis, process control chart and acoustic signal assisted nucleation detection. *Chemical Engineering Science* **2009b**, 65, (17), 4983-4995.
- (18) Simon, L. L.; Nagy, Z. K.; Hungerbuhler, K., Endoscopy-Based in Situ Bulk Video Imaging of Batch Crystallization Processes. *Organic Process Research & Development* **2009c**, 13, (6), 1254-1261.
- (19) Simon, L. L.; Oucherif, K. A.; Nagy, Z. K.; Hungerbuhler, K., Histogram Matching, Hypothesis Testing, and Statistical Control-Chart-Assisted Nucleation Detection Using Bulk Video Imaging for Optimal Switching between Nucleation and

- Seed Conditioning Steps. Industrial & Engineering Chemistry Research 2010, 49, (20), 9932-9944.
- (20) Dunuwila, D. D. B., K. A., ATR-FTIR spectroscopy for in situ measurement of concentration. *Journal of Crystal Growth* **1997**, 179.
- (21) Togkalidou, T.; Fujiwara, M.; Patel, S.; Braatz, R. D., Solute concentration prediction using chemometrics and ATR-FTIR spectroscopy. *Journal of Crystal Growth* **2001**, 231, (4), 534-543.
- (22) Borissova, A.; Khan, S.; Mahmud, T.; Roberts, K. J.; Andrews, J.; Dallin, P.; Chen, Z.-P.; Morris, J., In Situ Measurement of Solution Concentration during the Batch Cooling Crystallization of l-Glutamic Acid using ATR-FTIR Spectroscopy Coupled with Chemometrics. *Crystal Growth & Design* **2008**, *9*, (2), 692-706.
- (23) Hojjati, H.; Rohani, S., Measurement and Prediction of Solubility of Paracetamol in Waterâ^{*}Isopropanol Solution. Part 1. Measurement and Data Analysis. *Organic Process Research & Development* **2006**, 10, (6), 1101-1109.
- (24) Feudale, R. N.; Woody, N. A.; Tan, H.; Myles, A. J.; Brown, S. D.; Ferré, J., Transfer of multivariate calibration models: a review. *Chemometrics and Intelligent Laboratory Systems* **2002**, 64, (2), 181-192.
- (25) Honorato, F. A.; Galvão, R. K. H.; Pimentel, M. F.; de Barros Neto, B.; Araújo, M. C. U.; de Carvalho, F. R., Robust modeling for multivariate calibration transfer by the successive projections algorithm. *Chemometrics and Intelligent Laboratory Systems* **2005**, 76, (1), 65-72.
- (26) Cornel, J.; Lindenberg, C.; Mazzotti, M., Quantitative Application of in Situ ATR-FTIR and Raman Spectroscopy in Crystallization Processes. *Industrial & Engineering Chemistry Research* **2008**, 47, (14), 4870-4882.
- (27) Wold, H., Partial Least Squares. In *Encyclopedia of Statistical Sciences*, ed.; Kotz, S. J., N. L., Ed. Wiley and Sons: New York, 1985; Vol. 6, pp 581-591.
- (28) Griffiths, P. R. d. H., J. A., Fourier Transform Infrared Spectroscopy. Second ed.; John Wiley and Sons, Inc.: New Jersey, USA, 2007.
- (29) Massart, D. L. V., B.G.M.; Buydens, L.M.C.; De Jong, S.; Lewi, P.J.; Smeyersverbeke, J., *Handbook of Chemometrics and Qualimetrics: Part A.* ed.; Elsevier Science, B.V.: Amsterdam, The Netherlands, 1997; Vol. 20A.
- (30) Daudey, P. J. Crystallization of ammonium sulphate-secondary nucleation and growth kinetics in suspension Ph. D. Thesis, Technical University of Delft, The Netherlands, 1987.
- (31) Kalbasenka, A. N.; Spierings, L. C. P.; Huesman, A. E. M.; Kramer, H. J. M., Application of Seeding as a Process Actuator in a Model Predictive Control Framework

- for Fed-Batch Crystallization of Ammonium Sulphate. *Particle & Particle Systems Characterization* **2007**, 24, (1), 40-48.
- (32) Randolph, A. D. L., M. A. , *Theory of Particulate Processes*. ed.; Academic Press: San Diego, USA, 1988.
- (33) Daudey, P. J.; van Rosmalen, G. M.; de Jong, E. J., Secondary nucleation kinetcs of ammonium sulfate in a CMSMPR crystallizer. *Journal of Crystal Growth* **1990**, 99, (1-4, Part 2), 1076-1081.
- (34) Kalbasenka, A. N. Model Based Control of Industrial Batch Crystallizers. Ph. D. Thesis, Technical University of Delft, 2009.
- (35) Qamar, S.; Elsner, M. P.; Angelov, I. A.; Warnecke, G.; Seidel-Morgenstern, A., A comparative study of high resolution schemes for solving population balances in crystallization. *Computers & Chemical Engineering* **2006**, 30, (6-7), 1119-1131.
- (36) Mesbah, A.; Kramer, H. J. M.; Huesman, A. E. M.; Van den Hof, P. M. J., A control oriented study on the numerical solution of the population balance equation for crystallization processes. *Chemical Engineering Science* **2009**, 64, (20), 4262-4277.
- (37) Faber, N. M.; Rajkó, R., How to avoid over-fitting in multivariate calibration-The conventional validation approach and an alternative. *Analytica Chimica Acta* **2007**, 595, (1-2), 98-106.
- (38) Kalbasenka, A. V., C.; Huesman, A.; Kramer, H In *Application of an ultrasonic analyzer for supersaturation measurement in an 1100-l DTB crystallizer*, 16th International Symposium on Industrial Crystallization, Dresden, Germany, September 11-14, 2005; Chemieingenieurwesen, V.-G. V. a., Ed. VDI-Verlag GmbH: Dresden, Germany, 2005; pp 1105-1110.
- (39) Seber, G. A. F. W., C.J., Nonlinear Regression. ed.; Wiley: New York, USA, 1989.
- (40) Gunawan, R. M., D. L.; Fujiwara, M.; Braatz, R. D., *International Journal of Modern Physics B* **2002**, 16, (1-2), 367-374.
- (41) Bard, Y., Nonlinear Parameter Estimation. ed.; Academic Press: New York, 1974.

Chapter 6

Rapid Crystallization Process Development Strategy

This chapter is published as:

Kadam S. S., Vissers, J. A. W., Forgione, M., Geertman, R. M., Daudey, P. J., Stankiewicz, A. I., Kramer, H. J. M. "Rapid Crystallization Process Development Strategy from Lab to Industrial Scale with PAT Tools in Skid Configuration." Org. Process Res. Des., 2012,16(5), 769-780

Batch cooling crystallization is a commonly used separation and purification step in pharmaceutical industry. Various properties of the crystalline product from a batch crystallizer can have a strong impact on efficiency of downstream processes like filtration and drying. Development of crystallization processes presents a major challenge in process development of an active pharmaceutical ingredient (API). Therefore, it is beneficial to develop a rapid crystallization process development strategy to industrial scale. In this study we present a strategy for rapid process development, and apply this strategy for androsta-1,4-diene-3,17-dione, cyclic 17-(2,2dimethyltrimethylene acetal, a pharmaceutical intermediate produced by Merck Sharp and Dohme. The major advantages of the strategy lie in the facts that there is no requirement of crystallizer design modification, the calibration of the Process Analytical Technology (PAT) tools can be performed at industrial scale, and the determination of the operating window can be done directly at industrial scale. This strategy allows for process optimization directly at industrial scale thus eliminating the need of time intensive scale dependent study. The implementation of this strategy at industrial scale was performed with the help of Process Analytical Technology (PAT) tools arranged in a unique skid based configuration. The skid which contains both, the concentration sensors and the crystal size distribution (CSD) sensors, can be connected to the existing crystallizers thereby avoiding the time and cost intensive modifications in the crystallizer design. The modular nature of the skid offers opportunities to choose the PAT tools which compliments the solute-solvent model system. The skid makes it possible to gather the relevant information concerning the thermodynamics and the kinetics of the model system in situ during the crystallization runs at the industrial scale. A strategy for process development based on a sensor-skid is beneficial for industry as it is intrinsically rapid and it can be combined with the development of control strategies which lead to consistent product quality.

6.1 Introduction

Batch cooling crystallization is a commonly used separation and purification step in pharmaceutical industry as it is easy to operate, less energy intensive, can achieve high purity in a single step etc.¹ Although batch cooling crystallization has several advantages, batch-to-batch variations in crystalline product quality are commonly observed which have strong impact on product properties and also on the efficiency of the downstream processes like drying and milling.¹ Due to its critical role in the production process, crystallization presents a significant process development challenge when a new drug is to be synthesized commercially.

Attempts have been made in the past to develop crystallization strategies which are applicable to the existing crystallizers.²⁻⁴ Typical steps involved in such a process development strategy and its current limitations are schematically represented in Figure 6.1.

The steps in process development can be divided in three parts i.e. lab scale, pilot plant scale and industrial scale. The scale dependent study during conventional process development process is performed as the micromixing, macromixing and heat transfer effects vary with the scale. This leads to variable temperature and supersaturation profiles and hence variable crystallization kinetics. By scale dependent study, the amount of variations in the crystallization kinetics can be determined.⁵

The first set of experiments at lab scale is devoted to determine a solvent (Figure 6.1 block a). This set of experiments consists of inter-related steps for solvent screening, polymorph screening and determination of method of supersaturation generation. The second set of experiments at lab scale is performed to determine the operation window for the process and the crystallization kinetics (Figure 6.1 block b). Once the solvent, operation window and the crystallization kinetics are determined, process development continues at industrial scale through a pilot plant (Figure 6.1 block c and d) when performed without PAT tools and without a pilot plant when performed with PAT tools (Figure 6.1 block e). When PAT tools are available, process optimization becomes possible at the industrial scale directly which eliminates the need of scale dependent study. The details of the steps involved are described in sections 6.1.1 to 6.1.3.

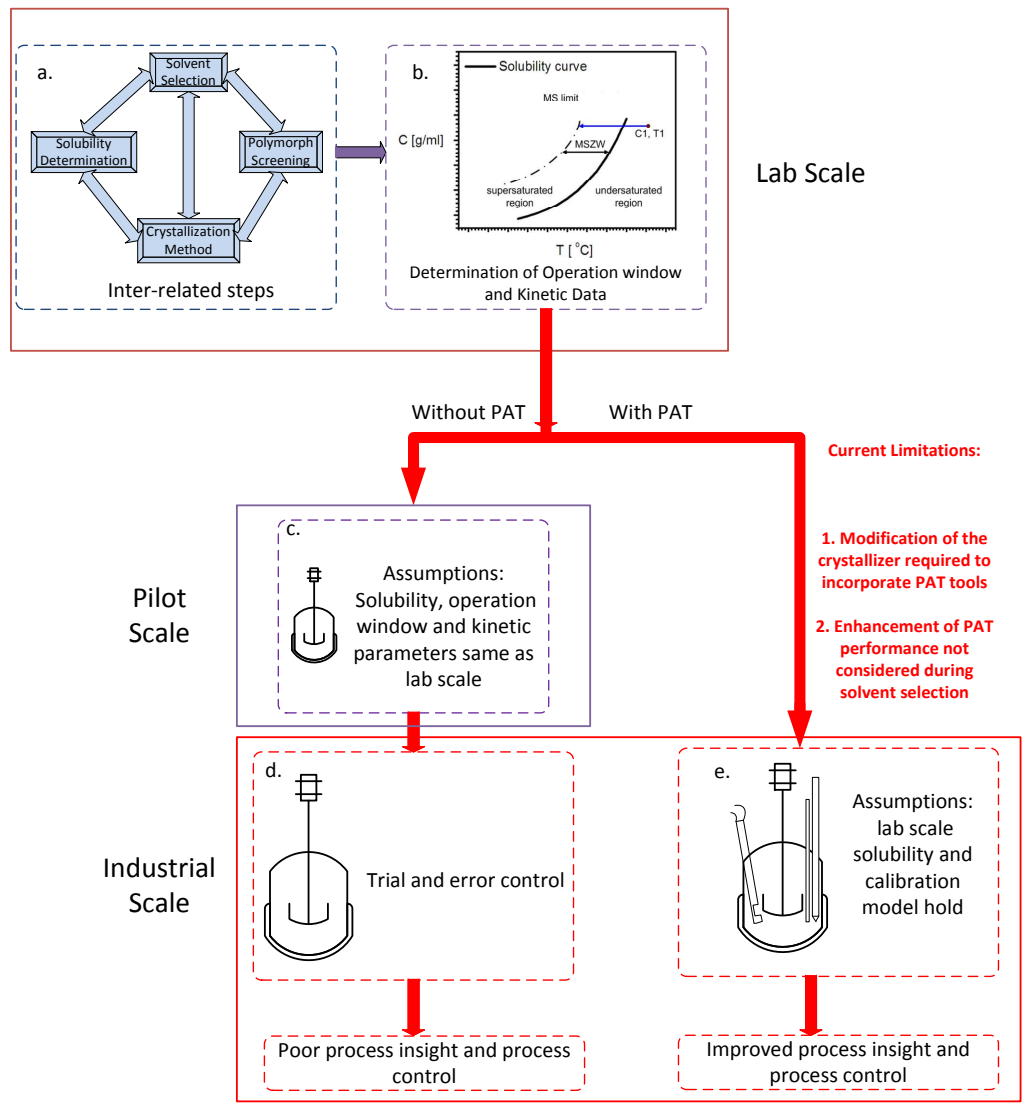


Figure 6.1: Typical process development strategies from lab to industrial scale with and without Process Analytical Technology (PAT) along with their limitations.

6.1.1 Lab scale

Solvent screening and method of supersaturation generation

The process development usually starts with solvent screening. For a cooling crystallization process, a solvent with a solubility that increases enough to yield approximately 10-20% solids over a reasonable cooling trajectory, is desirable. If the dependency of the solute solubility on temperature is not adequate, other methods of

supersaturation generation like evaporation, anti-solvent addition or combination of different methods can be employed.⁶ Solvent screening can be completely or only partially based on experiments. For the complete experimental approach, the solubility of the solute is determined in a wide variety of commonly used industrial solvents at room temperature. For solvents which display good solvation (between 5-200 mg/mL), the solubility is also determined at higher temperatures.² For the other, approach, an initial solvent screening is performed with models like UNIQUAC, COSMO-RS etc. which can predict the temperature dependent solubility of chemicals in different solvents.⁷⁻⁹ Based on the predicted yield by these models, a few solvents can be selected and the solubility in these solvents is experimentally determined as a function of temperature. Other considerations like the toxicity of the solvent and its environmental impact may also influence the choice of solvent.²

Polymorph screening

Polymorph screening is necessary to identify the most stable polymorph and to verify if the most stable polymorph is obtained directly after the batch. Polymorphs encountered in crystallization process depend amongst other factors on the solvent used. Solvent plays a crucial role in the polymorphic outcome of the crystallization process as it can promote or inhibit hydrogen bonding during formation of molecular clusters and hence control the nucleation of a specific solid form. There are several methods of polymorph screening which vary in their effectiveness of screening and time required for their implementation. Slurry testing is one of the commonly employed methods as it is very effective in identifying low energy polymorph and also in identifying solvates. 10, 12

Based on the outcome of solvent screening, polymorph screening and temperature dependent solubility measurements, a solvent is selected for the crystallization process.

Determination of the operation window and the crystallization kinetics

The Metastable Zone Width (MSZW) can be considered as the preferred operating region in the composition-temperature space. It forms the area between the solubility curve and the MSZ limit at which the crystals are detected at constant cooling rate.¹ A polythermal method¹³ is commonly used for determining the MSZW during cooling crystallization.

Along with the MSZW, the polythermal method can also be used for determining nucleation kinetics. The other common methods for determining nucleation kinetics are the induction time measurement method^{14, 15} and the double pulse method.¹⁶ Crystal growth rates are commonly determined by following the time evolution of a particular face of a crystal in stagnant solution with time,¹⁷ by using the Mixed Slurry Mixed Product Removal (MSMPR) crystallization experiments in combination with the population balance equations,⁶ by following CSD in time,¹⁸ or by using indirect methods like following desupersaturation curve after seeding with known amount of seeds.¹⁹ It is beneficial to use the PAT tools for determination of crystallization kinetics as it releases the requirement for sampling and the measurements can be automated thus resulting in sufficient amount of information on crystallization behaviour of the model system in short amount of time. However, PAT tools which deliver accurate measurement of process variables are scarce.

Based on the determined kinetic data at lab scale, an optimal or a near optimal cooling profile which could be implemented during crystallization at industrial scale can be determined.²⁰ The use of PAT tools at lab scale also enables implementation of interesting strategies within the operating window like temperature cycling which could allow control over polymorphic purity.²¹

6.1.2 Pilot and industrial scale

Depending on the accessibility, the crystallization process at industrial scale can be performed without PAT tools or with PAT tools.

Process development without PAT

As PAT tools are expensive and their implementation in industrial scale crystallizer might require substantial changes in the design of the crystallizer, the most common approach is to continue with the process development at industrial scale without PAT (Figure 6.1 block d) through a pilot plant stage (Figure 6.1 block c). Following this approach it is assumed that the solubility, MSZW and kinetic models determined at the lab remain valid at the pilot plant and industrial scale. Seeding is commonly employed at industrial scale to start the crystallization process.⁶ After seeding a cooling profile which is pre-determined offline is often followed to maintain the same level of supersaturation throughout the process.¹ This cooling profile is determined based on

the lab scale MSZW and the crystallization kinetics. During the implementation of the cooling profile, the crystal product quality evolution is not monitored and it is assumed that the product quality obtained would be similar to the lab scale. However the performance at pilot and industrial scale does not often match the performance at lab scale when this approach is implemented. This is primarily due to lack of scale-up rules and inhomogeneous mixing giving rise to areas of non-uniform energy dissipation, temperatures and supersaturation.^{5, 22} The effect of inhomogeneous mixing on crystallization kinetics will vary from one model system to other. The use of pilot plant can give an estimate for the amount of deviation from the expected product quality due to inhomogeneous mixing at larger volumes. Taking corrective measures at pilot scale or industrial scale would require redetermination of kinetic parameters or operating procedures. This approach of scale up without PAT is based on trial and error and poor process insight is often the result of this approach. Sampling and offline analysis could provide some insights in the process but the insights are not enough to develop rigorous control strategies.

Process development with PAT

The process development with PAT tools offers a better opportunity to obtain consistent product quality. The use of PAT tools allows for monitoring of crystal quality in real time. Process monitoring can be combined with process modelling and estimation tools to obtain kinetic parameters in situ at industrial scale. This enables designing of control strategies²³⁻²⁵ with minimum a-priori knowledge and capabilities to learn from batch-to-batch.

But the implementation of PAT tools at industrial scale currently requires time and cost intensive modifications in the design of the crystallizer.

6.2 Incentive for the work

In the current approach of process development to industrial scale there are several limitations:

1. Process development without PAT is based on the assumption that the solubility, the MSZW and the kinetic parameters determined at lab scale also hold at pilot and industrial scale. This approach ignores the fact that the MSZW is scale dependent²⁶, impurity profile may be different at the industrial scale

- and inhomogeneous mixing may lead to areas of variable supersaturation at pilot and industrial scale.
- 2. Process development to industrial scale with PAT requires several modifications in the design of the crystallizer to incorporate the PAT tools. The incorporated PAT tools are calibrated at lab scale and used at industrial scale. This approach results in time and cost intensive modifications of the industrial crystallizer and also leads to biased measurements as the calibration models are not developed at industrial scale.

In this study we present a rapid strategy for process development with PAT tools in an unique skid based configuration which addresses above mentioned limitations in shortest possible time. This strategy for process development does not make assumptions about the solubility and kinetic parameters being constant at lab and industrial scale, does not need major modifications in the design of the vessel and allows calibration of the concentration measuring instruments at industrial scale directly. The process development strategy is demonstrated for Androsta-1,4-diene-3,17-dione, cyclic 17-(2,2-dimethyltrimethylene acetal. The process development part at lab scale was performed at Merck Sharp and Dohme, Oss, the Netherlands while the industrial part was performed at Merck Sharp and Dohme, Apeldoorn, the Netherlands.

6.3 Skid design and its advantages

In order to overcome the limitations mentioned in section 6.2, the PAT tools were arranged in a unique skid based configuration as shown in Figure 6.2. The skid was manufactured by Zeton B.V. (the Netherlands).

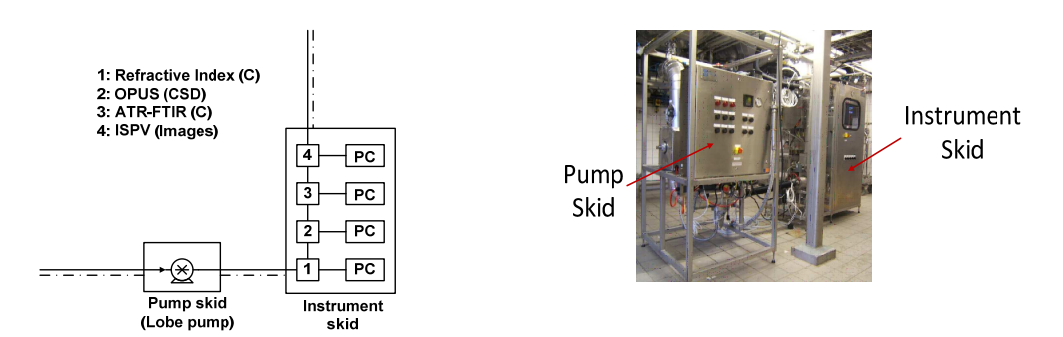


Figure 6.2a: Schematics of the pump and the instrument skid

Figure 6.2b: The pump and the instrument skid

The configuration consisted of two skids viz. the instrument skid and the pump skid

6.3.1 Instrument skid

The instrument skid consisted of a stainless steel pipeline with internal diameter of 2.54 cm for the flow of the slurry, four PAT tools and their computers enclosed in a pressurized cabinet as shown in Figure 6.2a and 6.2b. The PAT tools used in the skid are listed in Table 6.1.

Table 6.1: The PAT tools in the skid to monitor concentration (*C*) and crystal size distribution (*CSD*)

PAT tool	Supplier	Measured property	Monitored
BRIX sensor/	K-Patents (Finland)	Refractive index of the	С
process refractometer		solution	
OPUS	Sympatec	Ultrasound attenuation	CSD
	(Germany)		
ATR-FTIR	Bruker Optics	Absorption of the	С
(MATRIX-MF)	(Germany)	infrared radiations	
ISPV	Perdix Analytical Systems	(Images)	(CSD)

ATR-FTIR: attenuated total reflectance – Fourier transform infrared spectroscopy

The details of the working principles and the performances of the sensors listed in Table 6.1 are available in literature. $^{27\cdot30}$ The BRIX sensor was installed at the angle of 45° to the flow to allow for self-cleaning effect of the prism. The OPUS, ATR-FTIR and ISPV were installed perpendicular to the flow with the measuring sections of the instrument coinciding with the centre of the flow. The interferometer of the ATR-FTIR was flushed continuously with nitrogen gas to avoid the effect of atmospheric carbon dioxide and water vapour on the collected spectra. The ISPV sensor consisted of a set of two video microscopes with the resolutions of $10~\mu/\text{pixel}$ (low resolution) and $2~\mu/\text{pixel}$ (high resolution). Imaging can in principle be used to determine CSD during the process. During this work, imaging was used in qualitative manner to gain process insights. Hence CSD has been included in brackets in Table 6.1 for the ISPV. OPUS was included in the skid for Crystal Size Distribution (CSD) measurements but was not used during the experiments as it needs a-priori calibration which was not performed for ADD-

NEOP. The computers of the PAT tools were placed in the slightly pressurised skid cabinet along with the controller computer and software from IPCOS (the Netherlands). The controller software could interact with the control system of the crystallizer. The instrument skid was also equipped with a display screen on which measurement trends from individual PAT tools and from the IPCOS controller could be seen in real-time.

The instrument skid was connected to the pump skid and the crystallizer with the help of traced flexible hoses.

6.3.2 Pump skid

The pump skid consisted of a lobe pump (BF 330, OMAC, Italy) placed in the pressurized cabinet. The pump consisted of two lobes rotating in the direction opposite to each other. When the lobes moved away from each other, the slurry or solution flowed into the rotor case which was then discharged on the opposite side when the lobes moved towards each other. The inlet and outlet openings of the pump were three inch in diameter and the maximum flow-rate was approximately 120 L/min. The pump skid was connected to the instrument skid and the crystallizer with traced flexible hoses.

6.3.3 Advantages of the skid design

The configuration of the PAT tools in form of the skid leads to the following advantages

- a. The modification of the crystallizer is not required in order to connect the PAT tools. This saves the valuable industrial time and also the cost which would have been necessary for the design modification.
- b. The skid based design allows for the easy transportation of the skid from one location to the other.
- c. The skid is modular in nature allowing for the addition or removal of the PAT tools as per requirements.
- d. Good flow conditions through the skid ensures that the measurements by the PAT tool are representative of the conditions in the crystallizer.

6.4 Experimental

Experiments were performed with androsta-1,4-diene-3,17-dione, cyclic 17-(2,2-dimethyltrimethylene acetal) (Dutch name : androstadieen-3,17-Dion-17-Neopentylketaal, Acronym: ADD-NEOP) as a solute. ADD-NEOP (Figure 6.3) is a pharmaceutical intermediate synthesized by Merck Sharp and Dohme, the Netherlands and was used without further purification.

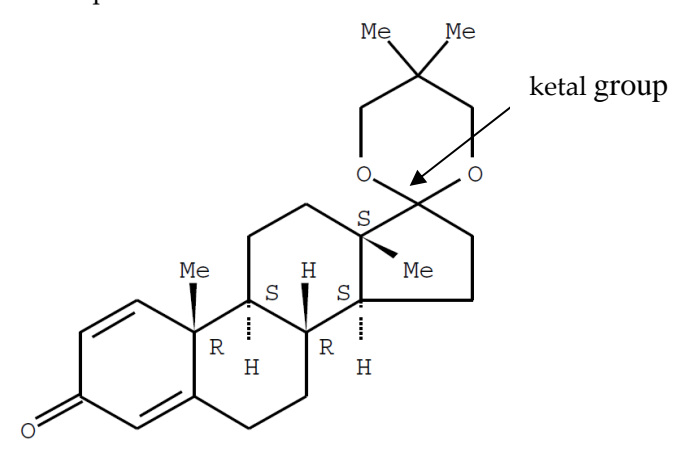


Figure 6.3: ADD-NEOP absolute stereochemistry³¹

ADD-NEOP consists of a ketal group which hydrolyzes in presence of acidic environment. Hence a small amount (0.5 % v/v) of base (triethyl amine, TEA, analysis grade, J.T. Baker) is added to stabilize ADD-NEOP solution when used in acidic environment.

6.4.1 Solubility measurements

Initial solvent screening was performed for 50 commonly used industrial solvents with COSMO-RS.9 Based on the differences in solubility of ADD-NEOP in these solvents predicted by COSMO-RS between 50 °C and 20 °C, four solvents were chosen. The solubility measurements were performed in these four solvents which were all analysis grade procured from J. T. Baker. For acidic solvents 0.5 % v/v of TEA was added to protect the ADD-NEOP molecule from hydrolysis. The solubility measurements were performed using a multiple reactor setup (Crystal16, Avantium Technologies). The setup consists of 16 magnetically stirred 1 mL vials in which transmission of light through the solution was recorded. Slurries with different concentrations were prepared in the vials and were stirred at 700 rpm. The heating and

cooling rates employed were 0.5 °C/min. Upon heating a vial in the setup, the transmission of the light through the solution became 100% at a certain temperature. That temperature was taken as the saturation temperature of that sample. The heating and cooling cycles were repeated at least 4 times per concentration to have a better estimate of the solubility.

6.4.2 Slurry test

Slurry tests were performed at room temperature to identify the most stable polymorph appearing from the four solvents chosen in section 6.4.1. Slurries were prepared with approximately 1000 mg of ADD-NEOP in 5 mL of solvents. They were stirred on IKA Ret basic werek stirring plate for 26 days continuously to allow any metastable polymorphic form to transform into a stable polymorphic form. After the end of the 26th day, the slurries were vacuum filtered through VitraPOR sintered glass filter (Gereate GmbH, Germany) with pore size of 16-40 µm. The filtered slurries were vacuum dried at 8 mbar for 48 hours and were analyzed by X-ray powder diffraction (XRPD). Batch cooling experiments between 40 °C and 20 °C were also performed at 5 mL scale in all four solvents in order to verify if the stable polymorph is obtained directly at the end of the batch.

6.4.3 Infrared spectra collection

The relative positions of the ADD-NEOP peaks and the solvent peaks was introduced as the new criteria for solvent selection which would enhance the performance of the ATR-FTIR spectroscopy. The details of the motivation behind introduction of this criteria are mentioned in section 6.5.3. Undersaturated solutions (25% w/w of the saturation concentration) were prepared in four solvents at room temperature. Midinfrared (MIR) spectra were collected in ATR mode with ReactIR45m (Mettler-Toledo) with resolution of 8 cm⁻¹ in the range of 2800-650 cm⁻¹. Each spectrum consisted of 256 co-added scans. Background spectrum was collected in air at room temperature. Collection of background spectra in air was preferred over collection in solvent as the solvent spectra are very sensitive to minute changes in temperature. ¹⁸

6.4.4 Combined characterization and PAT tool selection at lab scale

The operating region i.e. the MSZW is commonly determined on the lab scale without much consideration of the volume at which experiments are performed. Experiments at small volumes lead to distribution of MSZW while as the volume is increased, the MSZW gets reproducible within a small error margin.²⁶ Hence care must be taken to determine MSZW at sufficiently large volumes at which it is reproducible. The MSZW measurements can be combined with the identification of the PAT tool which works better for the model system under consideration. A given PAT tool will have different accuracy when used with different model systems ²⁹ and also different PAT tools used for the same model system will have different accuracies.³² Hence identifying the PAT tools which best suits the model system at lab scale itself will improve process monitoring at industrial scale.

The two steps mentioned above i.e. determination of the MSZW and selection of PAT tool can be combined together to make the process development rapid. In order to do so, experiments were performed in a 2 L baffled jacketed glass crystallizer which was agitated by anchor type impeller at 175 rpm to determine MSZW for ADD-NEOP in the solvent selected based on the experiments in section 6.4.1 to 6.4.3. The concentration of ADD-NEOP was 173 mg/mL which had a saturation temperature of 41.4 °C. The cooling was performed linearly at a cooling rate of 0.5 °C/min. The experiments were monitored by visual observation, Focused Beam Reflectance Measurements (FBRM) (Mettler-Toledo) and an In Situ Particle Viewer (ISPV) (Perdix Analytical Systems). The measurement was performed by FBRM every 10s while images were taken by ISPV every second. The ISPV had a resolution of 1 μ m/pixel. The experiment was performed twice to check the reproducibility of the MSZW measurements.

6.4.5 Combined calibration and characterization at industrial scale

Calibration models for the PAT tools which are developed at lab scale may not necessarily work at industrial scale. Especially the attenuated total reflectance Fourier transform infrared spectroscopy (ATR-FTIR) which is used for concentration measurements is sensitive to minute changes in the operating environment. Hence it is beneficial to perform calibration directly on the industrial scale. The calibration of the PAT tools can be combined with process characterization at the industrial scale to make process development rapid. The time and cost intensive step of modifying the design of

the crystallizer to incorporate PAT tools can be avoided by using the instruments in form of a skid as shown in Figure 6.4. The instrument skid can be connected to the crystallizer with help of a pump skid and flexible hoses. There are often inlet and outlet connections already in the original design of the crystallizer and hence the modification of the vessel is not necessary.

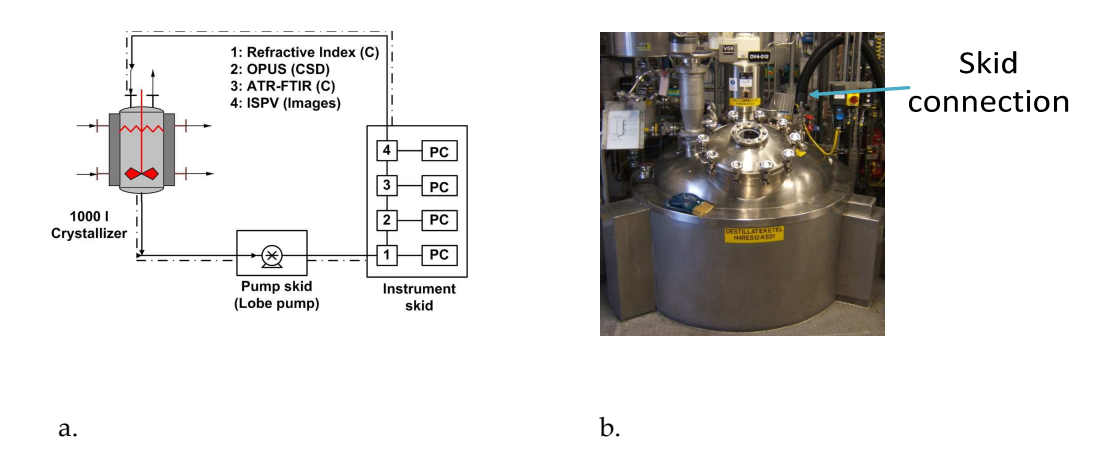


Figure 6.4: a. Schematics of the instrument skid and the pump skid connected to the crystallizer, b. Inlet connection to the crystallizer from the skid.

The industrial scale experiments reported here were performed at Merck Sharp and Dohme, Apeldoorn, the Netherlands. The crystallizer used for the experiments (Figure 6.4b) was a 1000 L jacketed stainless steel vessel equipped with a vacuum system and a condenser. The stirring was performed at 125 rpm with help of a 3 blade propeller. The crystallizer was connected to the pump skid and the instrument skid with help of traced insulated flexible hoses.

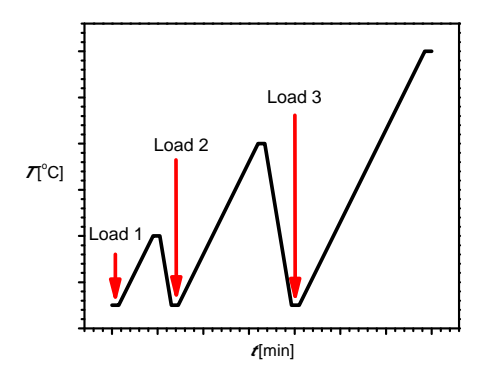


Figure 6.5: Schematics of combined calibration and characterization step.

Figure 6.5 shows the schematics of the combined calibration and characterization step. 904.5 L of solvent was added to the crystallizer at 5 °C. Background scan for ATR-FTIR was collected in air before the pumping of the solvent through the skid was started. 43.74 kg of ADD-NEOP was added to the crystallizer through the manhole. Vacuum was applied on the crystallizer to vaporize ethanol which was condensed and drained along the walls of the crystallizer to remove any ADD-NEOP sticking on the crystallizer wall. The crystallizer environment was made inert by purging in nitrogen gas and the slurry was heated at 0.3 °C/min. The spectra for ATR-FTIR and the BRIX readings were collected continuously. The slow heating allows for the determination of the saturation temperature at the given concentration and hence for determination of one side of the operation window. The crystallizer was maintained 5 °C above the saturation temperature for 30 minutes and then cooling was started at 0.4 °C/min to 5 °C. During the cooling process the onset of crystallization or the metastable limit which forms the other side of the operation window was determined. Cooling was always performed to 5 °C (which is below the flash point of solvent) so that the next batch of the ADD-NEOP can be added by opening the manhole of crystallizer. The process of heating and cooling was further repeated four times by adding loads of 27.4 kg each.

6.4.6 Gaining process insights

In situ imaging has been shown previously to provide valuable process insights.²⁶ In this contribution, in situ imaging was used to monitor the initial phases of an unseeded and seeded batch crystallization process in order to gain insights about secondary nucleation. For unseeded batch cooling crystallization, the crystallizer at 50 °C containing solution saturated at 40 °C was cooled to 36 °C linearly at the rate of 0.5 °C/min. The crystallizer was maintained at 36 °C for 1800 s and images were collected with both the high resolution and low resolution camera at an interval of 2s in order to check if crystals appear within 1800 s. The crystallizer was then heated back to 50 °C and was maintained at 50 °C for an hour in order to make sure that the solution is free from any crystalline material. Vacuum was applied in the crystallizer to evaporate part of the solvent which was then condensed and drained on the walls of the crystallizer was brought to 36 °C at 0.5 °C/min cooling rate and was seeded with a single seed crystal shown in Figure 6.6 which was approximately 10 mm in length, 2 mm in height and 2 mm in breadth.

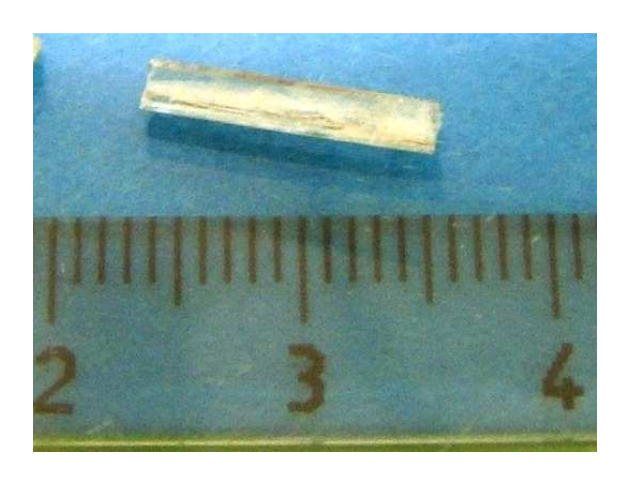


Figure 6.6: Single crystal used for seeding.

The single crystal was prepared by slow evaporation of solvent. The resulting evolution of the crystal number was followed with the help of in situ imaging.

6.5 Results

6.5.1 Solubility measurements

Of the 50 commonly used industrial solvents which were screened with COSMO-RS for solubility predictions, four viz. ethanol, propanol, ethyl acetate and acetone, were selected based on the difference in solubilities at 50 °C and 20 °C. As ethanol and propanol are slightly acidic, 0.5% v/v of triethyl amine (TEA) was added to them to prevent hydrolysis of ADD-NEOP. The solvent names (ethanol and propanol) are used henceforth in this paper without mentioning the name of the base. Based on the solubility measurements, a solvent which would lead to 10% solids when the crystallization process is operated between 40 °C and 10 °C was to be identified. The temperature window between 40 °C-10 °C and the solid concentration of 10% leads to economically favourable operation of the chosen crystallizer based on the experience of the staff and was chosen without further investigation.

As can be seen from Figure 6.7, the solubility of ADD-NEOP in ethyl acetate rises very steeply making it the least attractive of the solvents under consideration as the solids content would be more than 10% at the end of the batch when operated between $40~^{\circ}\text{C}$ and $10~^{\circ}\text{C}$. For acetone, propanol and ethanol the steepness of the solubility curve between $40~^{\circ}\text{C}$ and $10~^{\circ}\text{C}$ is approximately the same and would lead to 10% solid

concentration at the end of the batch. Based on the solubility criteria any of the solvent from acetone, propanol and ethanol could be used.

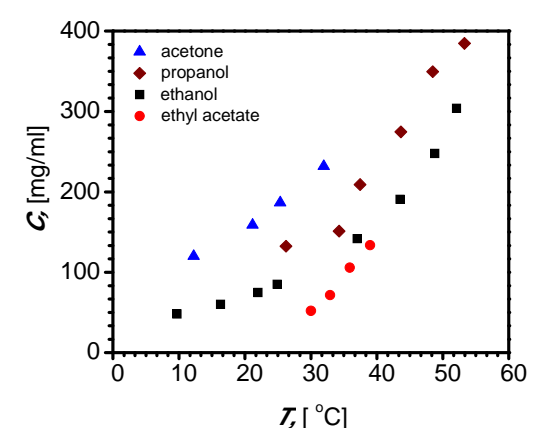


Figure 6.7: Temperature dependent solubilities of ADD-NEOP in acetone, propanol, ethanol and ethyl acetate.

6.5.2 Slurry test

The slurry test was performed to identify the most stable polymorph in the solvents under consideration. XRPD patterns of the crystals obtained after the slurry test are shown in Figure 6.8.

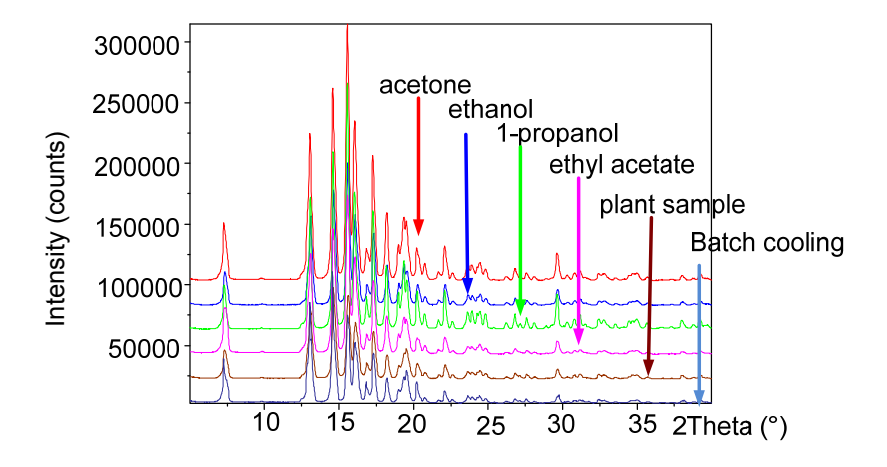


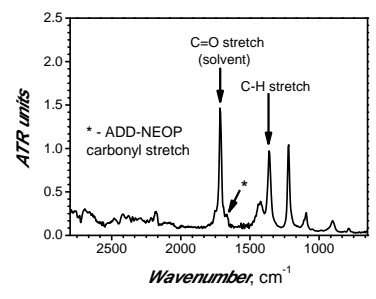
Figure 6.8: The XRPD patterns after the slurry tests and the batch cooling experiment in ethanol. Same stable polymorph is obtained from all the solvents and after batch cooling experiment.

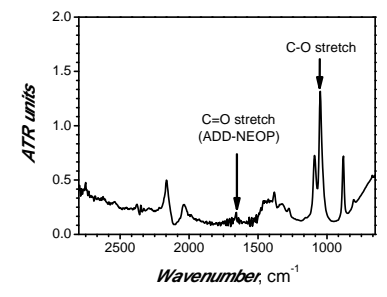
As can be seen from Figure 6.8, same stable polymorph was obtained from all the solvents. Also the ADD-NEOP which was supplied for the experiments from the plant was also in form of the stable polymorph. Batch cooling experiment at 5 mL scale in all the solvents also resulted directly in the stable polymorph. Based on polymorphic outcome, all four solvents are suitable for use.

6.5.3 Infrared spectra

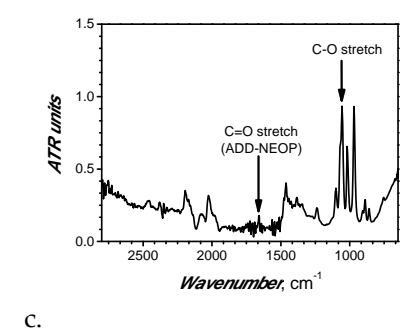
ATR-FTIR spectroscopy is one of the most suitable and commonly used technique for monitoring concentration during crystallization processes.^{29, 33} A multivariate calibration method is often used for obtaining concentration values based on the measured spectra.³⁴ The multivariate approach considers the intensity differences as a function of wavenumbers within the spectrum taken at a particular process condition and also the intensity differences between different spectra at a particular wavenumber taken during the changes in process conditions.³⁵ The change in concentration of the solute during the crystallization process would predominantly be seen as the change in peak height and the width of the solute peak. Performing multivariate calibration in the region around solute peak would increase chance of developing a calibration model with high accuracy and low rank.³⁴

The performance of the ATR-FTIR spectroscopy could be enhanced if the solute peak is distinct from the solvent peaks. Hence IR spectrum could be used as a criterion for solvent selection.





a.



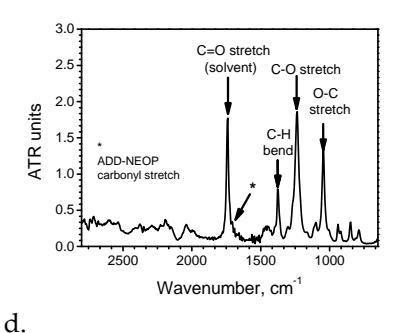


Figure 6.9: Mid-infrared spectra of ADD-NEOP in acetone (a), ethanol (b) propanol (c) and ethyl acetate (d).

As can be seen from Figures 6.9a and 6.9d, the mid-infrared spectrum of ADD-NEOP in acetone and ethyl acetate do not show distinct solute peaks. A small shoulder due to the ADD-NEOP carbonyl stretch is present (around 1700 cm⁻¹) on the peak due to carbonyl stretch of the solvent. On the other hand for ADD-NEOP in ethanol and propanol a distinct carbonyl peak is seen which makes them both attractive solvents. As the solubility of ADD-NEOP in ethanol is less than in propanol, ethanol was selected as the solvent for further experiments.

6.5.4 Combined characterization and PAT tool selection at lab scale

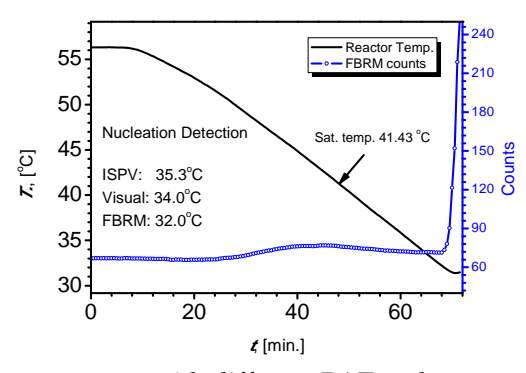


Figure 6.10: MSZW measurement with different PAT tools

The MSZ limit, which determines one side of the operation window, was determined for 173 mg/mL of ADD-NEOP in ethanol with help of visual observations, ISPV and FBRM at 2 L scale with cooling rate of 0.5 °C/min. As can be seen from Figure 6.10, ISPV detected the particles almost 3 °C (6 minutes) prior to FBRM and almost 1.5 °C (3 minutes) prior to visual observations. The experiment was repeated again and the MSZ

limit was reproducible within 0.3 °C. The smallest MSZW was measured by ISPV and was 6.1 °C. As ISPV was more sensitive in detecting particles, it was decided to use it at the industrial scale for detecting particles. The MSZW measurements can also be used for kinetic parameter estimation and determination of batch recipe. 36,37

6.5.5 Combined calibration and characterization at industrial scale

Calibration

For the calibration of ATR-FTIR and BRIX sensor, concentrations and temperature ranges used are shown in Table 6.2.

Table 6.2: Concentration and temperature ranges used for calibration of ATR-FTIR and BRIX sensor

Concentration [mg/mL]	Saturation temperature [°C]	Temperature range [°C]	
G	-	Upper	Lower
		temperature	temperature
48.3	10.0	15.0	5.0
78.6	22.5	29.0	17.5
108.9	30.0	34.5	25.0
139.3	35.5	41.5	30.0
169.6	39.8	45.2	34.7

Collection of spectra and BRIX values was carried out as described in section 6.4.5. For calibration of ATR-FTIR spectroscopy the region between 1816.9 cm⁻¹ and 794.7 cm⁻¹ was used and first derivative was used as the pre-processing step. The details of the calibration for ATR-FTIR spectroscopy and different spectral preprocessing steps can be found in literature²⁹ and are not described in details here. The root mean square error in prediction (RMSEP) for the calibration model was 0.521.

For calibration of BRIX sensor, a least square polynomial fit between the measured BRIX values was made with the known concentration values. The obtained polynomial is given as eq.6.1 and had a root mean square error of 0.955.

$$C_{brix} = P_{00} + P_{10}B + P_{01}T + P_{20}B^2 + P_{11}BT$$
(6.1)

where C is in mg/mL, T is in ${}^{\circ}C$ and B represents BRIX values measured by BRIX sensor. The obtained co-efficient of eq. 6.1 are

 $P_{00} = -139.5023$, $P_{10} = 2.4562$, $P_{01} = 0.3725$, $P_{20} = 0.2819$ and $P_{11} = -0.0126$.

Characterization

The calibration procedure used here allows for characterization i.e. determination of the operation window directly at industrial scale. The operation window at different concentrations is bound on one side by the solubility curve and on the other side by MSZ limit. As the calibration is performed directly at the industrial scale, the problems associated in concentration measurements due to minor misalignments of the hardware¹⁸ are avoided. Also as the solubility curve and the MSZ limit are determined directly at the industrial scale, the effect due to impurities and the scale of experiments will already be accounted for.

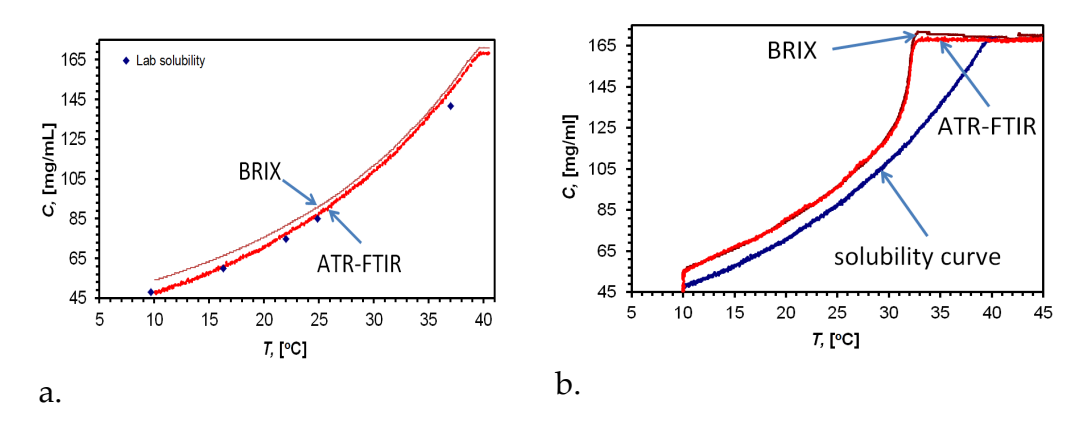


Figure 6.11: Process characterization at industrial scale, (a) solubility curve determined on industrial scale by ATR-FTIR and BRIX sensor, (b) the MSZW determined by ATR-FTIR and BRIX.

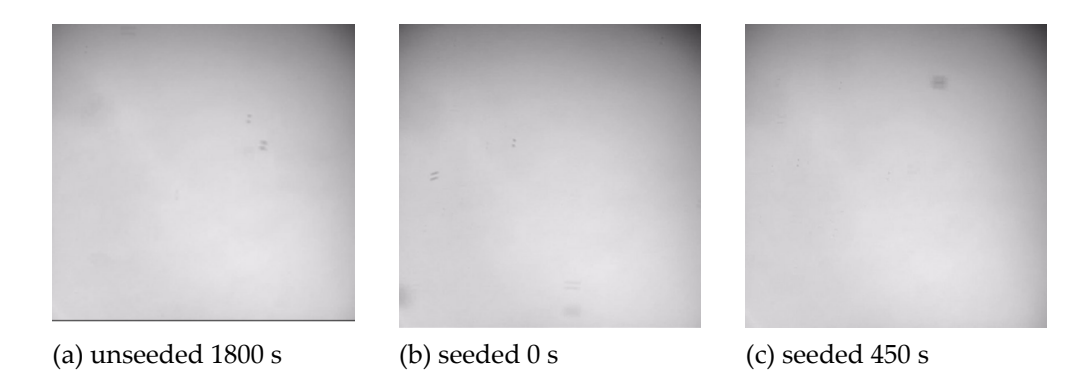
Figure 6.11a shows the solubility measured with ATR-FTIR and BRIX sensor for ADD-NEOP in ethanol at industrial scale. The lab scale solubility is plotted as a reference. As can be seen from Figure 6.11a, the solubility determined by ATR-FTIR agrees closely with the one measured at lab scale while the solubility determined by BRIX sensor is higher than the lab scale solubility. This is apparently due to the phase lag in the change of solution temperature and the change in the BRIX value associated with the temperature. The phase lag could be the result of the dynamics of the thermal path within the sensor and may be different while heating and cooling. Co-incidentally

the solubility determined at lab scale agreed reasonably with the solubility at industrial scale for ATR-FTIR. It might not be the case each time and in those cases the concentration of the clear solution after dissolution of individuals loads added during calibration could be used as a criteria. In this case, apart from the lab scale solubility the measured value of concentration by ATR-FTIR and BRIX agreed with the known value of concentration (amount of ADD-NEOP added to the solvent) at the end of last load.

When the clear solution is cooled at a constant rate of 0.4 °C/min, the MSZ limit can be determined. The MSZ limit is reached when the drop in concentration occurs for concentration measurement PAT tools. For both the ATR-FTIR and BRIX sensor, the MSZ limit was reached at 33 °C resulting in a MSZW of 6.8 °C. The larger MSZW, measured at industrial scale compared to lab scale is probably caused by the different detection techniques. Surprisingly, after nucleation and growth of the crystals the concentration did not reach the solubility curve towards the end of the batch. This might be due to the effect of impurity incorporation within the crystals but further research would be necessary before exact cause could be determined.

6.5.6 Gaining process insights

The results obtained during the unseeded and seeded experiments are shown in form of series of images in Figure 6.12. All the images in Figure 6.12 are taken at 36 °C with a high resolution camera in order to detect crystals as soon as possible. The time in the caption indicates the time elapsed after reaching 36 °C for unseeded experiment and for seeded experiments it indicates the time elapsed after seeding.



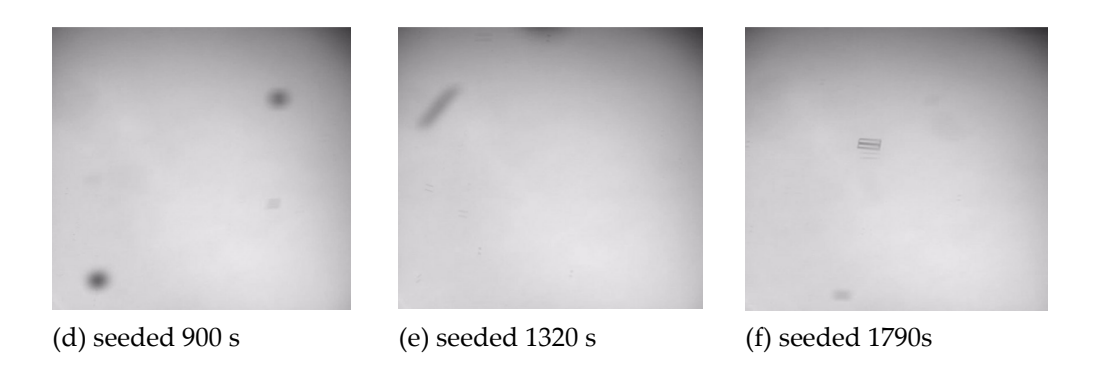


Figure 6.12: Images during the unseeded and seeded batch crystallization process by high resolution camera

As can be seen from Figure 6.12 there were no crystals seen during the unseeded experiment for 1800 s while for seeded experiment with the single crystal, crystals started appearing around approximately 1000 s. The low resolution camera gives a better indication of the amount of crystals as shown in Figure 6.13 as it has higher depth of field.

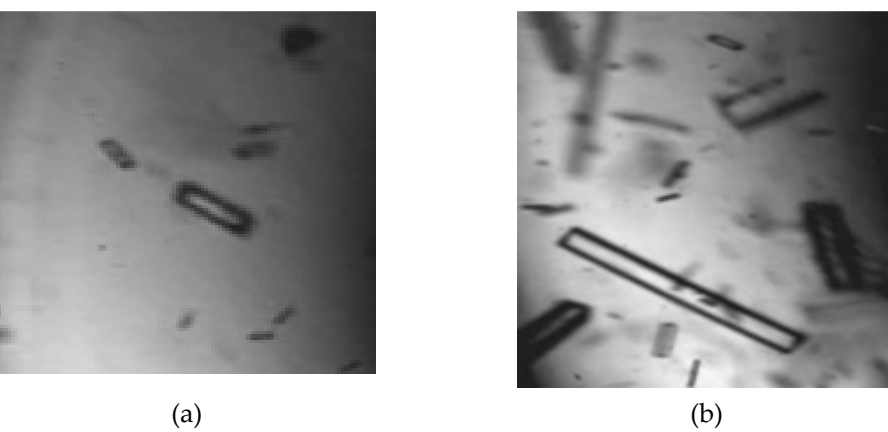


Figure 6.13: crystals after 1790 s (a) and 2595 s (b).

Both the seeded and unseeded experiments can be considered to be performed under constant supersaturation. For the unseeded experiment, not a single crystal was spotted for the first 1800 s while for seeded experiment with a single crystal, crystallization was seen around 1800 s. This indicates that the crystals appearing in the seeded experiment are the result of secondary nucleation induced by a single crystal. Substantial crystallization around 2600 s as seen in Figure 6.13b suggest that single crystal has a potential to act as a parent crystal and to lead to formation of the entire batch of crystals

through secondary nucleation. As seen from Figure 6.13 a and b under constant supersaturation of 1.25, number of crystals formed due to secondary nucleation increase with time. Amongst other factors, secondary nucleation rate is also proportional to the supersaturation.³⁸ Hence in a constant cooling mode of operation during batch crystallization, the amount of crystals formed by secondary nucleation would increase with time and supersaturation. This indicates that there exists a subregion within the MSZW close to the solubility curve where the secondary nucleation rate is minimal. Combining knowledge of this sub-region with seeded experiments with relatively few seeds in form of coarse crystals from the previous batch would lead to better control capabilities. Using few product crystals as seeds improves the descriptive capacity of the secondary nucleation model (Gahn and Mersmann)³⁹ as they form a system as described in the model of parent crystals giving rise to attrition fragments.⁴⁰

6.6 Conclusions

A rapid strategy for crystallization process development has been presented and demonstrated for ADD-NEOP using PAT tools both at lab scale and industrial scale. Integration of a number of PAT tools into a measurement skid which can be coupled to an existing crystallizer via a circulation flow allows for a flexible application of the PAT tools. The skid also circumvents the time and cost intensive design modifications which are conventionally necessary to incorporate the PAT tools at industrial scale. The presented process development strategy allowed for collection of thermodynamic and kinetic information at industrial scale without much a-priori knowledge. Monitoring of the process variables with the help of PAT tools enabled getting valuable process insights which can be used to optimize the process. This strategy of process development can also be combined with different control strategies to obtain better control over the product quality.

6.7 References

- (1) Mullin, J. W., Crystallization. Fourth ed.; Butterworth-Heinemann: Oxford, 2001.
- (2) Rohani, S.; Horne, S.; Murthy, K., Control of Product Quality in Batch Crystallization of Pharmaceuticals and Fine Chemicals. Part 1: Design of the Crystallization Process and the Effect of Solvent. *Organic Process Research & Development* **2005**, *9*, (6), 858-872.

- (3) Birch, M.; Fussell, S. J.; Higginson, P. D.; McDowall, N.; Marziano, I., Towards a PAT-Based Strategy for Crystallization Development. *Organic Process Research & Development* **2005**, 9, (3), 360-364.
- (4) Black, S. N.; Quigley, K.; Parker, A., A Well-Behaved Crystallisation of a Pharmaceutical Compound. *Organic Process Research & Development* **2006**, 10, (2), 241-244.
- (5) Kougoulos, E.; Jones, A. G.; Wood-Kaczmar, M. W., A HYBRID CFD COMPARTMENTALIZATION MODELING FRAMEWORK FOR THE SCALEUP OF BATCH COOLING CRYSTALLIZATION PROCESSES. *Chemical Engineering Communications* **2006**, 193, (8), 1008-1023.
- (6) Myerson, A. S., *Handbook of Industrial Crystallization*. 2nd ed.; Butterworth-Heinemann: Woburn, MA, 2002.
- (7) Prausnitz, J. M. L., R. N.; Azevedo, E. G., Molecular Thermodynamics of Fluid-phase Equilibria. ed.; Prentice-Hall: New Jersey, 1999.
- (8) Fredenslund, A.; Jones, R. L.; Prausnitz, J. M., Group-contribution estimation of activity coefficients in nonideal liquid mixtures. *AIChE Journal* **1975**, 21, (6), 1086-1099.
- (9) Eckert, F.; Klamt, A., Fast solvent screening via quantum chemistry: COSMO-RS approach. *AIChE Journal* **2002**, 48, (2), 369-385.
- (10) Lee, A. Y.; Erdemir, D.; Myerson, A. S., Crystal Polymorphism in Chemical Process Development. *Annual Review of Chemical and Biomolecular Engineering* **2011**, 2, (1), 259-280.
- (11) Anderton, C., A Valuable Technique for Polymorph Screening. *Eur. Pharm. Rev.* **2004**, 68-74.
- (12) Cui, Y.; Yao, E., Evaluation of hydrate-screening methods. *Journal of Pharmaceutical Sciences* **2008**, 97, (7), 2730-2744.
- (13) Jaroslav, N., Kinetics of nucleation in solutions. *Journal of Crystal Growth* **1968**, 3-4, (0), 377-383.
- (14) Jiang, S.; ter Horst, J. H., Crystal Nucleation Rates from Probability Distributions of Induction Times. *Crystal Growth & Design* **2010**, 11, (1), 256-261.
- (15) Christiansen, J. A., Nielsen, A. E., On the Kinetics of Formation of Precipitates of Sparingly Soluble Salts. *Acta. Chem. Scand.* **1951**, 673-674.
- (16) Galkin, O.; Vekilov, P. G., Direct Determination of the Nucleation Rates of Protein Crystals. *The Journal of Physical Chemistry B* **1999**, 103, (49), 10965-10971.
- (17) Hengstermann, A.; Kadam, S.; Jansens, P. J., Influence of Supercooling and Water Content on Crystal Morphology of Acrylic Acid. *Crystal Growth & Design* **2009**, 9, (4), 2000-2007.

- (18) Kadam, S. S.; Mesbah, A.; van der Windt, E.; Kramer, H. J. M., Rapid online calibration for ATR-FTIR spectroscopy during batch crystallization of ammonium sulphate in a semi-industrial scale crystallizer. *Chemical Engineering Research and Design* **2011**, 89, (7), 995-1005.
- (19) Glade, H.; Ilyaskarov, A. M.; Ulrich, J., Determination of Crystal Growth Kinetics Using Ultrasonic Technique. *Chemical Engineering & Technology* **2004**, 27, (7), 736-740.
- (20) Chung, S. H.; Ma, D. L.; Braatz, R. D., Optimal seeding in batch crystallization. *The Canadian Journal of Chemical Engineering* **1999**, 77, (3), 590-596.
- (21) Bakar, M. R. A.; Nagy, Z. K.; Rielly, C. D., Seeded Batch Cooling Crystallization with Temperature Cycling for the Control of Size Uniformity and Polymorphic Purity of Sulfathiazole Crystals. *Organic Process Research & Development* **2009**, 13, (6), 1343-1356.
- (22) Jones, A. G., *Crystallization Process Systems*. ed.; Butterworth-Heinemann: Oxford, 2002.
- (23) Mesbah, A.; Huesman, A. E. M.; Kramer, H. J. M.; Nagy, Z. K.; Van den Hof, P. M. J., Real-time control of a semi-industrial fed-batch evaporative crystallizer using different direct optimization strategies. *AIChE Journal* **2011**, 57, (6), 1557-1569.
- (24) Zoltan K, N., Model based robust control approach for batch crystallization product design. *Computers & Chemical Engineering* **2009**, 33, (10), 1685-1691.
- (25) Richard D, B., Advanced control of crystallization processes. *Annual Reviews in Control* **2002**, 26, (1), 87-99.
- (26) Kadam, S. S.; Kramer, H. J. M.; ter Horst, J. H., Combination of a Single Primary Nucleation Event and Secondary Nucleation in Crystallization Processes. *Crystal Growth & Design* **2011**, 11, (4), 1271-1277.
- (27) Rozsa, L., SeedMaster 2: A Universal Crystallization Transmitter and Automatic Seeding Device. *International Sugar Journal* **2006**, 108, (1296), 683-695.
- (28) Challis, R. E., Povery, M. J. W., Mather, M. L., Holmes, A. K., Ultrasound Techniques for Characterizing Colloidal Particles. *Rep. Prog. Phys.* **2005**, 68, (7), 1541-1637.
- (29) Kadam, S. S.; van der Windt, E.; Daudey, P. J.; Kramer, H. J. M., A Comparative Study of ATR-FTIR and FT-NIR Spectroscopy for In-Situ Concentration Monitoring during Batch Cooling Crystallization Processes. *Crystal Growth & Design* **2010**, 10, (6), 2629-2640.
- (30) Li, R. F.; Penchev, R.; Ramachandran, V.; Roberts, K. J.; Wang, X. Z.; Tweedie, R. J.; Prior, A.; Gerritsen, J. W.; Hugen, F. M., Particle Shape Characterisation via Image Analysis: from Laboratory Studies to In-process Measurements Using an in Situ Particle Viewer System. *Organic Process Research & Development* **2008**, 12, (5), 837-849.

- (31) ADD-NEOP absolute stereochemistry, obtained from SciFinder Scholar. (accessed on 24th September 2010),
- (32) Simon, L. L.; Nagy, Z. K.; Hungerbuhler, K., Comparison of external bulk video imaging with focused beam reflectance measurement and ultra-violet visible spectroscopy for metastable zone identification in food and pharmaceutical crystallization processes. *Chemical Engineering Science* **2009**, 64, (14), 3344-3351.
- (33) Dunuwila, D. D.; Berglund, K. A., ATR FTIR spectroscopy for in situ measurement of supersaturation. *Journal of Crystal Growth* **1997**, 179, (1-2), 185-193.
- (34) Brown, S. D.; Sum, S. T.; Despagne, F.; Lavine, B. K., Chemometrics. *Analytical Chemistry* **1996**, 68, (12), 21-62.
- (35) Bjørsvik, H.-R., Online Spectroscopy and Multivariate Data Analysis as a Combined Tool for Process Monitoring and Reaction Optimization. *Organic Process Research & Development* **2004**, 8, (3), 495-503.
- (36) Aamir, E.; Nagy, Z. K.; Rielly, C. D., Optimal seed recipe design for crystal size distribution control for batch cooling crystallisation processes. *Chemical Engineering Science* **2010**, 65, (11), 3602-3614.
- (37) Nagy, Z. K.; Fujiwara, M.; Woo, X. Y.; Braatz, R. D., Determination of the Kinetic Parameters for the Crystallization of Paracetamol from Water Using Metastable Zone Width Experiments. *Industrial & Engineering Chemistry Research* **2008**, 47, (4), 1245-1252.
- (38) Daudey, P. J.; van Rosmalen, G. M.; de Jong, E. J., Secondary nucleation kinetcs of ammonium sulfate in a CMSMPR crystallizer. *Journal of Crystal Growth* **1990**, 99, (1-4, Part 2), 1076-1081.
- (39) Gahn, C.; Mersmann, A., Brittle fracture in crystallization processes Part A. Attrition and abrasion of brittle solids. *Chemical Engineering Science* 54, (9), 1273-1282.
- (40) Kalbasenka, A.; Huesman, A.; Kramer, H., Modeling batch crystallization processes: Assumption verification and improvement of the parameter estimation quality through empirical experiment design. *Chemical Engineering Science* **2011**, 66, (20), 4867-4877.

Chapter 7

Conclusions and Recommendations

The main objective of this thesis was to develop domain knowledge and tools for rapid monitoring and characterization of crystal nucleation and growth. The domain knowledge and tools will enable understanding and quantifying of crystallization phenomena like nucleation and growth thus facilitating proper crystallizer design, an efficient and comprehensive route for process development and scale up, and developing appropriate process control strategy for existing crystallizers. The conclusions obtained while addressing the research objective and the recommendations for further research are summarized below.

7.1 Conclusions

Nucleation is one of the important crystallization phenomena as it initiates crystal formation in the initial phase of a batch process or new generations of crystals in a running crystallisation processes. The rate of the nucleation dictates the subsequent crystallisation phenomena like crystal growth, agglomeration etc. In spite of its importance, nucleation still remains an inadequately understood phenomenon. In chapters 2 and 3 of this thesis, the Metastable Zone Width (MSZW) or the operating window for batch crystallization was determined at different volumes and the obtained results were evaluated in the light of the Classical Nucleation Theory (CNT). Due to the high postulated values of the pre-exponential factor of the CNT, it was expected that the MSZW would be deterministic and also independent of volume. On the contrary for the paracetamol-water system large variations in MSZW values were observed in a range of approximately 25°C, when measured at 1 mL while the values were reproducible within 0.5°C when measured at 1 L for the same concentration and cooling rates. This indicates that the MSZW is a stochastic property at small volumes and the stochastic nature reduces as the volume is increased. This was confirmed by MSZW measurements at different volumes from 500 mL to 1 L for paracetamol-water system and isonicotinamide-ethanol system. The extent to which the reduction in the MSZW takes place is dependent on the model system. The stochastic nature of the MSZW is a result of low nucleation rates. The low nucleation rate also manifest itself in the volume dependent MSZWs. As the volume increases, the absolute number of molecular clusters increase with an increased probability of reaching the critical size early.

Nuclei which form as a result of primary nucleation have to grow before they are detected. Interestingly in several unseeded cooling crystallization experiments at 3 mL scale for multiple model systems under controlled conditions, it was observed that only a single crystal is seen before the outburst of the secondary nuclei. The secondary nuclei were visibly smaller than the parent crystal. This indicated that there were two distinct

generation of crystals in the small volume of 3 mL and these generations could have continued to multiply if the experimental volume was larger. The observation of only a single crystal in visualization experiment, the stochastic nature of the MSZW and its dependency on volume have led to the postulation of a Single Nucleus Mechanism (SNM). According to this SNM only a single primary nucleus is formed which grows to into a single parent crystal before undergoing extensive secondary nucleation. The appearance of only a single crystal in visualization experiments at 3 mL before outburst of secondary nuclei indicates that the coupling with secondary nucleation governs the number of crystals grown from primary nucleation. If the coupling between primary and secondary nucleation is strong, secondary nucleation would occur as soon as the first crystal is formed. On the other hand if the coupling is not strong, few more crystals would grow from primary nuclei, most likely one after another, before secondary nucleation becomes dominant.

In chapter 3 of this thesis a tool in form of a stochastic model based on the SNM was also developed which gives the probability of detecting crystals within a certain MSZW. The stochastic model enabled scale dependent study not only of nucleation but also of the MSZW. The stochastic model suggested that if the volume is increased the MSZW would become less stochastic . The effect of the volume on the MSZW was also investigated with the conventional population balance model used to describe crystallization processes. The conventional population balance model showed that there is no effect of the volume on the MSZW. The trends in the MSZW were compared with the experiments for 2 model systems at different volumes and they agreed well with the stochastic model. The experiments also revealed a scale up rule for the MSZWs: the smallest measured MSZW at each volume is the same.

Apart from the knowledge of phenomena it is also essential during crystallization to identify to which extent a particular phenomenon is active. This can be achieved by insitu measurement of the process variables. One of the important variables that must be monitored during crystallization is the concentration of solute in the solution. The actual value of concentration can provide the driving force for crystallization during the process. In chapter 4 of the thesis, the comparison between attenuated total reflectance Fourier transform infrared spectroscopy (ATR-FTIR) and Fourier transform near infrared spectroscopy (FT-NIR) for concentration monitoring during crystallization of four different crystallizing systems viz. α -lactose monohydrate in water, ammonium sulfate in water, ibuprofen in hexane, and L-glutamic acid in water was performed. It was found that ATR-FTIR performs better in pure liquid as well as in the vicinity of crystals and is more accurate. On the other hand, it is more sensitive to the stress in the fiber optics. Although FT-NIR has comparable performance in pure

liquid, it is inadequate in the presence of crystals as it is more susceptible to fouling. Also the spectra collection for FT-NIR is affected due to the crystals in the path of the radiations. The performance of both techniques is dependent on the crystallizing system. As spectra collected by ATR-FTIR consists of distinct peaks, it provides a distinct advantage in selecting regions of interest while developing the Partial Least Square (PLS) calibration models. The FT-NIR spectrum consists of broad bands resulting from the overtones and the combination vibrations and hence chemometrics must be relied on in selecting regions of interest.

Successful application of ATR-FTIR at lab scale does not necessarily warrant its success at the industrial scale or even when the instrument is moved from one vessel to the other in the lab scale. This is due to the changes in curvature of the fibre optics used to transmit the IR radiation to and from the probe. Due to changes in the curvature, the intensity of the IR radiations reaching the probe tip is altered which is reflected in the altered intensities of the peak heights. This leads to biased measurements. This bias can be corrected with the help of rapid online calibration method proposed in chapter 5 of this thesis. This method relies on another, possibly cheaper, measurement instrument which could measure concentration at least in absence of crystals. The advantage that rapid online calibration brings is that the time required to collect spectra and develop PLS calibration model at industrial scale is reduced by 90%. As the calibration of the instrument is performed with the fibre optics in the same position as will be used during the actual process measurements, bias in concentration measurement is not encountered.

Apart from the concentration measurement, another important process variable that must be monitored during crystallization is the Crystal Size Distribution (CSD). CSD measurements present more challenges than concentration measurements. It is mainly due to the assumption made by most CSD measurement techniques that the crystals are spherical in shape. For common CSD measurement techniques based on ultrasound attenuation and laser diffraction, the reconstruction of size distribution from the measurement signal is required. The reconstruction is complicated when the size distribution is not uni-modal. In-situ imaging can provide solutions to these problems as it does not make assumptions of the particle size distribution and shape. As the technique is based on direct observation of crystals, the interpretation of data is intuitive. In this thesis (chapters 2,3 and 6) in-situ imaging was used in a qualitative manner only as the extraction of CSD data from images is still challenging. This is due to the fact the quality of images obtained in-situ is not good for image segmentation, the sensor can handle low particle concentration and the image analysis algorithm are not robust yet.

Combination of different measurement instruments can provide possibilities of obtaining better parameter estimates and also of developing an optimized crystallization process. In chapter 5 of the thesis, concentration measurements were combined with CSD measurements to obtain better process insights. It was observed that the model used to describe the crystallization process based on parameters obtained just using CSD, over predicted the growth rate. When the growth rate parameters used in the model were re-estimated with the information of both the concentration and CSD, the model could better describe the process. In chapter 6 of the thesis a combination of different measurement instruments was used to propose and demonstrate a rapid strategy for crystallization process development of a pharmaceutical intermediate ADD-NEOP. The different measurement instruments or the Process Analytical Technology (PAT) tools were integrated into a measurement skid which could be coupled to an existing crystallizer via a circulation flow. The ease of connection of the measurement skid to the crystallizer and the modular design of the skid allowed for the flexible application of the PAT tools. The use of skid also circumvented the time and cost intensive design modifications which are conventionally necessary to incorporate PAT tools at industrial scale. The presented process development strategy facilitated collection of thermodynamic and kinetic information at industrial scale without much a-priori knowledge. Monitoring of the process variables with the help of PAT tools enabled getting valuable process insights which can be used to optimize the process.

The research presented in this thesis has led to advancements in crystallization domain understanding, process characterization and process monitoring. It has been shown contrary to the classical nucleation theory that the primary nucleation rates are extremely low and possibly a single parent crystal is responsible for the entire population of crystals in a batch. Also contrary to the conventional understanding of MSZW as a deterministic property, it has been shown in this thesis that MSZW is a stochastic property at small volume and its stochastic nature reduces with the increase in volume. Unlike the conventional population balance model which does not show the influence of volume on the MSZW, a newly proposed stochastic model based on the SNM can capture the influence of volume on the MSZW. In addition the work presented in this thesis is one of the pioneering work in the domain of process monitoring at industrial scale. The complications in introducing the PAT tools at industrial scale have been identified and solutions to overcome them have been proposed and demonstrated. The use of PAT tools in form of a measurement skid has been proposed and demonstrated. The measurement skid offers the needed flexibility and ease of implementation at industrial scale. The work presented in this thesis would make the crystallizer design, process development and scale up and designing

of crystallization control strategies more efficient and robust. In spite of the progress made due to the contribution of this thesis, there are several challenges which need attention. Some of those challenges are identified and possible solutions for those challenges are proposed in the following section.

7.2 Recommendations

- The CNT predicts high nucleation rates due to high values of the preexponential factor of the nucleation rate expression. According to the CNT, as large numbers of nuclei are formed simultaneously, MSZW is deterministic and also independent of volume. The pre-exponential factors estimated based on the experiments in this thesis are several orders of magnitude smaller than those postulated for CNT indicating very low primary nucleation rate. The precise reason for the discrepancy between the estimated pre-exponential factor based on the experiments and the one's postulated by the CNT is still obscure and should be investigated further. There are few possible means to investigate this which includes molecular modelling and experiments. Molecular modelling could provide insight in the clustering mechanism of the molecules under certain conditions thereby also providing means to determine nucleation rates. These nucleation rates can be compared with those determined based on the CNT and experiments. On the other hand experiments could be performed in controlled environment where values of the pre-exponential factor can be controlled. Such controlled environment can be envisaged in form of a tiny droplet with volumes in micro litre range or those provided by a template upon which nucleation would occur. The investigation would shed light on the sequence of molecular events which leads to the formation of a nucleus. The knowledge and mathematical description of the nucleation process will offer a chance to intervene and manipulate the outcome of molecular events. This would especially be interesting to obtain desired polymorphic form or a crystal with desired chiral symmetry.
- The mechanism of formation of a single crystal first followed by its rapid secondary nucleation, termed as the Single Nucleus Mechanism (SNM) in this thesis, raises three important questions
 - Why does only a single crystal appear initially at small volumes instead of a few simultaneously?
 - o What is the mechanism of secondary nucleation?

o If the volume is increased gradually (inhomogeneities in mixing would increase with volume), would there be a transition to the conventional nucleation mechanism from the single nucleus mechanism?

Molecular modelling could provide answer to the first question as it could help in understanding the sequence of molecular events which leads to the formation of the first nucleus. With molecular modelling it would be possible to investigate if the molecular cluster grows by the attachment of a single molecule or if two small clusters could combine to form one big cluster. Molecular modelling may also help in identifying the instance in cluster formation from which a structure starts to appear within the cluster, in determining if multiple molecular clusters could reach the critical size simultaneously and if they do why only a single crystal spotted is in small volumes.

Mechanism of secondary nucleation could be understood by carefully inducing secondary nucleation by different means and following the process by in-situ measurement of different process variables. An example of such a study would be to use high speed high resolution camera to observe secondary nucleation triggered by a single crystal in a small volume. It could be investigated if secondary nucleation occurs when the crystal is suspended in a stirred solution without physical contact with the stirrer. Also it would be interesting to investigate the effect of stirring speed and stirrer types on the secondary nucleation induced by such suspended single suspended crystal. Similar experiments could be performed by allowing contact between an unsuspended single crystal and the impeller.

In order to investigate if there would be a transition to the conventional nucleation mechanism as the volume and hence inhomogeneties in mixing increase, unseeded batch cooling experiments involving chiral or polymorphic systems could be performed. If crystals of same handedness are obtained for a chiral system or only a single polymorph is obtained from a mixture of solvents at the volume of interest, SNM holds at that volume. Experiments could be performed with computational fluid dynamics calculations to identify local cold spots and volumes of those cold spots within which the SNM would occur.

 ATR-FTIR can be used for concentration monitoring during crystallization at lab and industrial scale. Most of the times experimental perturbations are included in the spectral data in form of base line shifts or scatter due to interaction between particles and light. In order to eliminate the effect of perturbations, data pre-processing is necessary. Development of a good Partial Least Square model is also dependent on efficient data pre-processing. There are several pre-processing techniques available and a choice of any particular one is often based on trial and error rather than scientific reasoning. Hence it is essential to develop a protocol which would guide through the choosing of pre-processing techniques during PLS modelling.

Monitoring of the CSD distribution could be done by employing several different techniques. Most of the CSD measurement techniques make assumptions about shape of the crystals and the crystal distribution. In-situ imaging is free from such assumptions as it is based on direct observation. But in order to make in-situ imaging quantitatively applicable at industry, optics for better images must be developed. It must be complimented by robust image processing algorithm which could handle slightly un sharp images and images of overlapping crystals.

• A measurement skid provides a flexible way for application of the PAT tools at industrial scale. The drawback of calibration directly at industrial scale is that large volumes of solute and solvent would be necessary at industrial scale. Also the time for collecting relevant data for building calibration models would be high at industrial scale. These issues could be circumvented by building a small calibration loop within the skid-crystallizer loop. The calibration loop should be such that its temperature could be controlled and extra solute or solvent addition is possible. With the use of the calibration loop it would be possible to calibrate the instruments in short amount of time as amount of material handled would be low and the calibration can be performed in the same position of the instruments in which they would be used for process monitoring.

Summary Samenvatting

Summary

Batch crystallization is commonly used in pharmaceutical, agrochemical, specialty and fine chemicals industry. The advantages of batch crystallization lie in its ease of operation and the relatively simple equipment that can be used. On the other hand a major disadvantage associated with it is the inconsistent and usually poor product quality. Quality of the crystalline product, which is defined in terms of the Crystal Size Distribution (CSD), purity, kind of solid state etc., is related to its performance when used as an ingredient during subsequent processes. Also the quality of the product from batch crystallization process has a strong influence on the efficiency of downstream operations like filtration and drying. Hence it is essential to reduce the batch-to-batch variations in the product quality.

In this thesis three basic requirements for achieving consistent product quality have been identified. These requirements are a.) strong domain knowledge, b.) proper means of characterizing crystallization phenomena, and c.) adequate process monitoring capabilities. The results presented in this thesis help in meeting the above requirements and are summarized below.

- a. **Crystallization domain knowledge:** Three important results related to the Metastable Zone Width (MSZW) have been obtained in this thesis which cannot be explained by the conventional understanding. It has been shown in this thesis that
 - i. MSZW is not a deterministic property
 - ii. MSZW is volume dependent
 - iii. There exists a relationship between MSZWs measured at different volumes under similar conditions.

The MSZW measurements at small volumes of 1 mL show large variations while the variations in the measurements reduce as the volume is increased. The extent of variations in the MSZW measurements at a particular volume changes from one model system to the other. The smallest measured MSZW at all volumes between 1 millilitre and 1 litre is the same.

The dramatic deviation from the conventional understanding of the measured MSZWs is a result of inadequate understanding of the nucleation process. Conventionally, a multiple nuclei mechanism is assumed in which large number of nuclei are born together in a very short time interval. However in

this thesis evidence is presented for a mechanism in which only a single nucleus is formed initially in a supersaturated solution which grows into a single crystal. After growth to a certain size, this single crystal undergoes extensive secondary nucleation which results into multiple crystalline fragments. The newly postulated mechanism is called the Single Nucleus Mechanism. All the crystals produced in an unseeded batch crystallization therefore originate from a single primary nucleus by secondary nucleation. This indicates that during an unseeded industrial batch crystallization process, there will be different generations of crystals present. Hence, in order to achieve crystals with desirable quality, control strategies must be focused on controlling both primary and secondary nucleation.

b. Crystallization characterization: In this thesis novel methods to characterize crystal nucleation, growth and MSZW have been developed. The characterization of crystal nucleation and MSZW is done with the help of a stochastic model developed based on the Single Nucleus Mechanism. The stochastic model indicates that the nucleation rate is several orders of magnitude smaller than that postulated by the Classical Nucleation Theory. The low nucleation rate leads to the stochastic MSZWs. Unlike the conventional population balance model which shows that the MSZW is independent of volume, the stochastic model indicates that the MSZW is a function of volume. The stochastic model also enables scale dependent study of the MSZW.

The characterization of crystal growth is performed by the combination of information from both the concentration measurement sensor and the crystal size distribution (CSD) measurement sensor. It is shown that by combining of the concentration and CSD measurements a better parameter estimation and better process description could be achieved.

c. Crystallization process monitoring: In this thesis in situ measurement of several process variables has been successfully demonstrated not only at lab scale but also at industrial scale. A comparison has been performed between two spectroscopy based techniques viz. attenuated total reflectance Fourier transform infrared spectroscopy (ATR-FTIR) and Fourier transform near infrared spectroscopy (FT-NIR) for in situ concentration monitoring during crystallization at lab scale. Based on the comparison, ATR-FTIR is found to be more accurate than FT-NIR for different model systems. In spite of accurate concentration monitoring at lab scale, the concentration monitoring with ATR-

FTIR leads to biased measurements at industrial scale due to the differences in the curvature of fiber optics.

To facilitate the in situ concentration measurements in industrial environment, two calibration procedures have been investigated which circumvent problems associated with calibration transfer from lab to industrial scale. In the first procedure data from a cheap ultrasound based concentration probe is combined with the spectra from ATR-FTIR spectroscope. It is shown that this combination of data enables a rapid calibration of ATR-FTIR at industrial scale. In the second procedure, multiple Process Analytical Technology (PAT) tools that were arranged in a measurement skid were calibrated simultaneously at industrial scale. The skid configuration of the PAT tools allows for the combination of the calibration procedure with process characterization. The monitoring of the process at industrial scale with multiple sensors brings new process insights which can lead to better process control and optimization strategies.

The results presented in this thesis will enable achievement of consistent product quality by facilitating efficient process and equipment design, process development, and process control.

Samenvatting

Batch kristallisatie wordt vaak toegepast in de farmaceutische, agrochemische, speciale en fijne chemische industrie. De voordelen van batch kristallisatie liggen in het bedieningsgemak en in de relatief eenvoudige apparaten die hiervoor vereist zijn. Anderzijds is een er een groot nadeel aan verbonden en wel een niet consistente en meestal slechte productkwaliteit. De kwaliteit van een kristallijn product, dat wordt gedefinieerd in termen van de Crystal Size Distribution (CSD), zuiverheid, het type van vaste fase enz., is gerelateerd aan de prestaties bij gebruik als ingrediënt bij eventuele toepassingen. Ook heeft de kwaliteit van het product van batch kristallisatieprocessen een sterke invloed op de efficiëntie van vervolg behandelingen zoals filtratie en droging. Het is daarom essentieel dat de batch-to-batch variaties in de kwaliteit van het product te minimaliseren.

In dit proefschrift worden drie fundamentele eisen voor het realiseren van een meer consistente productkwaliteit geïdentificeerd. Deze eisen zijn a) een grote domeinkennis, b.) geschikte meetinstrumenten voor de karakterisering van verschillende kristallisatiestappen, en c.) adequate mogelijkheden voor procesbewaking. De resultaten gepresenteerd in dit proefschrift helpen bij het voldoen aan de bovenstaande vereisten en worden hieronder samengevat.

- a. Domeinkennis op het gebied van de industriële kristallisatie: Drie belangrijke resultaten met betrekking tot de breedte van de metastabiele zone (MSZW) zijn verkregen in dit proefschrift, die niet verklaard kunnen worden door de conventionele kristallisatie theorieën. In dit proefschrift is aangetoond dat
 - i. De MSZW is geen deterministisch eigenschap van het systeem is
 - ii. De MSZW afhankelijk is van het volume
 - iii. Er een relatie bestaat tussen de MSZW's gemeten in verschillende volumes onder vergelijkbare omstandigheden.

De MSZW metingen bij kleine volumes van 1 ml tonen grote variaties aan in de gevonden waarden, terwijl deze variaties afnemen met het toenemen van het volume. De grootte van de spreiding in de MSZW waarden bij een bepaald volume is verschillend van het ene modelsysteem tot het andere. Opmerkelijk is dat de laagste gemeten MSZW waarden hetzelfde is onafhankelijk van het meetvolume, althans in het volume bereik van één ml tot 1 liter.

Deze dramatische afwijking van de door de conventionele theorie voorspelde MSZW van die van de gemeten MSZWs waarden is het gevolg van onvoldoende begrip van de kiemvormingsproces. Gewoonlijk wordt in de theorie een zg "poly nucleus" mechanisme aangenomen waarbij grote aantal kiemen worden geboren in een zeer korte periode. In tegenspraak daarmee wordt in dit proefschrift bewijs gepresenteerd voor het bestaan van een mechanisme, waarbij in eerste instantie in een oververzadigde oplossing slechts één enkele kiem wordt gevormd welke vervolgens aangroeit tot een kristal. Na uitgroei tot een bepaalde grootte zal het aanwezige kristal uitgebreide secundaire kiemvorming tot gevolg hebben, wat resulteert in de vorming van een groot aantal kristalfragmenten. Het nieuw gepostuleerde mechanisme wordt het "Single Nucleus" mechanisme genoemd. Alle kristallen die in niet geënt batch kristallisatie worden geproduceerd, zijn dan ook afkomstig van één enkele primaire kiem geproduceerd door secundaire kiemvorming. Dit geeft aan dat er tijdens zo'n batch kristallisatieproces, verschillende generaties kristallen aanwezig zijn. Daarom moeten regelstrategieën voor de een gewenste kristalkwaliteit gericht zijn op het beheersen van primaire en secundaire kiemvorming.

b. Karakterisering van het kristallisatie proces: In dit proefschrift worden nieuwe methoden beschreven om kiemvorming, kristalgroei en de MSZW te karakteriseren.. De karakterisering van kiemvorming van de MSZW wordt gedaan met behulp van een stochastisch model ontwikkeld op basis van de het "Single Nucleus" mechanisme. Het stochastische model geeft aan dat de kiemvormingssnelheid enkele ordes van grootte kleiner is dan die gepostuleerd in de klassieke kiemvormingstheorie. De lage kiemvormingssnelheid leidt tot de stochastische MSZWs. In tegenstelling tot de conventionele populatiebalans modellen waaruit blijkt dat de MSZW onafhankelijk is van het volume, geeft het stochastische model aan dat de MSZW een functie is van volume. De stochastische model maakt het tevens mogelijk de MSZW afhankelijkheid van de schaal van opereren te bestuderen.

De karakterisering van kristalgroei is uitgevoerd door de gebruik te maken van de combinatie van data van zowel de concentratie sensor als de kristalgrootteverdeling (CSD) sensor. Aangetoond is dat door het combineren van concentratie en CSD metingen een betere parameterschatting en beter procesbeschrijving kan worden verkregen.

c. Bewaking van het kristallisatieproces: In dit proefschrift is het in situ meten van een aantal procesvariabelen met succes gedemonstreerd, niet alleen op laboratoriumschaal, maar ook op industriële schaal. Er is een vergelijking gemaakt tussen twee op spectroscopie gebaseerde technieken te weten. "Attenuated Total Reflection Fourier Transform Infrarood Spectroscopy", (ATR-FTIR) en "Fourier Transform Near-Infrared Spectroscopy" (FT-NIR) voor in-situ regeling van de concentratie tijdens kristallisatie op laboratorium schaal. Op basis van deze vergelijking, werd ATR-FTIR nauwkeuriger gevonden dan FT-NIR voor een aantal modelsystemen. Echter ondanks een nauwkeurige ijking van de concentratie op laboratorium schaal, leidde de concentratie meting met ATR-FTIR op industriële schaal tot metingen met een systematisch afwijking door verschillen in kromming van de gebruikte glasvezel kabel. Om de in-situ concentratie metingen in industriële omgeving te faciliteren, zijn er twee methodes onderzocht, die problemen verband houdend met het overzetten van de methode van ijking van laboratorium naar industriële schaal kunnen vermijden. In de eerste procedure worden gegevens van een op ultrasone metingen gebaseerde concentratie sensor gecombineerd met de spectra van de ATR-FTIR spectroscoop. De slimme combinatie van meetgegevens van twee verschillende sensoren maakte een snelle ijking mogelijk van de ATR-FTIR op industriële schaal. In de tweede procedure werden meerdere Process Analytical Technology (PAT) tools, die in een meetopstelling waren gerangschikt, gelijktijdig gekalibreerd op industriële schaal. De rangschikking van deze PAT tools in een externe meet unit maakt het mogelijk om de kalibratie methode te combineren met de karakterisering van het proces. De proces bewaking op industriële schaal met meerdere sensoren levert nieuwe proces inzichten die kunnen leiden tot een betere strategieën voor procesbeheersing en optimalisatie.

De resultaten gepresenteerd in dit proefschrift kunnen bijdragen tot een meer consistente product kwaliteit van industriële kristallisatieprocessen door middel van een meer efficiënte proces en apparaatontwerp, procesontwikkeling en procesbeheersing.

Vertaald door Dr. ir. H. J. M. Kramer.

List of Publications Curriculum Vitae Acknowledgements

List of Publications

Journal Papers

- 1. <u>Kadam, S. S.</u>; Vissers, J. A. W.; Forgione, M.; Geertman, R. M.; Daudey, P. J.; Stankiewicz, A. I., Kramer, H. J. M., Rapid Crystallization Process Development Strategy from Lab to Industrial Scale with PAT tools in skid configuration, manuscript in press, *Org. Process Res. & Dev.*, **2012**, 16(5), 769-780.
- <u>Kadam, S. S.</u>; Kulkarni, S. A.; Coloma, R.; Stankiewicz, A. I.; ter Horst, J. H.; Kramer, H. J. M., A New View on the Metastable Zone Width during Cooling Crystallization, *Chem. Eng. Sci.*, 2012, 72, 10-19.
- 3. <u>Kadam, S. S.</u>; Kramer, H. J. M.; ter Horst, J. H., The Combination of a Single Primary Nucleation Event and Secondary Nucleation in Crystallization Processes, *Cryst. Growth Des.*, **2011**, 11(4), 1271-1277.
- 4. <u>Kadam, S. S.</u>; Mesbah, A.; van der Windt, E.; Kramer, H.J.M., Rapid Online Calibration for ATR-FTIR Spectroscopy during Batch Crystallization of Ammonium Sulphate in a Semi-Industrial Scale Crystallizer, *Chem. Eng. Res. Des.*, **2011**, 89(7), 995-1005.
- 5. <u>Kadam, S.S.</u>; van der Windt, E.; Daudey, P.J.; Kramer, H.J.M., A Comparative Study of ATR-FTIR and FT-NIR Spectroscopy for In-Situ Concentration Monitoring during Batch Cooling Crystallization Processes, *Cryst. Growth Des.*, **2010**, 10(6), 2629-2640.
- Hengstermann, A.; <u>Kadam, S.</u>; Jansens, P.J., Influence of Supercooling and Water Content on Crystal Morphology of Acrylic Acid, *Cryst. Growth Des.*, 2009, 9 (4), 2000–2007.
- 7. Kulkarni, S. A.; <u>Kadam, S. S.</u>; Stankiewicz, A. I.; Meekes, H.; ter Horst, J. H, A Comparison between Nucleation Rates Obtained by Metastable Zone Width Measurements and Induction time measurements, manuscript in preparation.
- 8. Kulkarni, S. A.; <u>Kadam, S. S.</u>; Stankiewicz, A. I.; Meekes, H.; ter Horst, J. H., Validation of the Single Nucleus Mechanism by Polymorphism, manuscript in preparation.

Book Contributions

- Kramer, H. J. M. and <u>Kadam, S. S.</u> (2012) Imaging, in *Industrial Crystallization Process Monitoring and Control (eds A. Chianese and H. J. M. Kramer)*, Wiley-VCH Verlag GmbH & Co. KGaA, Weinheim, Germany. doi: 10.1002/9783527645206.ch5
- 2. <u>Kadam S. S.</u>, Kulkarni S. A., ter Horst J. H. (Editors), *Proceedings of 18th Industrial Workshop on Industrial Crystallization (BIWIC)*, ISBN: 978-94-6191-003-5, **2011**.

Selected Conference Proceedings

- 1. <u>Kadam, S. S.</u>; Kulkarni, S. A.; ter Horst, J. H.; Kramer, H. J. M, A New View on Crystal Nucleation in Industrial Crystallization, *In proceedings of 18th International Symposium on Industrial Crystallization (ISIC18)*, **2011**, 7-8.
- 2. <u>Kadam, S. S.</u>; Vissers, J. A. W.; Forgione, M.; Geertman, R. M.; Daudey, P. J.; Kramer, H. J. M., Rapid Determination of a Near-optimal Seeding Procedure at an Industrial Scale Batch Crystallizer, *In proceedings of 18th International Symposium on Industrial Crystallization (ISIC18)*, **2011**, 71-72.
- 3. Kulkarni S. A.; <u>Kadam S. S.</u>; Meekes, H.; ter Horst, J. H., Easy Access to Valuable Industrial Nucleation Kinetics, *In proceedings of 18th International Symposium on Industrial Crystallization (ISIC18)*, **2011**, 529-530.
- 4. Vissers, J.; Forgione, M.; <u>Kadam, S. S.</u>; Daudey, P.; Backx, T.; Huesman, A.; Kramer, H. J. M.; van den Hof, P., Novel Control of Supersaturation on an Industrial Scale Pharmaceutical Batch Cooling Crystallizer, *In proceedings of 18th Industrial Workshop on Industrial Crystallization (ISIC18)*, **2011**, 141-142.
- 5. Kulkarni S. A.; <u>Kadam S. S.</u>; Stankiewicz, A. I.; Meekes, H.; ter Horst, J. H, Validation of the Single Nucleus Mechanism, *In proceedings of 18th Industrial Workshop on Industrial Crystallization (BIWIC)*, **2011**, 75-80.
- Kadam, S.; Mesbah, A.; van der Windt, E.; Kramer, H.J.M., Application of ATR-FTIR Spectroscopy for In-situ Concentration Measurements of Ammonium Sulphate on Laboratory and Pilot Plant Scales, *In proceedings of 16th Industrial Workshop on Industrial Crystallization (BIWIC)*, 2009, 339-346.

Selected Oral Presentations

Plenary Lecture

1. A New View on Crystal Nucleation, 18th International Symposium on Industrial Crystallization (ISIC18), September 13-16, **2011**, Zurich, Switzerland.

Invited Lectures

- 1. A Probabilistic Approach to Characterize Nucleation Behavior by Metastable Zone Width Measurements, Dutch Association of Crystal Growth (DACG) Symposium, 12th November **2010**, Nijmegen, The Netherlands.
- 2. In-situ Concentration Monitoring by ATR-FTIR Spectroscopy, Bruker Optics R&D user meeting, 26th March 2010, Ridderkerk, The Netherlands.

Curriculum Vitae



Somnath Kadam was born in Mumbai, India on 18th January 1984. He attended secondary and higher secondary school at his native place Satara, India before starting Chemical Engineering studies at Dr. Babasaheb Ambedkar Technological University, Lonere, India. He received Bachelor of Technology degree with distinction in 2005. In the month of August the same year, he joined Master of Science program in Industrial Chemistry at Singapore. The master's program was a collaboration between the National University of Singapore and the Technical University of Munich. He was awarded the prestigious industrial sponsorship of 30,000 EUR by Degussa AG (now Evonik AG) to attend the master's program. He spent 8 months from June 2006 with Degussa AG at Marl, Germany to complete an internship and his master thesis. His master thesis titled "The Influence of Supercooling and Water Content on Crystal Morphology of Acrylic Acid" received the "Best Master Thesis Award" for the year 2007. He finished the Master of Science program with high distinction. The interest he developed in crystallization during his master thesis brought him to the Delft University of Technology in February 2008. During his PhD he contributed to both, the scientific and industrial aspects of crystallization. He spent 6 months with Merck Sharp and Dohme during his PhD and developed a rapid crystallization process development strategy with the project partners. During his PhD, he received guidance from Prof. A. I. Stankiewicz, Dr. H. J. M. Kramer, Dr. J. H. ter Horst and Dr. P. J. Daudey. Apart from his research, Somnath enjoys playing cricket, badminton and table-tennis. He loves swimming, cycling, ice skating, bowling, travelling, reading novels and photography.

Acknowledgements

I would like to express my deep sense of gratitude towards many who have contributed during my research and writing of this thesis. My words would hardly do justice to their immense contributions but nevertheless I do not want to miss on this opportunity of thanking them.

I would like to start by thanking Prof. Andrzej Stankiewicz for having me in his group and for providing me with the moral support during hard times of my thesis. You had accepted me gladly as one of your students when Prof. Peter Jansens made a transition from academia to industry. Whenever things went wrong with administration and management within the project, I could always count on you to be on my side. That sense of security allowed me to sail through turbulent situations with relative ease. Peter, I owe my interest in this department and the Delft University of Technology to you. After our meetings at Degussa AG, Marl; I very much wanted to be a part of P&E. During your transition to industry, you left me in the able hands of Prof. Andrzej Stankiewicz and Dr. Herman Kramer. Herman, I cannot thank you enough for bearing me in all those long meetings. You mentioned few times that, of all the meetings you have, you couldn't afford to miss a cup of coffee before the start of meetings with me. I always gained new insights through our discussions, and after the meetings I always felt that there is so much more to do. You also invited me to write a book chapter with you which I consider as a big honour. You gave ample freedom to implement my ideas and always encouraged me to question the conventional methods. Our collaboration with Dr. Joop ter Horst wouldn't have been so successful had it not been for your enthusiasm. Joop, you provided me with numerous opportunities which I couldn't have thought of having otherwise. You gave me a chance to chair a conference session, to be a part of the organizing committee of BIWIC 2011, to present at the Dutch Association of Crystal Growth and many more. I benefited a lot in my understanding of crystal nucleation because of you. You have played a big role in improving my technical writing and my oral presentation skills.

I would also like to thank Dr. Peter Daudey to accept me as a part of his team within the ISPT project. Peter, you are a very keen scientist with a good feel for fundamental as well as practical aspects of crystallization. I learnt a lot about secondary nucleation and seeding from you. A special thank goes to Dr. Rob Geertman for allowing me to work in his lab at Merck Sharp and Dohme. Rob, everybody at Oss and Apeldoorn makes a remark as soon as they hear your name. Rob is a scientist! I cannot agree more to that. I also learnt about the new directions in pharmaceutical industry, the working style of

the industry, culture within the company and much more from you. I would also like to thank Jochem Vissers and Marco Forgione, my fellow PhD students within the project. Without your support, it would have been difficult to do much during the experimental campaign at MSD and during the exploration of Apeldoorn city. Now that MSD will no longer be at Apeldoorn, the only place of interest for me over there is the Restaurant Roma. Prof. Paul Van den Hof, Prof. Ton Backx, Adrie Huesman, Prof. Siep Wieland, Dr. Xavier Bombois, Jeffrey Landlust, discussions with you enabled me to learn control perspectives on the same crystallization problem which I was approaching from the Chemical Engineering side. You echoed during the years the same thoughts that Paul had mentioned during my interview with him. Control engineers must be involved from early stages during the design of process and equipments rather than at later stages. Over the years, I have started to understand this notion in more details. I cannot mention all the people involved in the project due to the limited space but I would like to extend my gratitude to Dr. Pieter Vonk, Dr. Gerrit Westhoff, Dr. Marketta Uusipenttila, Fred Huygen, Jan Willem Gerritsen, Rob van Dongen, Ramon Harting, Edwin Stokkingreef, William de Wildt, Frido Roloff and Ger van der Veen. Eric van der Windt, a special thank also goes to you for teaching me about ATR-FTIR spectroscopy. You were always available when I had a problem with the instrument or with the modelling.

Most of the people mentioned above were brought together under one umbrella by ISPT. I thank ISPT for establishing such a consortium and providing the financial support during this project.

At P&E I have received a constant support from Leslie, Helma and Illona. Thank you for that. Also my gratitude towards Michel for his assistance during my experiments in the laboratory and Jan along with the entire workshop team for their help in the pilot plant Thank you Roger and Tim for all the painstaking experiments which helped me in collection of a lot of useful data.

My colleagues at P&E have provided the best atmosphere to do PhD in. When I enter my office the first thing I see is a closet full of candies and along the same diagonal in the corner I see another closet full of "interesting stuff". Creative juices indeed flow in such an office. I have received constant support and help from my colleagues here at P&E: Aditya (TT), Ali, Ana, Antonella, Aylin, Christian, Cristian, David, Dennis, Erin, Ernesto, George, Guido, Hrishikesh (tiggy), Jelan, Magda, Mahinder, Mahsa, Marloes, Marta, Martina, Michel, Norbert, Richard, Samir, Sayee, Shanfeng, Stephanie, Stijn,

Tomek, Widya, Xiaouhua, Yash. You guys have been instrumental in teaching me so many things.

Widya and Ali: You have been the constant source of support and knowledge. You are the first two people I think of when I am in trouble and that means every alternate day. Christian: you make the best Glühwein in the world. Jelan: Thank you for explaining the four years of PhD as four stages. In the first year, the PhDs don't do anything. In the second, they identify what to do. In the third, they actually do something. In the fourth year, they write. Xiaouhua: Chicken in Kitchen or Kitchen in Chicken is a matter to discuss decomratically or democratically. Marloes: Thank you for buurman en buurman and for introducing me to some nice beers. What were their names again? I actually did take more than a sip when you and Ana did proost every alternate second. Ana: I will eat one square cm of fish when you eat the entire Indian meal. The deal is still on. Norbert: Don't be afraid of snakes in India. They are quite friendly. Dennis: When I am away, I hope you can find a colleague who enters the office sharply at 10'o clock and 1'o clock. Martina: Thank you for remembering the rood lambrusco and the pizza I like. Samir: Life is complicated but finding simplicity amongst complexity is what keeps you going. Thank you for all the complicated discussions on chemistry, nucleation and life. Mahinder: Enjoy the fruits. They are specially packed for you every day. Thank you for the translations and help with the tax issues. Sayee: Cycling for more than a kilometre per day is actually possible. I hope you enjoy interesting proposals that keep on coming your way. Antonella: For some reasons you were the most discussed person even before arriving in Delft. David: I hope one day you can help the employees to win against the students in the soccer match. Tiggy, Yash, TT: talks with you were quite refreshing. I enjoyed playing badminton and ping-pong with you guys.

I would also like to express appreciation for some of my friends and housemates: Sameer anna, Butters, Amol, Roopali, Chulbul, Sudam, Pradyumna, Indu, Bhai, Swati vahini and Kedar. I always looked forward for the Friday evenings at San Marco or to enjoy Prosecco when at home, for the Saturday morning tea, for the Sunday afternoon kombdi and for the cricket matches when I am not eating or drinking during the weekend.

The acknowledgement would be incomplete before I thank few very special people in my life. Pappa, Mummy, Sweety, Chinu and Ashwini: your love for me kept me going in the lands far away from home. When I am back, I promise not to hide methi under the bowl...